

REFERENCE ONLY

SHL ITEM BARCODE



19 1774637 2

UNIVERSITY OF LONDON THESIS

Degree *PHD*

Year *2008*

Name of Author *BARRATT, TIMOTHY
ALAN.*

COPYRIGHT

This is a thesis accepted for a Higher Degree of the University of London. It is an unpublished typescript and the copyright is held by the author. All persons consulting the thesis must read and abide by the Copyright Declaration below.

COPYRIGHT DECLARATION

I recognise that the copyright of the above-described thesis rests with the author and that no quotation from it or information derived from it may be published without the prior written consent of the author.

LOAN

Theses may not be lent to individuals, but the University Library may lend a copy to approved libraries within the United Kingdom, for consultation solely on the premises of those libraries. Application should be made to: The Theses Section, University of London Library, Senate House, Malet Street, London WC1E 7HU.

REPRODUCTION

University of London theses may not be reproduced without explicit written permission from the University of London Library. Enquiries should be addressed to the Theses Section of the Library. Regulations concerning reproduction vary according to the date of acceptance of the thesis and are listed below as guidelines.

- A. Before 1962. Permission granted only upon the prior written consent of the author. (The University Library will provide addresses where possible).
- B. 1962 - 1974. In many cases the author has agreed to permit copying upon completion of a Copyright Declaration.
- C. 1975 - 1988. Most theses may be copied upon completion of a Copyright Declaration.
- D. 1989 onwards. Most theses may be copied.

This copy has been deposited in the Library of _____

This copy has been deposited in the University of London Library, Senate House, Malet Street, London WC1E 7HU.

Microwell Evaluation of Mammalian Cell Lines for
Large Scale Culture

A PhD thesis submitted to University College London

by

Timothy Alan Barrett



UMI Number: U591464

All rights reserved

INFORMATION TO ALL USERS

The quality of this reproduction is dependent upon the quality of the copy submitted.

In the unlikely event that the author did not send a complete manuscript and there are missing pages, these will be noted. Also, if material had to be removed, a note will indicate the deletion.



UMI U591464

Published by ProQuest LLC 2013. Copyright in the Dissertation held by the Author.
Microform Edition © ProQuest LLC.

All rights reserved. This work is protected against
unauthorized copying under Title 17, United States Code.



ProQuest LLC
789 East Eisenhower Parkway
P.O. Box 1346
Ann Arbor, MI 48106-1346

Declaration

I, Timothy Alan Barrett, confirm that the work presented in this thesis is my own. Where information has been derived from other sources, I confirm that this has been indicated in the thesis.

Abstract

Experimentation in shaken microplate formats offers a potential platform technology for the evaluation and optimisation of cell culture conditions. Provided that the results obtained are reliable, and indicative of large scale performance, it should be possible to obtain process design data early and cost effectively. This work describes a detailed engineering characterisation of liquid mixing and gas-liquid mass transfer in microwell systems and their impact on suspension cell cultures. Furthermore, an initial attempt at scaling a microwell culture to shake flasks and a 5-L stirred-tank reactor is made.

For suspension cultures of murine hybridoma cells producing IgG1, 24-well plates have been characterised in terms of power dissipation (P/V) (via CFD), fluid flow patterns and oxygen transfer rate as a function of shaking frequency and liquid fill volume. Predicted k_La values varied between 1.3 and 29 h^{-1} ; mixing time, quantified using decolourisation of iodine, varied from 1.7 s to 3.5 h; while the P/V ranged from 5 to 35 W m^{-3} . CFD simulations of the shear rate predicted hydrodynamic forces will not be lethal to cells. High shaking speed (≥ 250 rpm) was shown to be detrimental to cell growth, while a combination of low shaking speed and high well fill volume (120 rpm, 2000 μl) resulted in oxygen limited conditions. Using matched average energy dissipation as a basis for scale translation, cell growth and antibody titre were found to be similar in a 24-well plate, 250 ml shake flask and 5-L stirred-tank reactor.

Overall this work has demonstrated that cell culture performed in shaken microwell plates can provide data that is both reproducible and representative of larger-scale cultures. Linked with automation this provides a route towards the high throughput evaluation of robust cell lines under realistic process conditions.

Acknowledgements

I would like to thank my two supervisors, Gary Lye and Susana Levy, for their time, support and patience throughout my studies. From UCL, I would like to thank the following for their input and help: Andrew Wu, Sam Denby, Wellae Williams-Dalson, Betty Lin and Alfred Ding. In addition, I would like to thank my friends, my family and most of all Heather who has spurred me on and supported me over the last four years.

Contents

1	Introduction	14
1.1	Thesis Rationale and Overview	14
1.2	Antibodies	15
1.3	Expression Systems for Protein Production	18
1.3.1	Mammalian Cells	18
1.3.2	Bacterial Cells	19
1.3.3	Yeast Cells	20
1.3.4	Transgenic Plants	20
1.3.5	Insect Cells	21
1.3.6	Transgenic Animals	21
1.4	Bioreactor Systems for Bioprocess Development	22
1.4.1	Stirred Tank Reactors (STR)	22
1.4.2	Spinner Flasks	25
1.4.3	Shaken Bioreactors	25
1.4.4	Microwell Plates	28
1.5	Aim and Objectives of Thesis	39
2	Materials And Methods	41
2.1	Cell Culture	41
2.1.1	Cell Line Description and Medium Formulation	41
2.1.2	Creation of Cell Bank	41
2.1.3	Revival of Cells From Liquid Nitrogen Storage	42
2.1.4	Shake Flask Cultures	43
2.1.5	Shaken Microwell Cultures	43

2.1.6	Stirred-Tank Reactor (STR)	47
2.2	DOT Measurements in Microwell and Shake Flask Culture	48
2.3	Description of Liquid Phase Hydrodynamics	48
2.4	Oxygen Mass Transfer Coefficients (k_{La})	50
2.4.1	Prediction of K_{La} in Shaken Microwells	50
2.4.2	Measurement of k_{La} in the Stirred-Tank Reactor	50
2.4.3	Prediction of k_{La} in Shake Flasks	51
2.5	Liquid Phase Mixing Time Characterisation	53
2.6	Characterisation of Energy Dissipation Rates	55
2.6.1	Prediction of Energy Dissipation Rates in Shake Flasks	55
2.6.2	CFD Modelling of Shaken 24 Well Plates	56
2.6.3	Power Input to a 5-L STR	56
2.7	Derived Growth and Metabolic Parameters	59
2.7.1	Estimation of maximum specific growth rate	59
2.7.2	Integral of viable cell concentration (IVC)	59
2.7.3	Average specific antibody production rate	60
2.7.4	Specific glucose consumption rate	60
2.8	Analytical Techniques	60
2.8.1	Cell Number and Viability Quantification	60
2.8.2	Quantification of Antibody Concentration	61
2.8.3	Quantification Of Glucose, L-Lactate and Glutamine Concentration	61
2.8.4	pH and Osmolality Measurements	62
2.9	Statistical Tests	62
3	Engineering Characterisation Of Shaken Microwell Plates	63
3.1	Introduction and Aims	63
3.2	Prediction of Liquid Phase Hydrodynamics	64
3.3	Prediction of Oxygen Mass Transfer Coefficients	66
3.4	Liquid Phase Mixing Time Characterisation	68
3.4.1	Shaken Microwell Plates	68

3.4.2	Stirred-Tank Reactor	76
3.5	Characterisation of Energy dissipation rates	76
3.5.1	CFD Modelling of Shaken 24-Well Plates	76
3.5.2	Power Input to a 5-L STR	86
3.6	Evaporation From Shaken Microwell Plates	86
3.7	Consideration of a Basis for Scale Translation From Shaken Microwell Plates to Shake Flasks and Bench-Scale STR	91
3.8	Summary	93
4	Kinetic Analysis of Shaken Microwell Cultures	97
4.1	Introduction and Aims	97
4.2	Initial Assessment of Well Geometry	99
4.3	Effect of Shaking Speed on Cell Growth and Antibody Production in Shaken 24-SRW (ULA) Microtitre Plates	102
4.4	The Effect of Well Fill Volume on Cell Growth and Antibody Pro- duction in Shaken 24-SRW (ULA) Microtitre Plates	113
4.5	DOT measurements During Cell Culture in Shaken 24-SRW (ULA) Microtitre Plates	122
4.6	Influence of Well Coating and Baffles on Cell Growth and Antibody Production in Shaken 24-SRW (ULA) Microtitre Plates	123
4.6.1	Effect of Well Coating	123
4.6.2	Effect of Baffles	125
4.7	Summary	132
5	Scale Translation of Hybridoma Cultures Based on Energy Dissi- pation	135
5.1	Introduction and Aims	135
5.2	Cell Culture Performance Under Non-Matched P/V	136
5.3	Scale-up of Cell Culture Performance at Matched P/V	143
5.4	Summary	152
6	Conclusions and Future Work	153

List of Tables

3.1	Re, Fr and Ph numbers calculated for a 24-well (ULA) plate.	65
3.2	Mean volumetric oxygen mass transfer coefficient (K_{La}) predicted for a 24-well (ULA) plate.	66
3.3	Mean volumetric oxygen transfer coefficient (k_{La}) measured in a 5-L STR.	67
3.4	Summary of published liquid phase mixing time data for various geometries of mammalian cell bioreactor.	72
3.5	Energy dissipation rate per unit volume (P/V) and shear rate predicted for shaken 24-well plates using CFD	85
3.6	Mean energy dissipation in a 5-L STR as a function of stirrer speed .	88
3.7	Summary of the main engineering parameters established for shaken 24-well (ULA) plates.	95
3.8	Summary of the main engineering parameters established for a 5-L STR	96
4.1	Effect of shaking speed on growth, antibody production and metabolism during the culture of VPM 8 hybridoma cells in shaken 24-SRW (ULA) plates.	112
4.2	Effect of well fill volume on growth, antibody production and metabolism during the culture of VPM 8 hybridoma cells in 24-SRW (ULA) microtitre plates.	121
4.3	Effect of baffles on the growth and antibody production of VPM 8 hybridoma cells cultured in 24-SRW (ULA) plates	131

5.1	Scale-up of VPM 8 hybridoma cells based on matched average energy dissipation per unit volume: cell growth, antibody production and metabolism in shaken 24-SRW plates, 250 ml shake flasks and a 5-L stirred-tank reactor.	151
-----	---	-----

List of Figures

1.1	Schematic diagram of the structure of an antibody molecule	16
1.2	Values of the energy dissipation rate for various bioreactor environments and it's effect on various cell lines	19
1.3	Bioreactor options for high-throughput cell-culture process development	23
1.4	Schematic diagram of individual formats: 96-deep square well format (96-DSW); 24-round well format (24-SRW) and 96-round well format (96-SRW)	29
1.5	Dimensions of a single well from a 96-DSW microplate and the influence of increasing shaking speed on fluid motion and gas-liquid interfacial area available for oxygen transfer	31
1.5	Photographs showing details of the automated, high-throughput microwell platform currently used at UCL for stem-cell processing. . . .	37
1.6	Automated microscale sequence for the evaluation of linked fermentation and bioconversion processes	38
2.1	Schematic diagram of individual microwell formats used in this thesis: 96-deep square well format (96-DSW); 24-standard round well format (24-SRW (PS)) and 24-standard round well format with ultra-low attachment coating (24-SRW (ULA)).	44
2.2	Schematic diagram of baffled, 24-SRW (ULA) microwell plates	46
2.3	Schematic diagram of the 5-L STR and an image of the 3-blade segment impeller	47

2.4	Non-invasive measurements of dissolved oxygen in shaken microwell and shake flask cultures using a PreSens fibrox 3 meter and oxygen sensitive spots	49
2.5	Examples of the oxygen uptake curves used to quantify k_La in the 5-L STR	52
2.6	Perspex mimic of a single well from a 24-SRW (ULA) plate used for mixing time studies	53
2.7	Experimental set-up to measure power input to a 5-L STR	57
3.1	Mixing of a small liquid addition into the liquid contents of a single well from a 24-well (ULA) plate. Shaking speed = 120 rpm. 8 μ l of inert blue food dye was injected into 800 μ l of water and images were captured by high speed video	70
3.2	Mixing of a small liquid addition into the liquid contents of a single well from a 24-well (ULA) plate. Shaking speed = 300 rpm. 8 μ l of inert blue food dye was injected into 800 μ l of water and images were captured by high speed video	71
3.3	Mixing of a small liquid addition into the liquid contents of a single well from a 24-well (ULA) plate. Shaking speed = 120rpm. 8 μ l of 1.8 M sodium thiosulphate solution was injected into 800 μ l of 0.5 M iodine solution and images were captured by a high speed video camera	73
3.4	Mixing of a small liquid addition into the liquid contents of a single well from a 24-well (ULA) plate. Shaking speed = 300 rpm. 8 μ l of 1.8 M sodium thiosulphate solution was injected into 800 μ l of 0.5 M iodine solution and images were captured by a high speed video camera	74
3.5	Mean mixing time measured in shaken 24-well (ULA) plates as a function of Reynolds number (Re) and liquid fill volume (V_L)	75
3.6	Mean mixing time measured in baffled shaken 24-well (ULA) plates as a function of Reynold's number (Re)	77
3.7	Mixing of a small liquid addition into the liquid contents of a 5-L STR	78
3.8	Mean mixing time measured in a 5-L STR as a function of Re	79

3.9	Comparison of the liquid phase mixing times for a shaken 24-well (ULA) plate and 5-L STR	80
3.10	CFD simulations of shear rate performed on shaken 24-SRW (ULA) microtitre plates. Visual images, at identical shaken speeds, are also shown	83
3.11	Mean power number of a 3-blade segment impeller as a function of Re	87
3.12	Evaporation from the liquid bulk of a 24-well (ULA) microplate at 37°C covered with a breath-easy membrane	90
3.13	Variation of culture medium osmolality in shaken 24-well hybridoma cultures	92
4.1	Effect of well geometry on VPM 8 hybridoma cell growth in shaken 24-SRW (ULA) and 96-DSW plates	100
4.2	Effect of well geometry on VPM 8 hybridoma viability in shaken 24-SRW (ULA) and 96-DSW plates	101
4.3	Comparison of the cell growth and viability of VPM 8 hybridoma and CHO-S cells in shaken 96-DSW microtitre plates	103
4.4	Effect of shaking speed on VPM 8 hybridoma cell growth in shaken 24-SRW (ULA) plates.	107
4.5	Effect of shaking speed on VPM 8 hybridoma viability in shaken 24-SRW (ULA) plates	108
4.6	Effect of shaking speed on VPM 8 hybridoma antibody production in shaken 24-SRW (ULA) plates	109
4.7	Effect of shaking speed on VPM 8 hybridoma glucose consumption and L-lactate production in shaken 24-SRW (ULA) plates	110
4.8	Effect of shaking speed on VPM 8 hybridoma L-glutamine consumption in shaken 24-SRW (ULA) plates	111
4.9	Effect of well fill volume on VPM 8 hybridoma growth in 24-SRW (ULA) microtitre plates	116
4.10	Effect of well fill volume on VPM 8 hybridoma viability in 24-SRW (ULA) microtitre plates	117

4.11	Effect of well fill volume on VPM 8 hybridoma antibody production in 24-SRW (ULA) microtitre plates	118
4.12	Effect of well fill volume on VPM 8 hybridoma glucose consumption and L-lactate production in 24-SRW (ULA) microtitre plates	119
4.13	Effect of well fill volume on VPM 8 hybridoma L-glutamine consumption in 24-SRW (ULA) microtitre plates	120
4.14	In-situ dissolved oxygen tension (DOT) measurements in a 24-SRW (ULA) microtitre plate and a 250 ml shake flask during the culture of VPM 8 hybridoma Cells	124
4.15	Effect of well coating on VPM 8 hybridoma growth in 24-SRW microtitre plates	126
4.16	Effect of well coating on VPM 8 hybridoma antibody production in 24-SRW plates	127
4.17	Effect of baffles on the growth of VPM 8 hybridoma cells cultured in 24-SRW plates	129
4.18	Effect of baffles on the antibody production of VPM 8 hybridoma cells cultured in 24-SRW (ULA) plates	130
5.1	Effect of average energy dissipation (P/V) on VPM 8 hybridoma cell growth in 250 ml shake flasks.	137
5.2	Effect of average energy dissipation (P/V) on VPM 8 hybridoma viability in 250 ml shake flasks	138
5.3	Effect of average energy dissipation (P/V) on VPM 8 hybridoma antibody production in 250 ml shake flasks	139
5.4	Effect of average energy dissipation (P/V) on VPM 8 hybridoma glucose consumption and L-lactate production in 250 ml shake flasks	140
5.5	Effect of average energy dissipation (P/V) on VPM 8 hybridoma L-glutamine consumption in 250 ml shake flasks	141
5.6	Scale-up of VPM 8 hybridoma cells based on matched average energy dissipation per unit volume: cell growth in shaken 24-SRW (ULA) plates, 250 ml shake flasks and a 5-L stirred-tank reactor	146

5.7	Scale-up of VPM 8 hybridoma cells based on matched average energy dissipation per unit volume: cell viability in shaken 24-SRW plates, 250 ml shake flasks and a 5-L stirred-tank reactor	147
5.8	Scale-up of VPM 8 hybridoma cells based on matched average energy dissipation per unit volume: antibody titre in shaken 24-SRW plates, 250 ml shake flasks and a 5-L stirred-tank reactor	148
5.9	Scale-up of VPM 8 hybridoma cells based on matched average energy dissipation per unit volume: glucose and lactate concentrations in shaken 24-SRW plates, 250 ml shake flasks and a 5-L stirred-tank reactor	149
5.10	Scale-up of VPM 8 hybridoma cells based on matched average energy dissipation per unit volume: L-glutamine concentration in shaken 24-SRW plates, 250 ml shake flasks and a 5-L stirred-tank reactor	150

Nomenclature

a_i	Specific static interfacial area, m^{-1}
Bo	Bond number, $= \frac{\rho d_w^2 g}{\sigma}$, dimensionless
C_3	Constant in Equation 1.1, $= 1.94$
CFD	Computational fluid dynamics
d_w	Microwell diameter, m
d_s	Shaker diameter, m
d_f	Maximum inside shaking flask diameter, m
D	Oxygen diffusion coefficient, $\text{m}^2 \text{s}^{-1}$
DOT	Dissolved Oxygen Tension, % of air saturation
D_i	Impeller diameter, m
Fr	Froude number, $= \frac{(2\pi N)^2 d}{2g}$, dimensionless
$K_{L,a}$	Overall mass transfer coefficient, h^{-1}
$k_{L,a}$	Gas-liquid interface mass transfer coefficient, h^{-1}
k	Shake flask closure transfer resistance, $\text{m}^3 \text{h}^{-1}$. Used in Equation 2.4.
M	Equilibrium constant, dimensionless. Used in Equation 2.4.
N	Impeller rotation speed or shaking speed, s^{-1}
Ph	Phase Number, dimensionless
Po	Power number, $= \frac{P}{\rho N^3 D_i^5}$, dimensionless
P/V	Mean energy dissipation rate per unit volume, W m^{-3}
R	Perpendicular distance from direction of forced to pivot, m
Re	Reynolds number, $= \frac{\rho N d^2}{\mu}$, dimensionless
SD	Standard Deviation
SPR	Specific antibody production rate, $\text{mg} (10^9 \text{ cells.day})^{-1}$
STR	Stirred-Tank Reactor

T	Torque, N m
t	Time, s
V_L	liquid fill volume, m ³
vvm	volumes of gas per minute per unit volume of liquid, dimensionless
W	Wetting tension, N m ⁻¹
X_v	viable cell concentration, cells ml ⁻¹
24-SRW (ULA)	24-well standard round well coated with a ultra-low attachment film
24-SRW (PS)	24-well standard round wells fabricated from polystyrene
96-DSW	96-deep square well

Greek Symbols

ω	angular speed, s ⁻¹
ρ	density, kg m ⁻³

Chapter 1

Introduction

1.1 Thesis Rationale and Overview

Optimisation of suspension cell-culture is traditionally carried out in spinner flasks, shake flasks, and small bench-scale stirred-tank reactors (STR). The current need to reduce process development time necessitates the adoption of high throughput experimentation, however, the labour and material costs involved render this almost impractical at conventional scales (Lye et al., 2003)(Girard et al., 2001)(Micheletti and Lye, 2006). In contrast, experimentation in microwell formats offers a potential new platform technology to obtain key process design data early and cost effectively (Lye et al., 2003). Use of the microwell format readily lends itself to automation (Doig et al., 2002)(Nealon et al., 2005), and the implementation of advanced operating strategies such as liquid addition for pH control (Elmahdi et al., 2003) and fed-batch operation.

To date, microbial systems have been the main focus for the development of microwell technology as a high-throughput tool for bioprocess development (Section 1.4.4). In contrast, studies looking to use shaken microwells for the development of suspension-adapted mammalian cell cultures are very few (Girard et al., 2001)(Strobel et al., 2001). Those that have been published have tended to be process specific and ignore the engineering environment underpinning microwell operation. In this work, one of the main aims is to study the engineering environment that cells are exposed to

during shaken microwell cell culture, and then relate this understanding to culture performance (Section 1.5).

Of the biopharmaceutical products currently in development, a large proportion are monoclonal antibodies (Chadd and Chamow, 2001)(Dinnis and James, 2005). This class of therapeutic has certain advantages (Discussed in Section 1.2), and will therefore be used as a model protein in this study.

1.2 Antibodies

Antibodies are proteins of the immune system that bind to antigens. They are highly specific: one antibody binds to a particular antigen. Antigens (**Antibody Generating Substances**) are usually foreign to the organism and include disease inducing bacteria, viruses and other infectious agents.

All antibodies belong to a family of proteins called immunoglobulins. These Y-shaped molecules are formed from two types of polypeptides: heavy chains and light chains (Fig. 1.1). These two chains are linked by disulphide bonds. Three globular regions can be identified: two identical domains (Fab domain) corresponding to each arm and one corresponding to the stem (Fc domain). The N-terminal region of both heavy and light chains lie at the tip of each arm and are distinguished by highly variable amino acid sequence. The remaining portion of the sequences in both chains are nearly identical among antibodies with different specificities (Lodish et al., 1999). The antigen-binding sites lie at the end of each arm.

The constant region determines the mechanism used by the host organism to destroy any circulating antigen. Antibodies are divided into five major classes, IgM, IgG, IgA, IgD and IgE, based on their constant region structure and immune function.

Therapeutic antibodies are laboratory-engineered substances that recognize and

bind onto a protein on the surface of a pathogen's cell. Each therapeutic antibody recognises a different protein, or antigen, and in general can be used alone, in combination with chemotherapy or as a carrier of substances such as toxins or radiation. After binding to the targeted site, the therapeutic antibody can block the growth of the tumour and/or recruit the body's immune system to attack the target, and can also sensitize cancer cells to chemotherapy. Therapeutic antibodies can be classified as monoclonal or polyclonal, and human or humanised. A murine antibody is derived solely from mouse sequences and therefore is known as murine by the host body and can be used by antigen-antibody reactions in an in vivo system. A chimeric antibody is composed of both mouse and human sequences, usually a 30/70 ratio of mouse and human components and is used in immunotherapy. A human antibody is derived from human sequences and therefore is known as human by the host body and can be used by antigen-antibody reactions in an in vivo system.

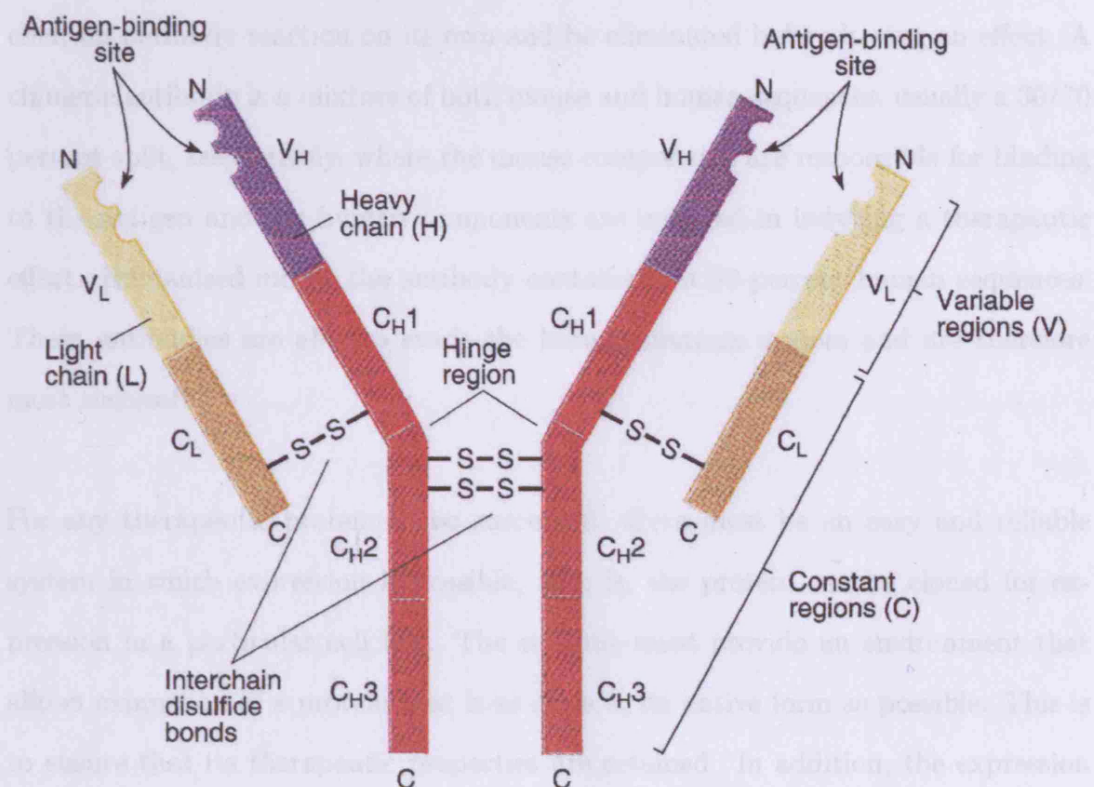


Figure 1.1: Schematic diagram of the structure of an antibody molecule

expansions, ranging from the use of horizontal cells through to transgenic animals. Each system has its advantages and disadvantages, and are discussed in the next section.

bind onto a protein on the surface of a patient's cell. Each therapeutic antibody recognises a different protein, or antigen, and in general can be used alone, in combination with chemotherapy or as a carrier of substances such as toxins or radiation. After binding to the targeted site, the therapeutic antibody can block the growth of the tumour and/or recruit the body's immune system to attack the target, and can also sensitise a cancer cell to chemotherapy. Therapeutic antibodies can be classified as follows: murine, chimeric and humanised. A murine antibody is derived solely from mouse sequences and therefore is viewed as foreign by the host body and can elicit an antibody reaction on its own and be eliminated before having an effect. A chimeric antibody is a mixture of both mouse and human sequences, usually a 30/70 percent split, respectively, where the mouse components are responsible for binding to the antigen and the human components are involved in inducing a therapeutic effect. Humanised means the antibody contains over 90 percent human sequences. These antibodies are able to evade the human immune system and are therefore most successful.

For any therapeutic protein to be successful, there must be an easy and reliable system in which expression is possible, that is, the protein can be cloned for expression in a particular cell line. The cell line must provide an environment that allows expression of a protein that is as close to its native form as possible. This is to ensure that its therapeutic properties are retained. In addition, the expression system should allow easy recovery of the recombinant protein using a cost effective process. There are a number of different systems available for recombinant protein expression, ranging from the use of bacterial cells through to transgenic animals. Each system has its advantages and disadvantages, and are discussed in the next section.

1.3 Expression Systems for Protein Production

1.3.1 Mammalian Cells

Suspension-adapted mammalian cells have become the dominant system for the production of recombinant proteins for clinical applications because of their capacity for proper protein folding, assembly and post-translational modification (Chadd and Chamow, 2001). Thus, the quality and efficacy of the protein can be superior when expressed in mammalian cells compared to other systems, such as bacteria, plants and yeast (Verma et al., 1998). Today, 60-70% of recombinant protein pharmaceutical are produced in mammalian cells (Chadd and Chamow, 2001). The majority of these proteins are expressed in chinese hamster ovary (CHO) cells, although other cells lines, such as myeloma (NS0), baby hamster kidney (BHK), human-embryo kidney (HEK-293) and human retinal cells have gained regulatory approval for recombinant protein production (Wurm, 2004). Mammalian cells have the advantage over transgenic plants and animals that protein can be produced approximately 6 months after the initial cloning. At present, the cost of production is very high in mammalian cells. Dove (2002) states that the estimated production cost from a mammalian cell process is \$150 / g raw material, compared to \$1-\$2 from transgenic animals. At present, recombinant protein produced by mammalian cells has reached approximately grams per litre after a three week culture, with a specific productivity of $90 \text{ pg cell}^{-1} \text{ day}^{-1}$ (Wurm, 2004)(Merten, 2006).

Mammalian cell systems have a number of potential disadvantages: they require complex media formulations, have low productivity, are slow growing and are relatively sensitive to changes in process conditions. In addition, one of the main concerns regarding mammalian cell culture is their susceptibility to “shear”, or, more correctly, hydrodynamic stress. It now thought that sparging, rather than agitation, is responsible for cellular damage in bioreactors (Nienow et al., 1996). In an attempt to quantify the affect of hydrodynamics on mammalian cells, Figure. 1.2 was compiled by Heath and Kiss (2007) using both literature and experimental

Figure 1.2: Values of the energy dissipation rate for various bioreactor environments and its effect on various cell lines. Reproduced from Heath and Kiss (2007).

data. This figure shows that energy dissipation rates that were found to lyse common mammalian cell-line are 2-4 order of magnitude greater than those experienced in typical stirred-tank reactors. Furthermore, these lethal values are comparable to those generated by a bursting bubble.

1.3.2 Bacterial Cells

Bacterial cells are commonly used for the production of simple proteins and polypeptides (Chadd and Chamow, 2001). They have the ability to produce large quantities of protein at a very fast rate compared to mammalian cells (typical doubling time of 20 minutes). The most commonly used organism is *Esheria Coli*. Transformation of *E. coli* cells with foreign DNA is easy and efficient. Antibody engineering using *E. coli* tends to be inexpensive. Despite the advantages, bacterial cells are not capable of glycosylating proteins. If whole antibody molecules are required, which are glycosylated in the C_{H2} domain, alternative expression systems are necessary (Verma et al., 1998). For this reason there are no commercially available therapeutic antibodies currently produced in bacteria.

1.3.3 Yeast Cells

The main advantage of yeast over *E. coli* is that it is both a microorganism and a eukaryote (Verma et al., 1998). Therefore it can provide advanced protein folding pathways for heterologous proteins. Like mammalian cells, it can secrete correctly folded proteins into culture media while being grown on simple growth media. Whole antibodies, single-chain antibodies and antibody fragments have been expressed using this system. Proteins which accumulate as insoluble inclusion bodies in *E. coli* are often soluble when expressed in yeast. In addition, the degradation of heterologous proteins, again a frequent problem in *E. coli* is usually reduced in yeast. Yeast cells are capable of glycosylation of proteins at Asn-X-Ser/thr motifs. However, this is not identical to that seen in hybridomas and myelomas since carbohydrates are not modified beyond the mannose addition. High levels of secreted recombinant antibody fragments have been achieved in yeast. Two single-chain antibodies, anti-CD7 and anti-DMI, were expressed at 0.25 mg l⁻¹ in *E. coli* but when the same fragments were expressed in *Pichia pastoris* their yields were increased to 60 mg l⁻¹ and 100-250 mg l⁻¹, respectively. Similarly, the yield of functional rabbit anti-recombinant human leukemia inhibitory sFv was 100-fold more in *Pichia pastoris* 100 mg l⁻¹ than in *E. coli*.

1.3.4 Transgenic Plants

Production of proteins using transgenic plants has a number attractions including low manufacturing cost, simple scale-up and the ability to produce correctly folded, glycosylated proteins. Cloning a foreign gene into a plant cell is commonly performed using agrobacterium infection or gene bombardment in the presence of a carrier molecule and gold particle (Chadd and Chamow, 2001). The public's concern over the GM crops represents a significant resistance to advances in technology in this area. At present transgenic plants have low yields: protein accounts for nearly 1% of the harvest leading to problems with downstream processing (Kusnadi et al., 1997). They also have a relatively long lead time before any protein material

can be produced. The antibodies produced in transgenic plants have carbohydrate structures that can be quite distinct in composition and structure compared to human glycoproteins (Chadd and Chamow, 2001)(Larrick and Thomas, 2001).

1.3.5 Insect Cells

Insect cells can produce proteins with similar post-translational modifications to mammalian cells. In fact, insect cells are second only to mammalian cells with regard to protein folding and post-translational modification. Slight differences in glycosylation, particularly N-glycosylation, separate the two expression systems (Altmann et al., 1999). Most insect cell expression systems are produced by infection of the cells with recombinant baculovirus particles (Verma et al., 1998). Upon infection, virus particles begin to replicate themselves, while expressing the heterologous gene. Although this method provides a convenient and simple way of producing large quantities of protein (1-500 mg of recombinant protein per litre of infected cells), it is disadvantaged by incorporating a very late viral promoter that peaks when the cells are dying from the viral infection. An alternative is to develop stable insect cell lines (Pfeifer, 1998). Stable transformation has been performed in *Drosophila* systems. Anti-E selectin sFv was expressed at 0.2-0.4 mg l⁻¹ in the culture supernatant (Verma et al., 1998). Compared to mammalian cell lines, insect cell lines have a greater oxygen demand and shear sensitivity, thus making the adaption to large-scale culture more difficult (Verma et al., 1998).

1.3.6 Transgenic Animals

Protein production using transgenic animals is commonly initiated by the microinjection of a genetic construct fused to a milk-specific regulatory element into a single cell embryo (Larrick and Thomas, 2001). Protein titers obtained from transgenic animals are in the same range as those from mammalian cell culture (2-10 g per litre

of milk)¹. Along with goats; mice, chickens, rabbits and cows have been used to produce proteins. Once established, transgenics are a very cost effective way of producing therapeutic proteins, and scale-up is based on agricultural economics (Dove, 2002). The generation of a transgenic herd to produce material for phase 1 clinical trials takes between 18 - 24 months (Chadd and Chamow, 2001) which could prove an unacceptable delay for development purposes. At present there are no human therapeutic proteins produced in transgenic animals as a result of regulatory issues ².

In the next section, the various different bioreactors that are currently used or have the potential to be used for bioprocess development will be discussed; in particular their various strengths and weaknesses. The main criteria for a successful scale-down model is it's ability to generate data that is both reproducible and representative of larger scales. However, with the ever increasing number of new drug candidates to be evaluated, factors such as labour requirements, raw material costs and throughput become ever more important. The trade-off between throughput and generation of cell culture data is shown in Fig. 1.3. At each step in the development of the culture process, careful consideration of a bioreactor's limitations is required to efficiently generate data that is both relevant and predictive of larger scales.

1.4 Bioreactor Systems for Bioprocess Development

1.4.1 Stirred Tank Reactors (STR)

Benchtop stirred-tank reactors, along with spinner flasks (Section 1.4.2) and shake flask (Section 1.4.3) are the primary systems used in the development of a new fermentation/cell culture process (Girard et al., 2001). Indeed, while spinner flasks and shake flask are generally used for seed-trains and screening raw materials, STRs are

¹<http://www.gtc-bio.com/science/questions.html> Cited: 28/10/2007

²<http://news.bbc.co.uk/1/hi/sci/tech/4740230.stm> Cited: 22/02/2006

used as a scale-down model for bioprocess design (Li et al., 2006). The advantages of using STRs include the ability to implement control parameters such as pH, dissolved oxygen (DO), foam levels, nutrient concentrations and temperature.

The engineering constraints in STRs are best summarized as follows. For a typical cell culture in a STR, the average energy dissipation rate is between 1 and 10 W m⁻³ (Shaw et al., 1995) (Vince and Birch, 1995) (Langenhovek and Novak, 1994).



Figure 1.3: Bioreactor options for high-throughput cell-culture process development. Reproduced, with permission, from Doig et al. (2006).

and in 24-deep well microtiter plates (1–10 ml). The advantages of this approach include the ability to operate with higher average transfer rates than stirred tank bioreactors, online measurement of dissolved oxygen, pH and optical density (Lampard et al., 2003) (Ge et al., 2004); and the ability to maintain zero or low shear with the production bioreactor. Furthermore, the engineering environment has been extensively characterized in terms of energy dissipation rate, k_{La} and mixing time (Lampard et al., 2003) (Vailly-Jos et al., 2005) (Derts et al., 2006). Using this

^a Volumetric flow rate per volume per unit volume of liquid

used as a scale-down model for bioprocess design (Li et al., 2006). The advantages of using STRs include the ability to monitor and control parameters such as pH, dissolved oxygen (DOT), foam height, nutrient concentration and temperature.

The engineering environment in STR has been extensively characterised. For a typical cell culture in a STR, the average energy dissipation rate is between 1 and 12 W m⁻³ (Nienow et al., 1996)(Varley and Birch, 1999)(Langheinrich and Nienow, 1999). Typical values of k_La are between 1 and 10 h⁻¹ (Varley and Birch, 1999)(Fenge et al., 1993), while mixing times are generally less than 200 s (Table 3.4). Given this understanding of the hydrodynamics and gas-liquid mass transfer, a variety of bases for scale-translation of suspension cell cultures have been successfully implemented including fluid turnover rate (Chisti, 1993); superficial gas velocity (Xie et al., 2003); vvm³ and impeller tip speed (Marks, 2003); and average energy dissipation rate (Li et al., 2006).

The disadvantages of using STRs as a scale-down tool for bioprocess development are the low throughput, the large requirements for raw material (> 1 L), the labour requirement for inoculation, sampling, harvesting and then cleaning; and the potential damage to mammalian cells caused by sparging.

The use of miniature STRs for bioprocess development has received much interest in recent years (Lamping et al., 2003)(Vaillejos et al., 2006)(Betts et al., 2006)(Gill et al., 2007). These systems operate with a working volume comparable to that used in 24-deep well microtitre plates (5 - 10 ml). The attraction of this approach includes the ability to operate with higher oxygen transfer rates than surface aerated bioreactors; online measurement of dissolved oxygen, pH and optical density (Lamping et al., 2003)(Ge et al., 2006); and the ability to maintain geometric similarity with the production bioreactor. Furthermore, the engineering environment has been extensively characterised in terms of energy dissipation rate, k_La and mixing time (Lamping et al., 2003)(Vaillejos et al., 2006)(Betts et al., 2006). Using this

³Volumetric flow rate per minute per unit volume of liquid

knowledge, both $k_L a$ (Lamping et al., 2003) and energy dissipation rate (Betts et al., 2006), have been used successfully as a basis for scale translation of *E. coli* culture with bench-scale STRs. The disadvantage of using miniature STRs is that they are not applicable to automation and they do not have the same level of throughput compared to microwell plates and shake flasks. Furthermore, they are not disposable and so a considerable amount of time is required to clean and then sterilise before inoculation.

1.4.2 Spinner Flasks

A spinner flask is a vessel filled with between 1 and 12 L of diluted culture and placed on a magnetic stirring platform in a suitable incubator. Agitation is provided by a magnetic paddle coupled to a glass shaft that runs through the headplate. Two “arms” on either side of the vessel allow sampling and additions during the cultivation. Spinners have been used for many years and thus have been the subject of many studies looking to characterise the hydrodynamic and mass transfer environment (Aunins et al., 1989)(Sucosky et al., 2004). The disadvantages of spinners for cell culture process development is that they are not high-throughput, not applicable to automation and require significantly greater amounts of labour and raw materials when compared to systems such as microwell plates.

1.4.3 Shaken Bioreactors

Shaken bioreactors, especially Erlenmeyer flasks, are widely used in academia and the biotechnology industry for screening and process development projects (Büchs, 2001) (Weuster-Botz, 2005) (Freyer et al., 2004). They are easy to operate, require small amounts of material (typically 50 - 500 ml) and cost very little (Kumar et al., 2004). Following inoculation, the flask is typically placed on an orbital shaker platform in a suitable incubator. Gas-exchange, if necessary, is made possible using a loose fitting bung or perforation in the cap. It has been estimated that nearly 90%

of all laboratory cell culture and fermentation experiments are performed in shaken bioreactors, yet only 2% of all relevant publications in the area have dealt with engineering aspects of the shake flask (Zhang, Williams-Dalson, Keshavarz-Moore and Shamlou, 2005)(Büchs, 2001).

Recently, numerous studies have been published on the characterisation of liquid hydrodynamics and oxygen mass transfer in various size of flasks. Büchs et al. (2000a) measured mean power dissipation in unbaffled shake flasks via torque measurements made on the drive shaft of the shaker platform. A correlation, Equation 1.1, was then fitted to this data with a reported accuracy of $\pm 30\%$.

$$\frac{P}{V_L} = C_3 \rho \frac{N^2 d_f^4}{V_L^{\frac{2}{3}}} Re^{-0.2} \quad (1.1)$$

In this case P = energy dissipation rate, V_L = liquid fill volume, $C_3 = 1.94$ (a constant), ρ = liquid density, N = shaking speed, d_f = maximum inner diameter of the shake flask and Re = Reynold's number. Besides measurement of the torque on the drive shaft, other techniques, such as the temperature method (Sumino et al., 1972)(Kato et al., 2004)(Raval et al., 2007) and CFD (Zhang, Williams-Dalson, Keshavarz-Moore and Shamlou, 2005), have been used to measure energy dissipations of up to 1 KW m^{-3} in shaken bioreactors. However, these studies have not published a simple correlation to accurately predict mean energy dissipation from known operating conditions. Besides quantification of mean energy dissipation rate, a few studies have been published looking at local energy dissipation rates (Büchs and Zoels, 2001)(Peter et al., 2006). Knowledge of spatial variation in energy dissipation can be important for bioprocesses that are limited by hydromechanical stress, such as animal cell culture (Chisti, 2001) and filamentous cultures (van Suijdam and Metz, 1981).

Oxygen mass transfer coefficients, k_{La} , have been extensively studied in shake flasks, especially for microbial systems (Mrotzek et al., 2001),(Büchs, 2001),(Freyer et al., 2004),(Maier and Büchs, 2001),(Maier et al., 2004). These studies have tended to focus on interfacial gas-transfer, ignoring the resistance of the cap. This was addressed by Gupta and Rao (2003), who measured oxygen mass transfer resistance at both parts and combined them into a simple prediction of k_{La} in Erlenmeyer flasks. For microbial systems, k_{La} values of up to 280 h^{-1} have been reported in shake flasks (Kumar et al., 2004). These values are comparable to those found in medium-sized stirred-tank reactors. Under typical shake flask conditions for the growth of mammalian cells, CFD predicted k_{La} values of between 10 and 100 h^{-1} (Zhang, Williams-Dalson, Keshavarz-Moore and Shamlou, 2005).

The term “in-phase” operation applies to shaken systems where the fluid motion follows the movement of the shaker platform (Büchs et al., 2000b)(Büchs et al., 2001). In contrast, “out of phase” operation is characterised by a large fraction of the liquid remaining stationary on the bottom of the flask during shaking. Consequently, both mixing and oxygen transfer are reduced. The demarcation between these two flow regimes is described by the Phase number and may be predicted using Equation 1.2, where d_s = shaker diameter; d_f = maximum inside shaking flask diameter; ρ = liquid density; N = shaker speed; μ = liquid viscosity and V_L = liquid fill volume. “In-phase” operation is assumed to exist for $Ph > 1.26$.

$$Ph = \frac{d_s}{d_f} \left\{ 1 + 3 \log_{10} \left[\frac{\rho (2\pi N) d_f^2}{4\mu} \left(1 - \sqrt{1 - \frac{4}{\pi} \left(\frac{V_L^{\frac{1}{3}}}{d_f} \right)^2} \right)^2 \right] \right\} \quad (1.2)$$

Besides Erlenmeyer flasks, other shaking bioreactors have been considered. These include 50 ml centrifuge tubes (De Jesus et al., 2004), cylindrical shaped containers with a 5 - 10 L working volume (Liu and Hong, 2001) and square-shaped Duran bottles (Muller et al., 2005).

In general, all the shaking bioreactors discussed in this section have similar disadvantages with regard to bioprocess development. Firstly, they are not applicable to automation, hence considerable labour is required during large screening and optimisation studies. Secondly, compared to alternative systems such as microwell plates and microfluidic chips, shake flasks require large volumes of expensive raw materials and offer considerably lower throughputs. Thirdly, shake flasks are almost always non-instrumented, meaning shifts and deviations of important parameters like pH and DOT are not captured during a culture. This problem was addressed by Weuster-Botz et al. (2001), who used a custom shake flask design to monitor and then control pH during a microbial culture. In addition, this design was further extended to allow fed-batch operation. Finally, with the exception of Erlenmeyer flasks, no engineering characterisation studies have been performed on other shaken bioreactors. This knowledge would be vital to ensure predictive and reproducible scale-translation.

1.4.4 Microwell Plates

Microwell plates are available in various formats: 6, 12, 24, 48, 96, 385 to 1536 wells per plates; round, flat or pyramidal shaped bottoms; round or square cross section; and deep or shallow wells. Typically, they are fabricated from plastics such as polycarbonate or polypropylene. Fig. 1.4 show three typical microwell geometries with corresponding geometries.

Traditionally, microwell plates have been used for analytical purposes in areas such as medical diagnostics, combinatorial chemistry and biotechnology; whenever a large number of small liquid volumes have to be handled in parallel. Examples of the applications for use include: ELISA (Severns et al., 1984)(Ruitenberg et al., 1976), cell culture (Brody and Huntley, 1965)(Girard et al., 2001)(Strobel et al., 2001)(Deshpande and Heinzle, 2004), tissue culture (Sullivan and Rosenbaum, 1967),

PCR (Hosoga et al., 1994) and high-throughput screening (Hersberg and Papp, 2001; Battersby and Truu, 2003).

Recently, microfluidic processing techniques have emerged as a potential option to



Figure 1.4: Schematic diagram of individual formats: (a) 96-deep square well format; (b) 24-round well format; (c) 96-round well format. V_w represents the total well volume, SA represents the static surface area available for gas exchange. Reproduced, with permission, from Lye et al. (2003).

$$\eta_{\text{static}} = \sqrt{\frac{SA}{4 \times V_L}} \quad (1.1)$$

where σ = surface tension, d_w = microwell diameter, V_L = liquid "fill" volume, ρ =

PCR (Hataya et al., 1994) and high-throughput screening (Hertzberg and Pope, 2000)(Battersby and Trau, 2002).

Recently microscale processing techniques have emerged as a potential means to increase the speed of bioprocess design (Lye et al., 2003). Rapid and efficient mixing during liquid addition to individual wells underpins the reproducibility of all bioprocess studies (Micheletti and Lye, 2006). Examples include pH control and nutrient additions during fed-batch operation. Liquid phase mixing times in flat and round bottomed 96-well plates, based on the dispersion of pH indicator dyes, were found to vary between 5 - 500 seconds (Weiss et al., 2002). These values were found to be a function of well geometry, shaking speed and the method of liquid addition. Nealon et al. (2006) demonstrated how rapid jet-mixing can be achieved in static 96-well plates using large addition volume ($\geq 20\%$ of the initial volume). For small additions commonly used in high-throughput assay protocols, insufficient energy is imparted into the liquid resulting in mixing times of the order of minutes or longer.

Shaking of microwell plates is the simplest and most efficient way of promoting liquid mixing. The concept of a critical shaking frequency (N_{crit}), above which the surface tension forces are overcome by the centrifugal force and a significant increase in the fluid motion and oxygen transfer is observed, has been described by Hermann et al. (2003). This is shown in Fig. 1.5. The photographs from left to right were taken with increasing shaking speed. The first is below the N_{crit} . The next two show the increase in the gas-liquid interfacial area responsible for the increase in $k_L a$. The value of N_{crit} can be calculated from Equation 1.3 (Hermann et al., 2003).

$$n_{crit} = \sqrt{\frac{\sigma d_w}{4\pi V_L \rho d_s}} \quad (1.3)$$

where σ = surface tension, d_w = microwell diameter, V_L = liquid fill volume, ρ =

liquid density and d_w = shaker diameter.

Numerous studies on gas-liquid mass transfer in shaken microwell systems have been published. This is due to the predominance of studies on microbial fermentation (Dunst et al., 2002)(Dunst and Wubbolt, 2001)(Dong et al., 2003). In general, reduction in culture volume, increase in shaking diameter, and increasing shaking speed all result in an increase in oxygen transfer rate (OTR) (Dunst et al., 2002)(Dunst and Wubbolt, 2001)(Kency, Zimmermann, Koschke, Anderts, Trutkewitz, Hoopendoren



Figure 1.5: Dimensions of a single well from a 96-DSW microplate (left-hand side) and the influence of increasing shaking speed (600, 1000 and 1400rpm, $V_L = 400 \mu\text{l}$) on fluid motion and gas-liquid interfacial area available for oxygen transfer. Reproduced, with permission, from Micheletti and Lye (2006).

where D = the diffusion coefficient, a_L = the initial specific surface area, Re = Reynolds number, Sc = Schmidt number, Fr = Froude number, α = coefficient that depends on the microplate geometry (0.50 for 24-well plates, 0.04 for 96-well plate and 0.01 for 384-well plates), Bo = Bond number and γ = second coefficient that depends on the microplate geometry (0.03 for 24-well plates, 0.15 for 96-well plates and 0.18 for 384-well plates). The stated accuracy of the $k_L a$ prediction is $\pm 30\%$.

For 96-well plates, OTR obtained in deep, square wells were approximately twice

liquid density and d_s = shaker diameter.

Numerous studies on gas-liquid mass transfer in shaken microwell systems have been published. This is due to the predominance of studies on microbial fermentation (Duetz et al., 2000)(Duetz and Witholt, 2001)(Doig et al., 2002). In general, reduction in culture volume, increase in shaking diameter, and increasing shaking speed all result in an increase in oxygen transfer rate (OTR) (Duetz et al., 2000)(Duetz and Witholt, 2001)(Kensy, Zimmermann, Knabben, Anderlei, Trauthwein, Dingerdissen and Büchs, 2005)(Kensy, John, Hofmann and Büchs, 2005). For 96-well plates, k_La values of between 130 and 188 h^{-1} have been reported under conditions suitable for microbial cell growth, which are similar to those reported for stirred-tank reactors (Duetz et al., 2000)(John et al., 2003). Also in 96-well format, a k_La of 0.9 h^{-1} has been reported under conditions suitable for growth of CHO cells (Deshpande and Heinzle, 2004).Kensy, Zimmermann, Knabben, Anderlei, Trauthwein, Dingerdissen and Büchs (2005) quantified the k_La in shaken 48-well plates and reported values of up to 1,600 h^{-1} . They stated that the well format had superior oxygen transfer rates to both 96-well plates and shake flasks. In 24-well plates, k_La values of between 75 and 250 h^{-1} have been reported (Kensy, John, Hofmann and Büchs, 2005). Doig et al. (2005) have measured k_La and used dimensional analysis to establish a first correlation (Equation 1.4) for predicting k_La in shaken microplates.

$$k_La = 31.35Da_iRe^{0.68}Sc^{0.36}Fr^xB_o^y \quad (1.4)$$

where D = the diffusion coefficient, a_i = the initial specific surface area, Re = Reynolds number, Sc = Schmidt number. Fr = Froude number, x = coefficient that depends of the microplate geometry (0.86 for 24-well plates, 0.64 for 96-well plate and 0.51 for 384-well plates), Bo = Bond number and y = second coefficient that depends on the microplate geometry (0.03 for 24-well plates, 0.15 for 96-well plates and 0.18 for 384-well plates). The stated accuracy of the k_La prediction is $\pm 30\%$.

For 96-well plates, OTR obtained in deep, square wells were approximately twice

those obtained in round wells (Duetz and Witholt, 2004). Similarly, Hermann et al. (2003) showed a significant improvement in interfacial area and OTR using deep, square wells compared to standard round wells. It is thought that the square wells disrupt the flow and promote more turbulent mixing (Hermann et al., 2003)(Duetz and Witholt, 2004).

Despite this progress, knowledge of the basic fluid mechanics in shaken microwells is still far from complete. For example, although the Reynolds number has been published for some microwell systems (Weiss et al., 2002), information on how it relates to laminar and turbulent flow regimes is still lacking. Understanding the engineering environment in microwell systems will ultimately underpin their use in bioprocess studies, ensuring the generation of reproducible, quantitative and scalable information. With regard to this latter point, two recent studies have shown good quantitative agreement between *E. coli* fermentation kinetics obtained in microwells and STR format. In both studies, matched $k_L a$ was used as a basis for scale-translation (Micheletti et al., 2006)(Ferreira-Torres et al., 2005).

Evaporation from microwells has been shown to be a problem, particularly for slow growing organisms such as mammalian and insect cells (Girard et al., 2001)(Bahia et al., 2005). However this can be overcome by using a suitable membrane or closure on the top of the plate (Duetz et al., 2000). Careful selection of membranes or an enclosure is required for a particular application to ensure sufficient oxygen permeability yet minimise evaporation. Zimmermann et al. (2003) describe rapid techniques to measure the oxygen permeability and water loss for a particular microwell-membrane combination.

The ultimate goal for microscale bioprocessing techniques would be to apply the approach to as many unit operations as possible in a given bioprocess sequence. This information would either directly mimic larger scales of operation or provide insight into key scale-up issues or process options. Furthermore, important interactions be-

tween steps could be captured, for example fermentation and primary recovery. To date, microbial fermentation has been the most studied of all microwell unit operations (Duetz et al., 2000)(Doig et al., 2002)(Micheletti et al., 2006)(Ferreira-Torres et al., 2005) In general, good agreement is seen in terms of biomass growth and product titres compared with commonly used laboratory formats. Work on the cultivation of yeast (Kensy, Zimmermann, Knabben, Anderlei, Trauthwein, Dingerdisen and Büchs, 2005)(Jansen et al., 2003), filamentous organisms (Minas et al., 2000)(Elmahdi et al., 2003), insect cells (Bahia et al., 2005) and immobilisation of enzymes (Brandt et al., 2006) in microwell format has also been reported. In contrast, little work has focused on suspension-adapted mammalian cells. To date, just two studies (Girard et al., 2001)(Strobel et al., 2001) have been published. The former investigated the potential of shaken 12-well plates for the development and optimisation of a transient transfection process in CHO cells. Compared to the titre from a lab scale STR, two-fold more protein was achieved in microwell plates. In addition, they reported that evaporation from the microwells was more significant at the edges leading to systematic errors in the data. The second study by Strobel et al. (2001) investigated the potential of substituting a shake flask with a 96-deep well plate for media development. Using design of experiment techniques to assess the data; growth and protein production data from the two geometries were accepted as equivalent. However, both studies failed to perform an engineering study to understand the underlying mixing and mass transfer environment. To enable predictive scale-up of microwell data, it will be first necessary to establish how key parameters such as the volumetric oxygen mass transfer coefficient (k_{La}) and shear rate vary with agitation and well fill volume.

To improve fermentation performance, modifications to standard microwell plates have been made. One such approach has been to improve the control of microwell environments by invoking, for example, pH control. During microwell fermentations of *Saccharopolyspora erythraea* CA340 this led to significant improvements in product synthesis and yield (Elmahdi et al., 2003). Another strategy has been

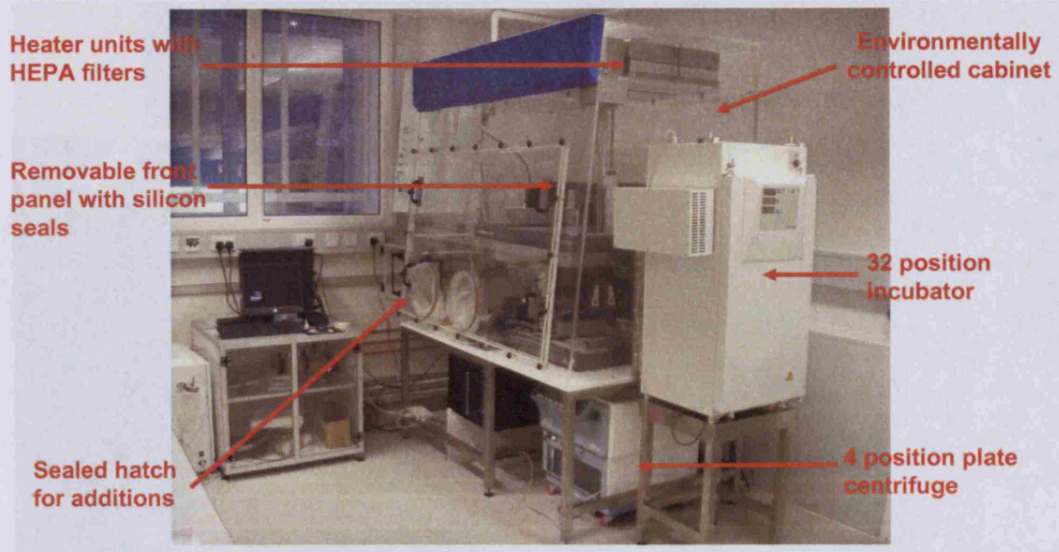
to promote better oxygen mass transfer. Puskeiler et al. (2005) have developed a novel gas-sparging impeller that provides k_La values of up to 1440 h^{-1} while Doig et al. (2005) created a novel microplate bubble column based on a 48-well plate. k_La values of up to 220 h^{-1} were reported.

To date, there has been little work on downstream processing operations in microwell format. Jackson et al. (2006) have established an automated microscale normal flow filtration technique able to quantitatively evaluate the influence of upstream processing conditions on the microfiltration behaviour of *E. coli* fermentation broths. Similarly, Chandler and Zydney (2004) studied membrane resistance during the filtration of baker's yeast under varying conditions using a custom 96-well filter plate. The data obtained was in good agreement with results from larger-scale filters. In addition to microscale approaches to primary recovery, advances are being made to miniaturise chromatography (Mazza et al., 2002)(Rege et al., 2004). This is a particularly difficult operation to mimic in microwell formats owing to the dynamics of product binding and influence of the phase flow rate on mixing and mass transfer. Therefore, these studies have tended to focus on the screening of suitable resins and the selection of binding conditions (Rege et al., 2006).

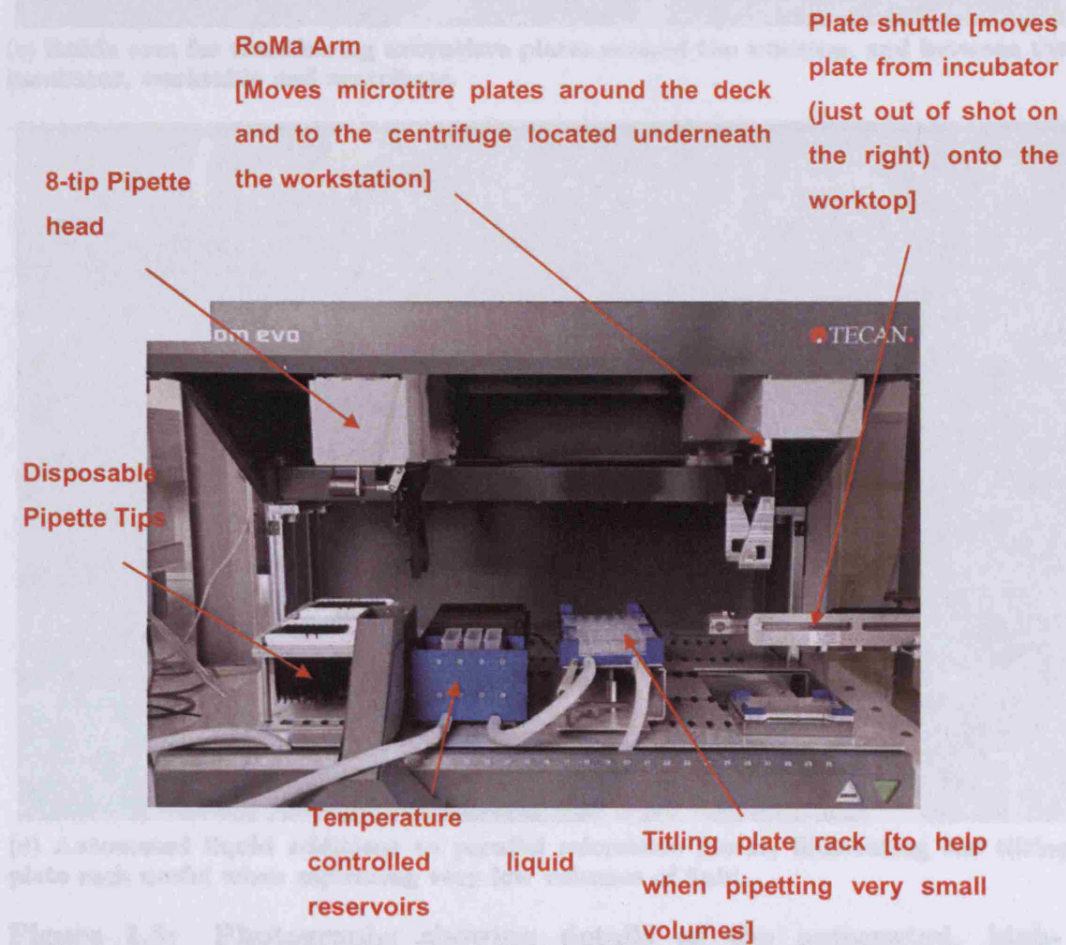
Once the procedure for a microwell experiment has been established, microplate handling can be automated using robots with liquid-handling systems and integrated centrifuges, incubators, plate readers and flow cytometers (Lye et al., 2003)(Harms et al., 2002)(Fig. 1.5). Such robots are currently available through commercial suppliers such as Tecan⁴ and Perkin Elmer⁵. Research here has tended to focus on the automation of individual unit operations such as fermentation (Doig et al., 2002) and filtration (Jackson et al., 2006). However, recently studies have looked at automating whole process sequences, such as the interaction between fermentation, induction and bioconversion (Ferreira-Torres et al., 2005). The sequence of events in this last study are shown in Fig. 1.6.

⁴www.tecan.com

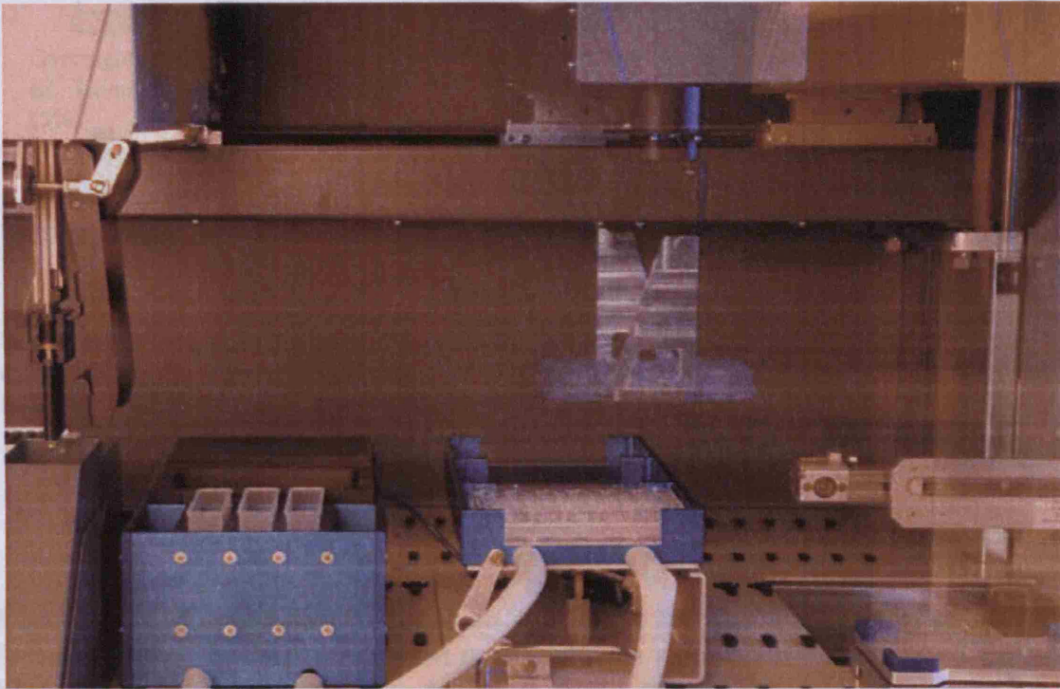
⁵www.perkinelmer.com



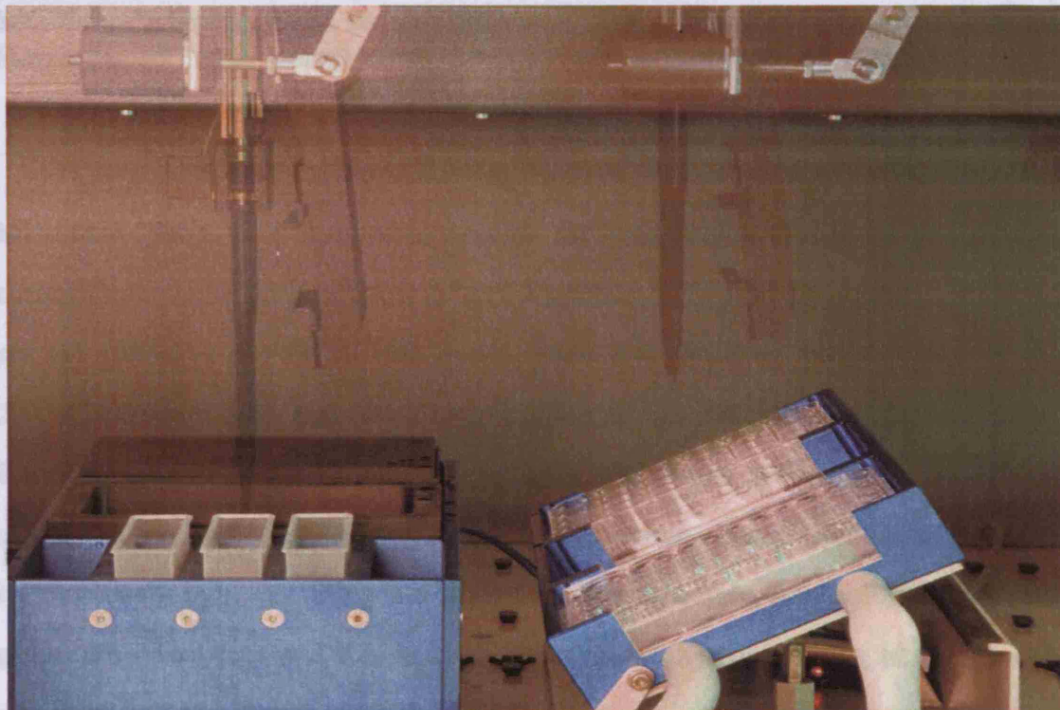
(a) Layout of the automated, high-throughput microwell platform used at UCL for stem-cell processing.



(b) Typical features of a liquid handling robot including pipette head, RoMa arm and plate shuttle.



(c) RoMa arm for transferring microtitre plates around the worktop, and between the incubator, worktable and centrifuge.



(d) Automated liquid additions to parallel microtitre plates, illustrating the tilting plate rack useful when aspirating very low volumes of fluid.

Figure 1.5: Photographs showing details of the automated, high-throughput microwell platform currently used at UCL for stem-cell processing.

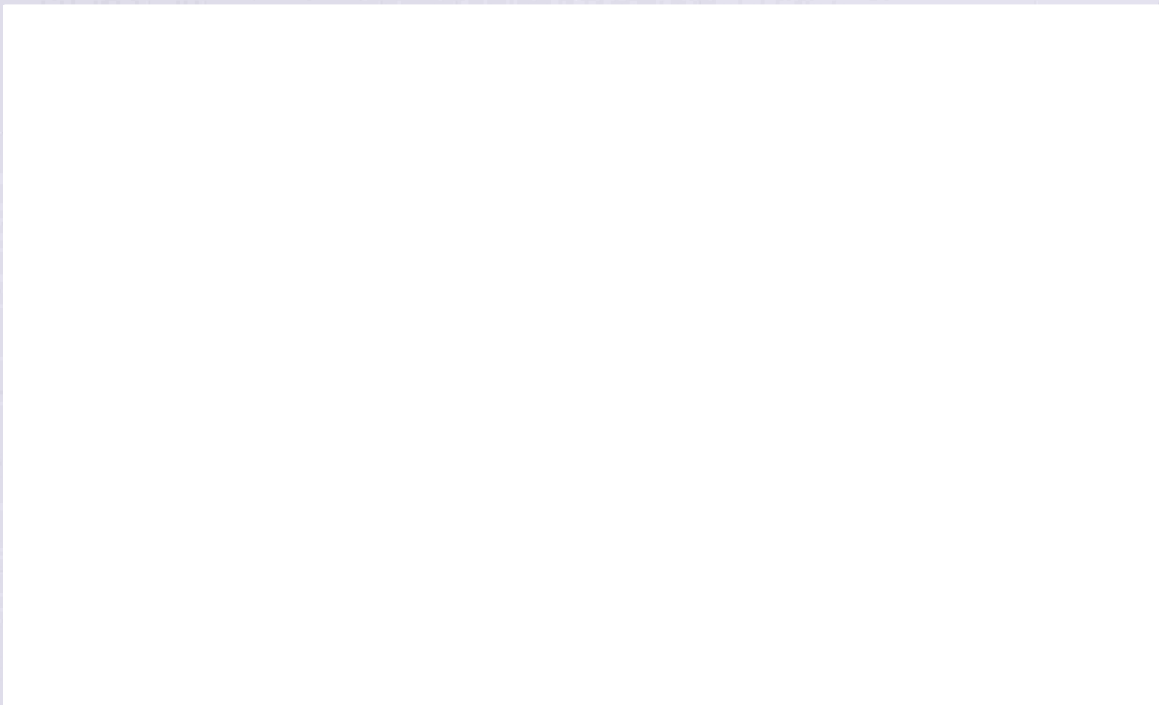


Figure 1.6: Automated microscale sequence for the evaluation of linked fermentation and bioconversion processes. A recombinant *E. coli* TOP10 biocatalyst was first produced at two different carbon source concentrations. The specific Baeyer-Villiger monooxygenase activity of whole cells from each fermentation process was then determined for three different ketone substrates, each as two different initial substrate concentrations. Reproduced, with permission, from Ferreira-Torres et al. (2005).

Microtitre plates with integrated sensors are presently available on the market through companies such as PreSens⁶ and Applikon⁷. Typical parameters measured are pH (Weiss et al., 2002)(John et al., 2003) and dissolved oxygen (John et al., 2003)(Deshpande and Heinzle, 2004)(Guarino et al., 2004)(Kensy, Zimmermann, Knabben, Anderlei, Trauthwein, Dingerdissen and Büchs, 2005)(Kensy, John, Hofmann and Büchs, 2005). Samorski et al. (2005) developed a non-invasive technique to monitor the light scattering and NADH fluorescent of microbial cultures in 96 well plate. The data captured was used to distinguish differences in lag phase, growth velocities and inoculation densities during the screening of clonal libraries.

More recently there has been growing interest in the use of microfluidic devices for

⁶www.presens.de/html/start.html

⁷www.applikon-bio.com/cgi-bin/applikonbio/basis-micro-bioreactor-u24

high-throughput bioprocess development. This technology permits a further reduction in culture volume to the micro-litre level. Already groups have looked at the culture of microbial (Zhang, Szita, Boccazzi, Sinskey and Jensen, 2005)(Zanzotto et al., 2006)(Szita et al., 2005)(Balagadde et al., 2005) and animal cells (Schulz et al., 2002)(Lee et al., 2006) on microfluidic chips, often with integrated sensors for pH, DOT and biomass monitoring. The advantages of using microfluidic chips to obtain bioprocess data are the greatly reduce working volume, their compatibility with standard laboratory automation equipment⁸, and precise control of their microenvironment through rapid heat and mass transfer (Lee et al., 2006). At present there is no engineering basis to relate microfluidic culture conditions with large-scale bioreactors. More importantly, the high surface area to volume ratio of these systems could lead to problems with quantification and reproducibility.

1.5 Aim and Objectives of Thesis

The overall aim of this thesis is to establish a potentially automated, microwell approach for rapid cell culture process development. As described in Section 1.4.4, microwell cell culture was chosen because the advantages of such an approach would include :

- a reduction in the quantity of often expensive media required for cell culture process development.
- the potential to operate automated whole process sequences in microwell format.
- a more rapid translation of processes from discovery to pilot plant scale.
- the rapid generation of design data for use in process or economic models.

The culture of mammalian cells in these systems is also poorly described in the literature and yet as described in Section 1.3.1 they are now the expression system

⁸www.bioprocessors.com

of choice for therapeutic antibody production. Consequently the production of IgG in hybridoma cell cultures will be examined. The specific objectives are described below:

- Initially, it will be important to characterise the engineering environment in shaken microwells under conditions that are relevant to the culture of suspension-adapted mammalian cells. This will be covered in Chapter 3.
- Next, characterise hybridoma growth, antibody production and metabolism in batch shaken microwell cultures within the characterised engineering environment. This will allow the impact of the fluid hydrodynamics on culture performance to be understood and also help define optimal culture conditions. This work will be described in Section 4.
- Finally, make an initial attempt at scaling-up a microwell culture to shake flasks and a bench-scale stirred-tank reactor using matched average energy dissipation as a basis for scale-translation. This is covered in Section 5.

Chapter 2

Materials And Methods

2.1 Cell Culture

2.1.1 Cell Line Description and Medium Formulation

Two suspension adapted cell-lines were used in this work. A VPM 8 hybridoma cell line (ECACC, Salisbury, UK: Catalogue number: 93113024) expressing IgG1 (directed against a 27 kDa light chain of ovine immunoglobulin) and a null CHO-S cell-line (Invitrogen, Paisley, Scotland).

Hybridoma cells were cultured in RPMI-1640 medium supplemented with 10% (v/v) fetal bovine serum (FBS), 1% (v/v) sodium pyruvate and 1% (v/v) 200 mM L-glutamine. For cultures conducted in the stirred-tank reactor, the media was supplemented with 1 g l⁻¹ Pluronic F68 (Invitrogen, Paisley, UK) and 6 mg l⁻¹ silicone antifoam to allow direct sparging. Unless stated, all media components were purchased from Sigma (Poole, UK) and were of the highest purity available. The CHO cell line was cultured in CHO-S-SFM II, a proprietary serum-free, low protein media (Invitrogen, Paisley, UK).

2.1.2 Creation of Cell Bank

Cells were cultured in 250 ml shake flasks (50 ml) until 48 hours, transferred into 50 ml centrifuge tubes and centrifuged at 200g for 5 minutes. The cells were resuspended

at a density of 1×10^7 viable cells ml^{-1} in 1 ml of freezing media (see below) and transferred into 1 ml sterile cryovials (Fisher, Loughborough, UK). These cryovials were loaded into a Nalgene Mr Frosty freezing container (Sigma, Poole, Dorset, UK) and placed in a -70°C freezer. After 24 hours, the vials were transferred to cryocanes and stored in a liquid nitrogen dewar.

Hybridoma cells were frozen in 90% (v/v) FBS (Sigma, Poole, Dorset, UK) and 10% (v/v) DMSO. CHO-S cells were frozen in 50% (v/v) fresh growth medium and 50% (v/v) conditioned growth medium (day 2 to 4 cell conditioned media collected from CHO-S cultures during subculture procedure) and DMSO to a final concentration of 7.5% (v/v). DMSO was purchased from Sigma (Poole, Dorset, UK). Both freezing media were prepared immediately before use. In addition, they were filter sterilised and chilled to 4°C .

2.1.3 Revival of Cells From Liquid Nitrogen Storage

Hybridoma cells were removed from liquid nitrogen and rapidly thawed in a 37°C water bath. The liquid contents of the vial were then transferred into a sterile 15 ml centrifuge tube followed immediately by 9 ml of cold (4°C) RPMI-1640 media added drop-wise. The tube was centrifuged at 200g for 5 minutes. Following removal of the supernatant, the pellet was resuspended in 15 ml of pre-warmed (37°C) RPMI media and then transferred into a 125 ml shake flask. This flask was then placed on a shaker platform (IKA KS 260 control, Fisher Scientific, Loughborough, UK) (100 rpm) in a 37°C incubator containing a humidified atmosphere of 5% CO_2 (v/v) in air.

Likewise, CHO-S were removed from liquid nitrogen and rapidly thawed in a 37°C water bath. The contents of the cryovial was transferred into a 125 ml shake flask containing 27 ml of pre-warmed CD-CHO medium supplemented with 8 mM L-glutamine and 10 ml l^{-1} of HT supplement. This flask was incubated in a 37°C incubator containing a humidified atmosphere of 5% CO_2 (v/v) in air on an orbital shaker platform (IKA KS 260 control, Fisher Scientific, Loughborough, UK) rotat-

ing at 130 rpm.

2.1.4 Shake Flask Cultures

Cells were routinely maintained in plastic shake flasks (Corning 125 ml or 250 ml polycarbonate Erlenmeyer flasks with vent caps; Sigma, Poole, UK) at volumes between 25 and 50 ml. These were kept on an orbital shaker in a 5% (v/v) CO₂, 37°C incubator. The shaking platform was set to agitate at either 100 rpm (hybridoma) or 130 rpm (CHO-S). Cells were seeded at a density of 1x10⁵ cells ml⁻¹ (hybridoma) or 2x10⁵ cells ml⁻¹ (CHO) and sub-cultivated every 2-3 days.

2.1.5 Shaken Microwell Cultures

Three individual microwell formats were used in this work:

1. 96-deep, square wells (96-DSW) (ABgene, Epsom, Surrey, UK) (Fig. 2.1).
2. 24-standard round wells (24-SRW (PS)). The plate was fabricated from polystyrene. (TPP, Trasadingen, Switzerland) (Fig. 2.1).
3. 24-standard round wells (24-SRW (ULA)). All wells were coated with an Ultra-low attachment layer to inhibit cell and protein attachment (Corning, New York, USA) (Fig. 2.1)

Two baffle configurations, single-wall (Fig. 2.2) and double-wall (Fig. 2.2), were designed and fitted into the wells of a 24-SRW (ULA) plate (Fig. 2.2). All baffles were 1.5 mm x 1.5 mm perspex cylinders that spanned the complete height of the wells. Baffles were affixed to the walls using silicone glue. Before use, the baffled microwell plate was sterilised by gamma irradiation (Isotron, Swindon, UK).

Cells were seeded at a density of 1x10⁵ cells ml⁻¹ (hybridoma) or 2x10⁵ cells ml⁻¹ (CHO) using diluted mid-exponential (48 hr) culture. 24-SRW plates were inoc-

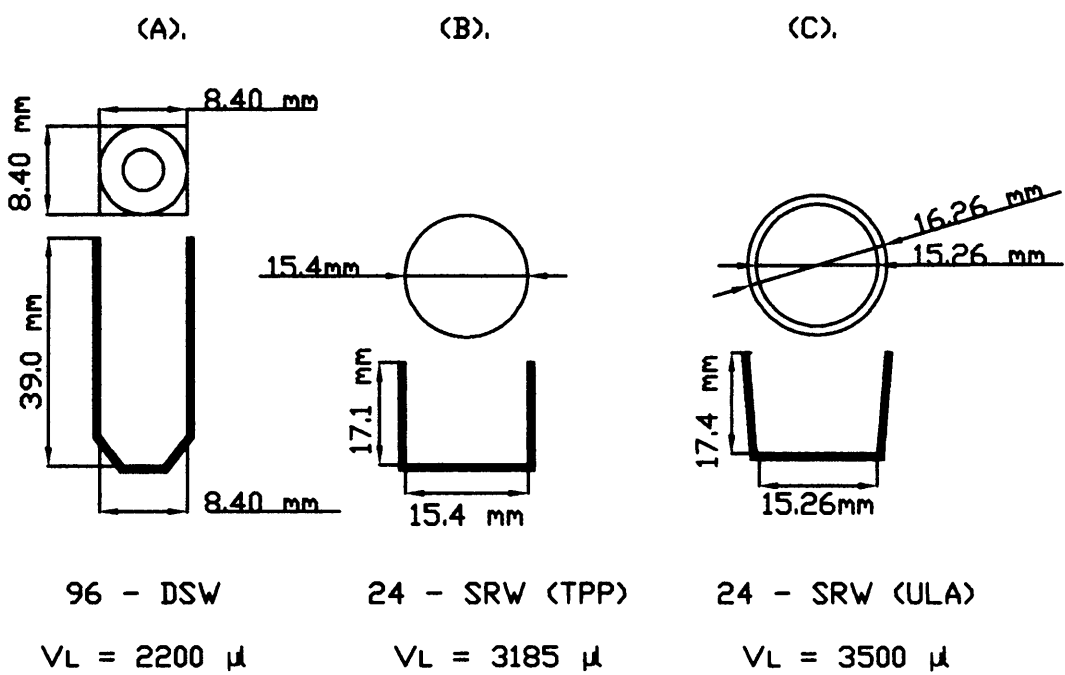


Figure 2.1: Schematic diagram of individual microwell formats as described in Section 2.1.5: (a) 96-deep square well format (96-DSW); (b) 24-standard round well format (24-SRW (PS)); (c) 24-standard round well format with ultra-low attachment coating (24-SRW (ULA)). V_L represents the total well volume.

ulated using 1 - 2 ml sterile, serological pipettes while the 96-SRW plate was inoculated using a 12-channel pipette, sterile 300 μl Eppendorf biopur tips (VWR, Lutterworth, Leicestershire, UK) and a Corning reagent reservoir (Sigma, Poole, Dorset, UK). Before inoculation of a 24-SRW (ULA) plate, the surface coating was conditioned by filling the wells with cell-culture media and then incubating at 37°C for 1 hr; prior to inoculation this media was aspirated. All microwell cultures were covered with a Diversified Biotech Breathe-easy membrane (Sigma, Poole, Dorset, UK) to minimise evaporation over extended periods of culture. These cultures were incubated in a 37°C incubator containing a humidified atmosphere of 5% CO₂ (v/v) in air on an orbital shaker platform (Heidolph rotamax 120, Wolf labs, York, UK) (shaking diameter (d_S) = 20mm) rotating at speeds between 120 - 250 rpm. Well fill volumes (V_L) were between 800 μl and 2000 μl for 24-SRW plates and 300 μl - 600 μl for the 96-DSW plate. For analysis (Section 2.8), the entire contents of triplicate sacrificial wells were removed. Evaporation of the culture was monitored throughout by weighing the sample in microcentrifuge tubes of predetermined weight. All culture data was corrected for evaporation losses using the ratio between initial volume and the measured volume at each time point in order to allow direct comparison with shake flask and STR culture data where no evaporation was considered to occur.

Before each experiment, the temperature of the liquid contents of each well was calibrated to 37°C by manipulation of the incubator chamber temperature. A microwell plate was filled with distilled water to the required working volume, covered with a membrane and shaken at the correct speed. Fluid temperature was monitored overnight using a thermocouple. The incubator chamber temperature was then adjusted to achieve 37°C in each well.

Unless stated, all microwell cultures were performed in triplicate. All data was averaged and standard deviations were calculated.

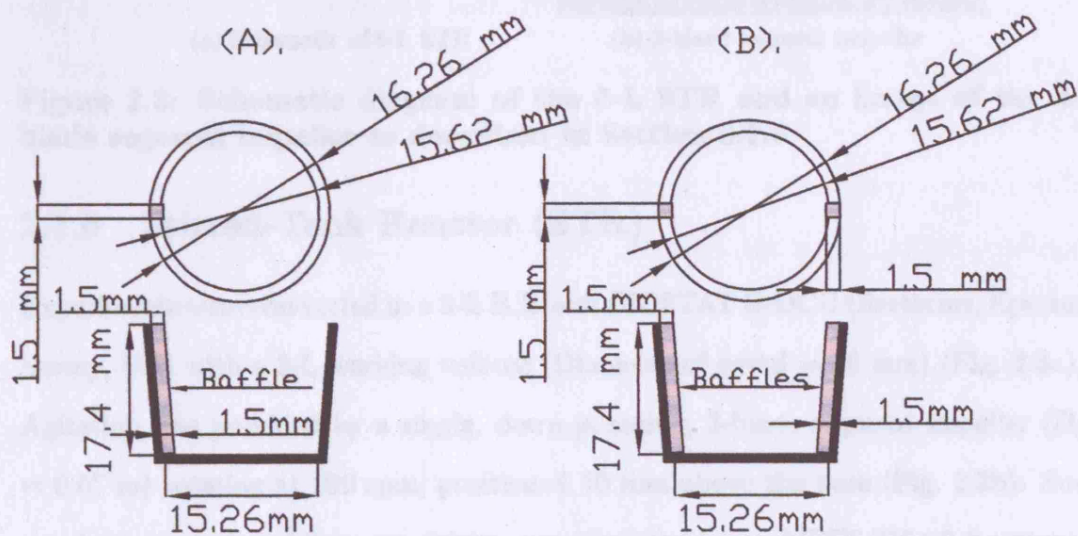
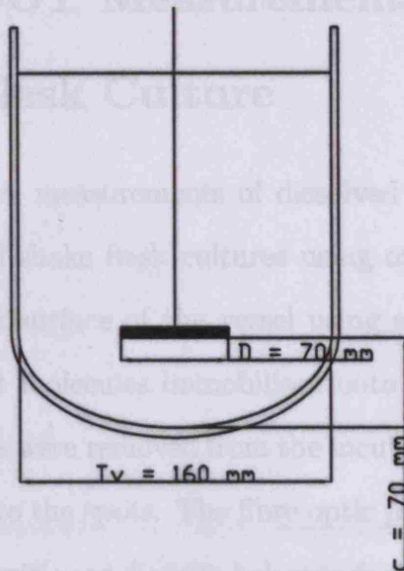
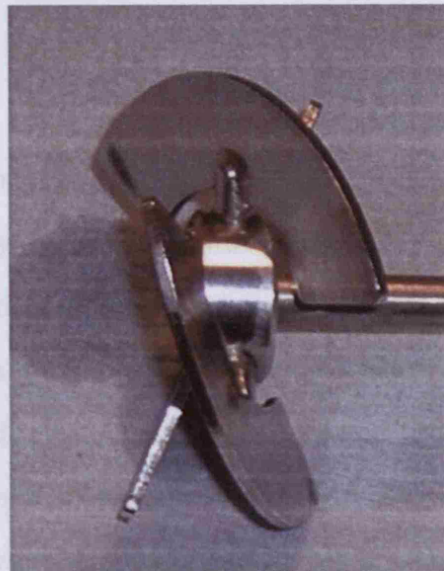


Figure 2.2: Schematic diagram of baffled microwell configuration as described in Section 2.1.5. (a) Single wall baffle configuration; (b) double wall baffle configuration. 24-standard ultra-low attachment plates (24-SRW (ULA)) were fitted with both baffle designs.



(a) Schematic of 5-L STR



(b) 3-blade segment impeller

Figure 2.3: Schematic diagram of the 5-L STR and an image of the 3-blade segment impeller as described in Section 2.1.6

2.1.6 Stirred-Tank Reactor (STR)

Experiments were conducted in a 5-L B.Braun BIOSTAT B-DCU (Sartorius, Epsom, Surrey, UK) with a 3-L working volume (Diameter of vessel = 16 mm) (Fig. 2.3a). Agitation was provided by a single, down-pumping, 3-blade segment impeller ($D_i = 0.07$ m) rotating at 200 rpm, positioned 70 mm above the base (Fig. 2.3b). Supervisory control and data acquisition was managed by an MFCS/Win 2.0 system. Temperature was controlled at 37°C using an electrical heating blanket. pH was controlled at 7.2 ± 0.1 using pure CO₂ in the inlet gas. The dissolved oxygen tension (DOT) was maintained at $30\% \pm 1\%$ of saturation using air, oxygen and nitrogen. Headspace aeration was found to be sufficient for the first 48 hours of culture, thereafter intermittent direct sparging was necessary; a gas flow rate of $100 \text{ cm}^3 \text{ min}^{-1}$ was used throughout. A ceramic, microporous sparger was used for all cultures. The vessel, containing 3-L of distilled water, was sterilised on a fluids cycle at 121 °C for 20 minutes; before inoculation this water was aseptically removed. Cells were seeded at a density of 1×10^5 cells ml^{-1} using diluted mid-exponential (48 hr) culture. The STR cultures (Section 5.3) were performed in duplicate.

2.2 DOT Measurements in Microwell and Shake Flask Culture

Non-invasive measurements of dissolved oxygen tension were made in shaken microwell and shake flask cultures using oxygen sensor spots. The spots, affixed to the bottom surface of the vessel using silicone glue, consisted of oxygen sensitive fluorescent molecules immobilised onto a glass support. To make measurements, the cultures were removed from the incubator and clamped onto a retort stand to allow access to the spots. The fibre optic probe, attached to a Fibrox 3 oxygen meter, was then positioned directly below each spot to excite the oxygen sensitive molecules and record the subsequent fluorescence (Fig. 2.4). Fluorescence measurements were converted into the equivalent DOT reading using Oxyview software, installed on a PC. Before each culture, dissolved oxygen tension in the microwell plates was calibrated using air and pure nitrogen. This plate was then sent to be gamma-sterilised (Isotron, Swindon, UK). The oxygen sensitive spots, the Fibrox 3 oxygen meter and its fibre optic probe; and oxyview software were purchased from PreSens (Regensburg, Germany).

2.3 Description of Liquid Phase Hydrodynamics

Predictions of the liquid-phase hydrodynamics in shaken microwells, shake flasks and STRs were made using Reynold's number (Re), Froude number (Fr), Phase number (Ph) and the critical shaking frequency (N_{crit}); the results of which are discussed in Section 3.2 and 2.6.2. Equations 2.1, 2.2, 1.2 and 1.3 were used to calculate the respective values.

$$Re = \frac{\rho N d^2}{\mu} \quad (2.1)$$

$$Fr = \frac{(2\pi N)^2 d}{2g} \quad (2.2)$$

where ρ = liquid density, μ = liquid viscosity, N = shaking speed or impeller stirring speed, d = characteristic length (see below for explanation), g = acceleration due to gravity ($= 9.81 \text{ m s}^{-2}$). Liquid properties were assumed to be those of water at 37°C . The characteristic length (d) was taken as the microwell diameter ($d_w = 15.94 \text{ mm}$), maximum inside diameter of the shake flask ($d_f = 3.0 \text{ cm}$) and the impeller diameter ($D_i = 7.0 \text{ cm}$) (Fig. 2.3a). The original diameter of the shaker chamber (d_s) was 19 mm .

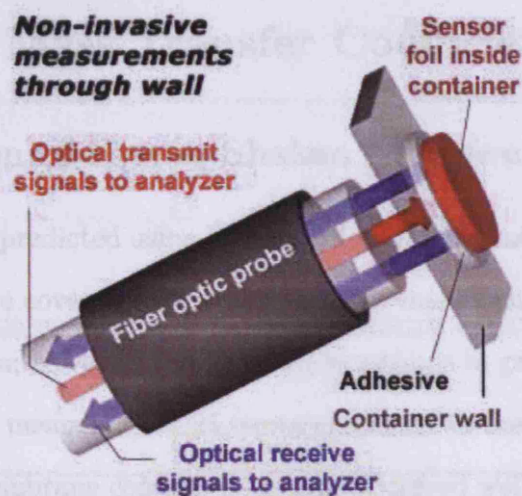


Figure 2.4: Non-invasive measurements of dissolved oxygen in shaken microwell and shake flask cultures using a PreSens (Regensburg, Germany) fibrox 3 meter and oxygen sensitive spots. Spots were affixed to the bottom surface of the vessels using silicone glue. Before gamma-sterilisation, the dissolved oxygen tension was calibrated using air and pure nitrogen. Figure reproduced courtesy of PreSens.

were assumed to be those of water at 37°C . Predictions of $k_{L,a}$ in shaken microwell plates are discussed in Section 3.3.

2.4.3 Measurement of $k_{L,a}$ in the Stirred-Tank Reactor

$k_{L,a}$ in the 6-L STR (Section 2.1.6) was measured experimentally using the static gassing-out method discussed by Leppin et al. (2006) and Betts et al. (2006). 3-L of 100mM PBS pH 7.4 at 37°C was used to represent a non-coalescing media. A sparging rate of $100 \text{ cm}^3 \text{ min}^{-1}$ was used in all experiments. Measurements were collected at 50, 150 and 200 rpm. Before measuring $k_{L,a}$, the response



where ρ = liquid density, μ = liquid viscosity, N = shaking speed or impeller stirring speed, d = characteristic length (see below for explanation), g = acceleration due to gravity ($= 9.81 \text{ m s}^{-2}$). Liquid properties were assumed to be those of water at 37°C . The characteristic length (d) was taken as the microwell diameter ($d_w = 15.94 \text{ mm}$), maximum inside diameter of the shake flask ($d_f = 8.0 \text{ cm}$) and the impeller diameter ($D_i = 7.0 \text{ cm}$)(Fig. 2.3a). The orbital diameter of the shaker platform (d_s) was 20 mm .

2.4 Oxygen Mass Transfer Coefficients (k_La)

2.4.1 Prediction of K_La in Shaken Microwells

K_La in microwells was predicted using Equation 1.4. As discussed in Section 2.1.5, all microwell cultures were covered with a breathe-easy membrane to maintain sterility and reduce evaporation; however, they provide resistance to gas exchange. Pickering (2007) experimentally measured a 2.25 times reduction in the k_La of a well covered with a breath-easy membrane compared to the uncovered well. The following physical properties were used in Equation 1.4: orbital shaking diameter (d_s) = 20 mm , microwell diameter (d_w) = 15.94 mm , oxygen diffusion coefficient (D) = $2.69 \times 10^{-9} \text{ m}^2 \text{ s}^{-1}$ (Micheletti et al., 2006), initial air-liquid specific surface area (a_i) = 249.9 m^{-1} and wetting tension (w) = 0.0012 N m^{-1} (Doig et al., 2005). Liquid properties were assumed to be those of water at 37°C . Predictions of K_La in shaken microwell plates are discussed in Section 3.3.

2.4.2 Measurement of k_La in the Stirred-Tank Reactor

k_La in the 5-L STR (Section 2.1.6) was measured experimentally using the static gassing-out method discussed by Lamping et al. (2003) and Betts et al. (2006). 3-L of 100mM PBS pH 7.4 at 37°C was used to represent a non-coalescing cell-culture media. A sparging rate of $100 \text{ cm}^3 \text{ min}^{-1}$ was used in all experiments. Measurements were collected at 50, 150 and 200 rpm. Before measuring k_La , the response

time (τ_p) of the calibrated probe was measured by equilibrating the DOT reading at 100% in air and then rapidly plunging the probe into the STR containing nitrogen gas. The response time was defined as the time taken for the DOT reading to fall to 37% of air saturation and was found to be 20 ± 2 s ($n = 3 \pm 1$ sd) Before each experiment, the DOT probe was calibrated *in-situ* at 100% and 0% of air saturation by sparging air and nitrogen respectively. A typical experiment began by sparging nitrogen to reduce the DOT to 0%, then the gas supply was switched to air and the rise in DOT monitored using the MFCS logging software, described in Section 2.1.6. Fig. 2.4.2 shows the increase in DOT, at 50 and 200 rpm, following the initiation of air sparging. k_La was determined, as discussed by Lamping et al. (2003) and Betts et al. (2006), by entering the τ_p and DOT values into the Marquardt algorithm (Equation 2.3) and solving using Microsoft Excel. All k_La measurements were conducted in duplicate. A mean and standard deviation were then calculated.

$$C_p = \frac{1}{t_m - \tau_p} [t_m \exp(-t/t_m) - \tau_p \exp(-t/\tau_p)] \quad (2.3)$$

where C_p = normalised DOT measured by the probe; $t_m = 1/k_La$ and τ_p = probe response time.

2.4.3 Prediction of k_La in Shake Flasks

The mass transfer coefficient in 250 ml shake flasks was predicted using Equation 2.4. This equation was developed by Gupta and Rao (2003) and takes into account the resistances of the closure and the gas-liquid interface:

$$(k_La)_{eq} = \frac{1}{V_L} \left[\frac{1}{MK} + \frac{1}{V_L k_La} \right]^{-1} \quad (2.4)$$

where: $(k_La)_{eq}$ = equivalent oxygen mass transfer coefficient; V_L = volume of liquid in flask; M = equilibrium constant of oxygen between the gas and liquid phases;

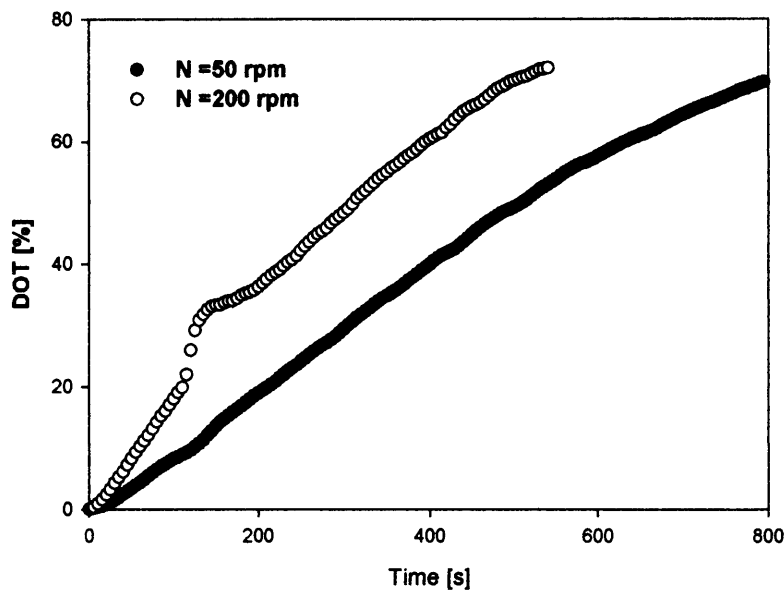


Figure 2.5: Examples of the oxygen uptake curves used to quantify k_La in the 5-L STR described in Section 2.1.6. A fill volume of 3-L (PBS pH 7.4) and sparge rate of $100 \text{ cm}^3 \text{ min}^{-1}$ were used at the two agitation speeds (N): 50 and 200 rpm. Nitrogen gas was used to reduce the DOT reading to 0 %, following this, the gas supply was switched to air and the subsequent rise in DOT captured using MCFS data-logging software. For each curve, the k_La was determined using the Marquardt algorithm described in Section 2.4.2.



Figure 2.6: Perspex mimic of a single well for a 24-SRW (ULA) plate used for mixing time studies. Dimensions of the well were the same as the actual wells from the microplate. The faces were square to avoid image distortion during high-speed video footage.

k_{La} = interfacial oxygen mass transfer coefficient and k = oxygen mass transfer resistance due to the closure.

In the estimation of k_{La} , M was assumed to be 41 (Gupta and Rao, 2003). The closure of the shake flask was assumed to be a milk filter with $k = 5.7 \times 10^{-3} \text{ m}^3 \text{ h}^{-1}$ (Gupta and Rao, 2003). An interfacial oxygen mass transfer coefficient (k_{La}) of 10 h^{-1} was assumed. This value was predicted for a 250 ml shake flask, operating at 100 rpm with a 100 ml fill using CFD (Zhang, Williams-Dalson, Keshavarz-Moore and Shamlou, 2005).

2.5 Liquid Phase Mixing Time Characterisation

All microwell mixing studies were conducted in a perspex mimic of a single well from a 24-SRW (ULA) plate (Fig. 2.5). The mimic was designed with square faces to avoid distortion of video images, in addition, it was mounted on a large perspex block to improve stability during shaking.

All liquid additions to the wells were made using a 10 μl pipette tip held directly over the center of the well using an expanded polystyrene cap. All experiments were conducted on an orbital shaker platform with a shaking diameter (d_s) of 20 mm. To make an addition, the 10 μl tip was connected to a 10 μl Gilson pipette, held stationary and vertically above the well with a retort stand and clamp, using PEEK tubing. The tip was removed from the cap, loaded with liquid, then replaced into cap. The liquid was then aspirated into the liquid in the well when required.

Mixing times studies in the 5-L STR were also performed. All liquid additions to the STR were made from the same position, located 2 cm under the liquid surface (Hadjiev et al., 2006). Additions were made in \approx 2-3 s using a serological pipette .

Images of the mixing kinetics were captured using a NAC HSV 500 digital high speed video system (NAC Image technology, Simi Valley, CA, USA). Images were recorded at a speed of 250 frames per second. The images were transferred to a PC and converted to TIFF format. Furthermore, to reduce memory requirements, TIFF files were converted into JPEG format.

To initially visualise the mixing of a small liquid addition into the liquid content of a well, 1% (v/v) inert blue food dye (Supercook, Leeds, UK) was injected into water. This dye has been shown not to significantly alter the physical properties of the fluid (Nealon et al., 2006). Each flow visualisation experiment was performed in triplicate.

Iodine decolourisation using sodium thiosulphate was used to actually quantify liquid phase mixing times (Nienow et al., 1996). Upon addition of thiosulphate, iodine solution changes from an orange colour to completely colourless. The duration of this colour transition was defined as the mixing time. 1% (v/v) additions of 1.8 M sodium thiosulphate were made to 0.5 M iodine solution using the apparatus described above. Both reagents were purchased from Sigma (Poole, Dorset, UK).

The progression of the decolourisation was monitored using a stop watch and a digital video camera. To estimate mixing times using the video footage, the number of frames between addition and complete decolourisation were divided by the frame speed. All mixing time measurements were made in triplicate. Values were averaged to obtain a mean and standard deviation.

For 24-SRW (ULA) plates, both the flow visualisation and mixing time quantification experiment were performed for 800, 1000 and 2000 μl fill volumes, over the range of shaking speeds 0 - 300 rpm. For the 3-L STR, both experimental procedures were conducted using a 3-L fill volume and stirrer speed ranging from 50 - 250 rpm. The vessel remained unaerated throughout.

2.6 Characterisation of Energy Dissipation Rates

2.6.1 Prediction of Energy Dissipation Rates in Shake Flasks

Energy dissipation in shake flasks was predicted using Equation 1.1, as discussed in Section 1.4.3. Predictions were made for a 250 ml shake flask with a maximum inner diameter (d_f) of 8.0 cm, shaken on a orbital shaking plate with diameter (d_s) of 10 mm. The properties of water at the working temperature of 37°C were assumed. C_3 was 1.94 (Büchs et al., 2000a).

For experiments investigating the effect of energy dissipation rate on cell performance (Section 5.2), diluted culture in 250 ml shake flasks was incubated in a 37°C incubator containing a humidified atmosphere of 5% CO_2 (v/v) in air. To produce mean energy dissipation rates (P/V) of 0, 40 and 810 W m^{-3} , the following conditions were used: 100 ml (liquid fill volume) and 0 rpm; 100 ml and 120 rpm; and 20 ml and 250 rpm respectively. The orbital shaker platform had a diameter of 10 mm. Samples were taken every 12 - 24 h.

2.6.2 CFD Modelling of Shaken 24 Well Plates

The volume of fluid (VOF) method was used to solve the transient forms of the Navier-Stokes equation that govern the motion of the gas and liquid phases. In addition, the continuum-surface-force (CSF) model was invoked to model surface tension acting at the gas-liquid interface. All equations were solved using the commercial software packages CFX 4 and CFX 5 (AEA Technology, Didcot, Berks, UK). Full details of this method can be found in Zhang, Williams-Dalson, Keshavarz-Moore and Shamlou (2005).

All CFD models presented in this thesis were developed and analysed by Dr. Hu Zhang.

2.6.3 Power Input to a 5-L STR

Power input to the 5-L STR was measured using an air-bearing and pressure transducer as shown in Fig. 2.7. The impeller was held in a position identical to that used to culture cells. 3-L of water was used to simulate cell culture media. Changes in the pressure exerted on the transducer by the air-bearing's cue were logged on a PC using Winso software (HEL Ltd, Barnet, Herts, UK). Before all power measurements, the transducer was calibrated at 0 g and 1.3 g. Power input through stirring manifests itself as pressure changes on the transducer. For each experiment, a step-change in the mass reading from the transducer was obtained following the commencement of agitation. Changes in the mass exerted were converted to a force using Equation 2.5:

$$F = mg \quad (2.5)$$

where F = force, m = mass and g = acceleration due to gravity (9.81 m s^{-2}).

This derived force value was then converted to torque using Equation 2.6:

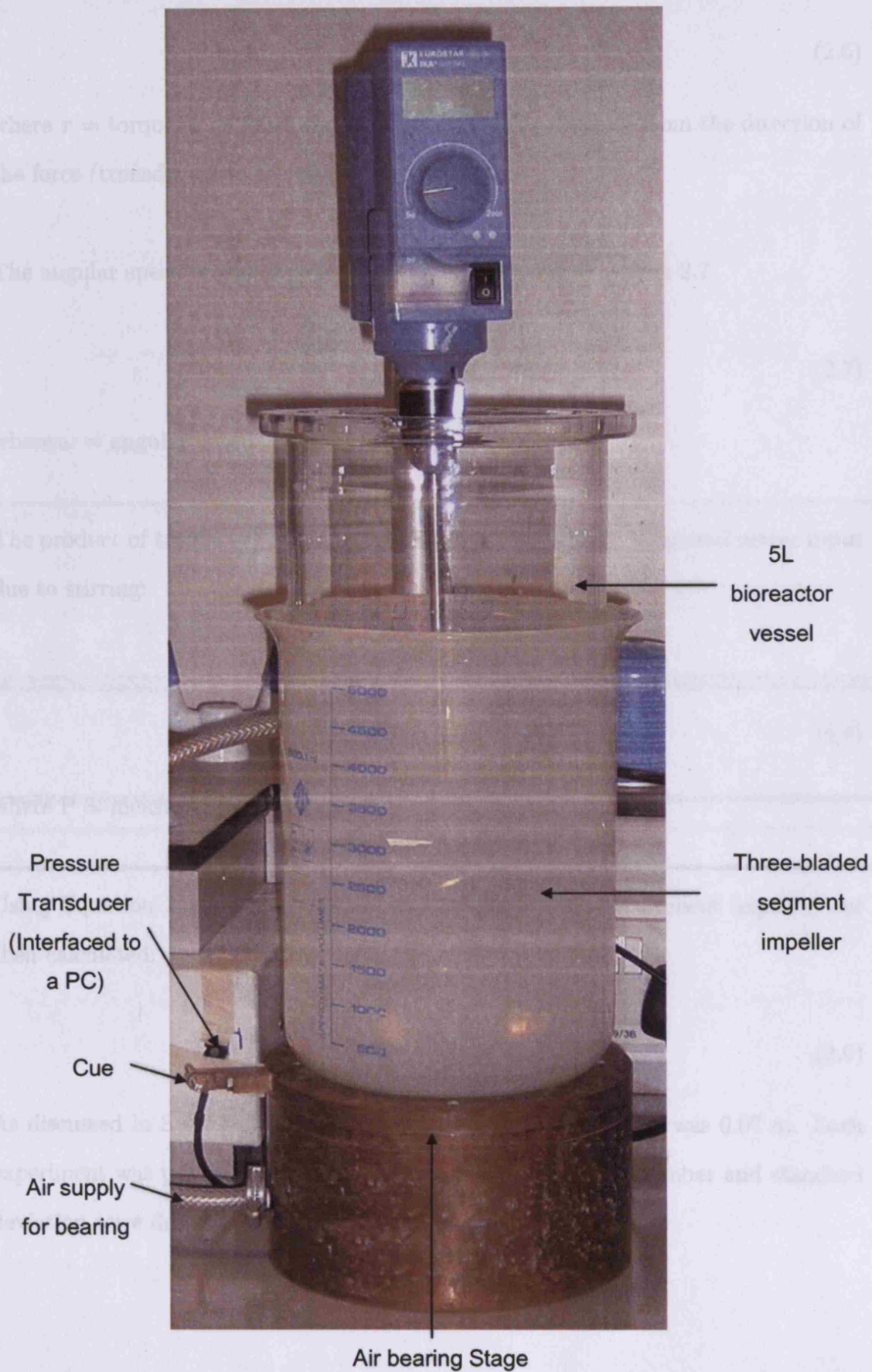


Figure 2.7: Experimental set-up to measure power input to a 5-L STR as described in Section 2.6.3.

$$\tau = FR \quad (2.6)$$

where τ = torque, F = force and R = perpendicular distance from the direction of the force (transducer) to the pivot (14 cm).

The angular speed of the impeller was calculated using Equation 2.7:

$$\omega = \frac{2\pi}{60}N \quad (2.7)$$

where ω = angular speed of stirrer and N = stirrer speed.

The product of torque (τ) and angular speed (ω) yielded the measured power input due to stirring:

$$P = \tau\omega \quad (2.8)$$

where P = measured power input.

Using Equation 2.9, the Power Number (P_o) of the 3-blade segment impeller was then calculated:

$$P_o = \frac{P}{\rho N^3 D_i^5} \quad (2.9)$$

As discussed in Section 2.1.6, the diameter of the impeller (D_i) was 0.07 m. Each experiment was performed in triplicate. Both a mean Power number and standard deviation were derived.

2.7 Derived Growth and Metabolic Parameters

2.7.1 Estimation of maximum specific growth rate

Growth rate was estimated by plotting the natural logarithm of viable cell concentration measured during the growth period against time. The gradient of the resultant straight line was taken as the maximum specific growth rate.

The following equations were adapted from those given by Sauer et al. (2000).

2.7.2 Integral of viable cell concentration (IVC)

The integral of viable cells for each discrete time interval was obtained using Equations 2.10 and 2.11, where $(X_v V_L)_1$ and $(X_v V_L)_2$ are the total number of viable cells at times t_1 and t_2 , respectively. $(X_v V)_{ave}$ is the average total number of viable cells for the time interval $t_2 - t_1$. X_V = viable cell concentration.

$$\int_{t_1}^{t_2} X_v V_L dt = (X_v V_L)_{ave} (t_2 - t_1) \quad (2.10)$$

$$(X_v V_L)_{ave} = \frac{(X_v V_L)_1 + (X_v V_L)_2}{2} \quad (2.11)$$

The integral of viable cells was estimated by summing all of the discrete time interval values at $t = (t_1 + t_2) / 2$:

$$\int_{t_{initial}}^{t_{final}} X_v V_L dt = \sum_t (X_v V_L)_{ave} (t_2 - t_1) \quad (2.12)$$

The integral of viable cell concentration was obtained by dividing Equation 2.12 by the final culture volume.

$$\frac{\int_{t_{initial}}^{t_{final}} X_v V_L dt}{V_{final}} \quad (2.13)$$

2.7.3 Average specific antibody production rate

The average specific antibody production rate, q_{Ab}^{ave} , was calculated using Equation 2.14, where Ab_t was the antibody concentration at time t . The average specific antibody production rate was obtained by dividing the cumulative antibody produced by the integral of viable cells; this expression was evaluated at the end of the culture. Lactate production was calculated in the same manner.

$$q_{Ab}^{ave} = \frac{Ab_{t_{final}} \cdot V_{t_{final}} - Ab_{t_{initial}} \cdot V_{t_{initial}}}{\int_{t_{initial}}^{t_{final}} X_v V_L dt} \quad (2.14)$$

2.7.4 Specific glucose consumption rate

The average specific glucose consumption rate q_{gluc}^{ave} was calculated using Equation 2.15, where $gluc_t$ was the cultures residual glucose concentration at time t . The average specific glucose consumption rate was obtained by dividing the cumulative glucose consumed by the integral of viable cells; this expression was evaluated at the end of the culture.

$$q_{gluc}^{ave} = \frac{gluc_{t_{initial}} \cdot V_{t_{initial}} - gluc_{t_{final}} \cdot V_{t_{final}}}{\int_{t_{initial}}^{t_{final}} X_v V_L dt} \quad (2.15)$$

2.8 Analytical Techniques

2.8.1 Cell Number and Viability Quantification

Cell number and viability were assessed immediately post sampling using a CASY TTC cell counter (Sedna Scientific, Derbyshire, Uk) and trypan-blue exclusion. The supernatants harvested from each sample were stored at -20°C for subsequent analysis of metabolites and antibody titer once the cultivation was complete.

2.8.2 Quantification of Antibody Concentration

A “sandwich” ELISA technique was used to quantify antibody titers in supernatant samples. All 96 wells of a NUNC Maxisorp plate (VWR, Lutterworth, Leicestershire, UK) were coated with 100 μl of anti-mouse IgG (Fab specific) at a concentration of 2 $\mu\text{g ml}^{-1}$ and incubated at 4°C overnight. Each well was then washed three times with 100 μl of PBS-Tween20, pH 7.4. Following aspiration, 200 μl of 1% (w/v) skimmed milk was added to each well to block unbound sites, and the plate was incubated for 1 hour on a reciprocating shaker. Following another wash cycle, 100 μl of blocking solution (1% (w/v) skimmed milk) was added into each well except row A. 200 μl of IgG standard (1 $\mu\text{g ml}^{-1}$) and diluted sample (10 fold) were loaded into row A in duplicate. Using a 12-channel pipette, the standards and samples were then serially diluted down the plate, by taking 100 μl from row A and transferring to row B, pipette mix 5 times and transfer of 100 μl to row C and this was repeated until to row H. Wells H1 and H7 were used as blanks. The plate was covered in cling film and incubated for 2 hours at room temperature. Following incubation, the plate was washed and 100 μl of anti-mouse IgG (Fc specific) peroxidase conjugate added to each well at a concentration of 1.4 $\mu\text{g ml}^{-1}$. This was incubated for 1 hour at room temperature. After washing, 100 μl of 3, 3', 5, 5' tetramethylbenzidine liquid substrate was added to each well, and allowed to develop for 3 minutes. Subsequently 100 μl of 1N HCl was added to each well to stop the reaction and the absorbance was measured at 450nm using a microplate spectrophotometer (Tecan, Reading, UK). Unless stated, all reagents were purchased from Sigma (Poole, Dorset, UK).

2.8.3 Quantification Of Glucose, L-Lactate and Glutamine Concentration

Glucose, L-lactate and glutamine were all measured using an YSI 2700 select bio analyser (YSI inc., Yellow Springs, Ohio, USA). All three assays work on the same principle: An enzyme specific for the substrate of interest is immobilized between two membrane layers, polycarbonate and cellulose acetate. The substrate is oxidized

as it enters the enzyme layer, producing hydrogen peroxide, which passes through cellulose acetate to a platinum electrode where the hydrogen peroxide is oxidized. The resulting current is proportional to the concentration of the substrate.

2.8.4 pH and Osmolality Measurements

pH was measured using a Thermo microcombination pH electrode 16Ga needle tip (World Precision Instruments Ltd, Stevenage,UK) and Hanna pH meter. Before each reading the probe was calibrated with pH 7 and pH 4 buffer heated to 37°C. The meters' manual temperature compensation was set to 37 °C.

Osmolality measurements were made using a Camlab automatic osmometer (Camlab, Cambridge,UK). Zero osmolality was set using distilled water and the span was calibrated with a 300 milliosmol standard solution (Camlab).

2.9 Statistical Tests

One-way ANOVA and a student's t-test were used to compare mean viable cell concentrations. All calculations were performed using Minitab software (Minitab ltd, Coventry, UK). A 95% confidence interval was used throughout.

Chapter 3

Engineering Characterisation Of Shaken Microwell Plates

3.1 Introduction and Aims

Optimisation of suspension cell-culture is traditionally carried out in spinner flasks, shake flasks, and small bench-scale stirred-tank reactors (STR) as previously described in Chapter 1. The current need to reduce process development time necessitates the adoption of high throughput experimentation, however, the labour and material costs involved render this almost impractical at conventional scales (Lye et al., 2003)(Girard et al., 2001)(Micheletti and Lye, 2006). In contrast, experimentation in microwell format offers a potential new platform technology to obtain key process design data early and cost effectively (Lye et al., 2003). The use of microwell format readily lends itself to automation (Doig et al., 2002)(Nealon et al., 2005), and the implementation of advanced operating strategies such as liquid addition for pH control (Elmahdi et al., 2003) and fed-batch operation. For such an approach to be implemented, it is first necessary to understand the influence of the engineering environment in microwells on cell-cultures. This will be vital for defining optimal operation for cell-cultures and ultimately a reliable basis for process scale-up.

The aim of this first chapter is to characterise the engineering environment in shaken microwells under conditions that are relevant to the culture of suspension adapted

mammalian cells. As a model system the culture of VPM 8 hybridoma cells in shaken 24-well plates will be considered. The specific objectives of this chapter are thus to:

- Use existing correlations, as described in Section 1.4.3, to predict fluid hydrodynamics and oxygen mass transfer coefficients over the range of likely operating conditions.
- Experimentally measure liquid phase mixing times in shaken 24-well (ULA) plates, and a laboratory scale STR, based on the iodine decolourisation method, as described in Section 2.5.
- Use CFD modelling of shaken microwells to obtain an initial insight into the energy dissipation and shear rate within individual microwells. In addition, use high-speed video footage to observe fluid motion and the deformation of the gas-liquid interface in microwells.
- Consider potential basis for scale-up of microwell culture conditions based on parameters such as mixing time, energy dissipation and oxygen mass transfer coefficient.

3.2 Prediction of Liquid Phase Hydrodynamics

In Section 2.3, the Reynolds (Re), Froude (Fr), and Phase (Ph) numbers were introduced as parameters used to characterise liquid phase hydrodynamics. Re is defined as the ratio of inertial forces to viscous forces, and may be defined for shaken systems using Equation 2.1. Fr is defined by Equation 2.2 as the ratio of radial to axial forces for shaken systems (Büchs et al., 2000b). Ph is defined by Equation 1.2, and marks the boundary between “in-phase” and “out of phase” shaking conditions (Büchs et al., 2000b). During “in-phase” conditions ($Ph > 1.62$, $Fr > 0.4$), the whole of the liquid moves with the rotation of the shaker platform. Operation under “out of phase” conditions is characterised by a significant proportion of the liquid not following the motion of the shaker. As a direct result, both the oxygen transfer rate

Table 3.1: Re, Fr and, Ph numbers calculated for a 24-well (ULA) plate. All calculations used a microwell diameter (d_w) = 15.94 mm, shaker diameter (d_s) = 20 mm, and assume the fluid properties of water at 37°C. Re, Fr and Ph were calculated using Equations 2.1, 2.2 and 1.2 respectively.

	$V_L [\mu l]$	N [rpm]					
		120	160	200	225	250	300
Re	-	730	973	1220	1370	1520	1830
Fr	-	0.16	0.29	0.45	0.57	0.70	1.0
Ph	800	8.2	8.7	9.0	9.2	9.4	9.7
	1000	8.8	9.2	9.6	9.8	10	10
	2000	11	11	12	12	12	12

and mixing intensity are reduced (Büchs et al., 2000b).

Table 3.1 presents the calculated Re, Fr and Ph numbers for the microwell plate and range of conditions to be used in this work. To date, there have been no studies linking Re to flow regimes in shaken microwell plates (Micheletti et al., 2006). So while the values are presented in Table 3.1, it is not possible to say whether the flow is turbulent or not. “In-phase” operation is predicted to exist in 24-well plates when $N \geq 200$ rpm since $Fr > 0.4$ and $Ph > 1.26$. Between 120 - 160 rpm, a large fraction of the liquid is likely to remain in contact with the base and not follow the motion of the shaker platform. This may result in reduced mixing intensity and oxygen transfer.

By comparison, the Re of the shake flask, conditions to be used as an experimental comparison (Section 3.7), was calculated as 18,000. Recently, it has been proposed that turbulence prevails in non-baffled shake flasks when $Re > 60,000$ (Peter et al., 2006). Given that laminar flow is highly unlikely from visible observations, it seems sensible to suggest transitional flow in the shake flask. The value of Re calculated in the 5-L STR ranged from 5,900 at 50 rpm, to 29,000 at 250 rpm. For an unbaffled STR, turbulent flow is not fully developed until $Re > 10^5$ (Doran, 1995). The values predicted suggest the flow for the STR to also be in the transitional region. “In-phase” conditions were predicted for the shake flask comparison ($Fr = 0.64$, $Ph = 2.68$). While the “In-phase”, “out-of-phase” concept does not apply to the STR

Table 3.2: Mean volumetric oxygen mass transfer coefficient (K_{La}) predicted for a 24-well (ULA) plate covered with a breathe-easy membrane. Equation 1.4 was first used to generate the values corresponding to an uncovered well. A correction factor was then applied to compensate for the membrane as described in Section 2.4.1. All calculations used a microwell diameter (d_w) = 15.94 mm, shaker diameter (d_s) = 20 mm, oxygen diffusion coefficient (D) = $2.69 \times 10^{-9} \text{ m}^2 \text{ s}^{-1}$ (Micheletti et al., 2006), initial air-liquid specific surface area (a_i) = 249.4 m^{-1} and wetting tension (W) = 0.0012 N m^{-1} (Doig et al., 2005). Liquid properties were assumed to be those of water at 37°C . All units are h^{-1} .

$V_L [\mu\text{l}]$	N [rpm]					
	120	160	200	225	250	300
800	3.2	6.3	11	14	19	29
1000	2.5	5.1	8.6	12	15	23
2000	1.3	2.5	4.3	5.7	7.4	11

experiments.

3.3 Prediction of Oxygen Mass Transfer Coefficients

One of the key challenges for shaken microwell systems is to provide sufficient oxygen for the cells to grow. Under oxygen limited conditions, cells may grow slowly and synthesis products inefficiently. Results obtained under such conditions are likely to be misleading particularly for scale-up purposes (Doig et al., 2005)(Maier and Büchs, 2001).

K_{La} was calculated for uncovered wells using Equation 1.4 and then corrected for the added transfer resistance of the breath-easy membrane used to cover the wells (Section 2.4.1) (Doig et al., 2005).

The predicted values of K_{La} for 24-well (ULA) plates are summarised in Table 3.2. The predicted oxygen mass transfer coefficient (k_{La}) were, under all conditions investigated, greater than 1 h^{-1} . k_{La} values greater than 1 h^{-1} are generally considered

Table 3.3: Mean volumetric oxygen transfer coefficient (k_{La}) measured in a 5-L STR ($V_L = 3\text{-L}$) using the dynamic-gassing out method. PBS, at pH 7.4, was used to approximate cell-culture media. All experiments were conducted at 37°C with an aeration rate of $100\text{ cm}^3\text{ min}^{-1}$ as described in section 2.4.2. ($n = 2 \pm 1\text{ SD}$)

N [rpm]	k_{La} [h^{-1}]
50	4.35 ± 0.63
150	7.25 ± 0.92
200	9.30 ± 0.28

sufficient to support the oxygen demand of $10^6 - 10^7$ cells ml^{-1} (Fenge et al., 1993), while 10^8 cells ml^{-1} require a k_{La} of between $5\text{-}55\text{ h}^{-1}$ (Ozturk, 1996). These predictions suggest that oxygen transfer into a 24-well (ULA) plates, covered with a breathe-easy membrane, will not be limiting for hybridoma cells. Equation 1.4 has a reported accuracy of $\pm 30\%$ (Doig et al., 2005), therefore oxygen may just become limiting under the extreme operating conditions of $V_L = 2000\ \mu\text{l}$ and $N = 120\text{ rpm}$. Although the hybridoma cell line used in this work typically reaches cell densities of 1.5×10^6 cells ml^{-1} (Section 4.3), the predicted values of k_{La} suggests the majority of conditions studied will support at least 10^7 cells ml^{-1} . Currently, recombinant cell lines used in industry can reach densities in the order of 1×10^7 cells ml^{-1} (Wurm, 2004). It is therefore unlikely that production cell lines will also be limited by oxygen transfer if cultured in the shaken 24-well plates under the shaking conditions used here.

k_{La} was measured in the 5-L STR using the dynamic gassing-out method, as described in Section 2.4.2. Table 3.3 presents the results. All values of k_{La} were again $> 1\text{ h}^{-1}$ suggesting that oxygen transfer into the STR will not limit the hybridoma cell line to be used here.

k_{La} was predicted in the shake flask (100 ml, 120 rpm) using the method described in Section 2.4.3. The value (10 h^{-1}) was again $> 1\text{ h}^{-1}$ suggesting that oxygen transfer into the shake flask will not limit the hybridoma cell-line to be used in this work.

3.4 Liquid Phase Mixing Time Characterisation

3.4.1 Shaken Microwell Plates

In this section, an experimental investigation into the mixing of small liquid addition made to shaken microwell cultures is described. This work is directed towards future automation of microwell mammalian cell culture process development, when automated liquid additions of reagents, for pH control (Elmahdi et al., 2003), DNA complexes (Girard et al., 2001) or concentrated feeds may be made to microwell cultures. Poor mixing in microwells has the potential to affect cell growth, productivity and product quality as at larger scales (Ozturk, 1996) (Sen et al., 2001). Clearly this would impact on the validity of small scale process studies/characterisation, or the success of scale-up work.

Two distinct mixing patterns were observed following the addition of small liquid aliquots to shaken 24-well (ULA) plates. These patterns are shown in Fig. 3.1 and Fig. 3.2. A small aliquot of inert blue food dye, 1% of the bulk volume, was injected into the water bulk using the apparatus described in Section 2.5. Images were captured using a digital video camera operating at 250 frames s^{-1} . Fig. 3.1 shows the mixing pattern representative of those observed between 0 and 225 rpm. Initially, the dye flowed to the bottom of the well (Fig. 3.1a). This was followed by dispersion along the bottom surface (Fig. 3.1b). Finally, the dye ascends the liquid bulk as a continuous, horizontal front (Fig. 3.1c). In contrast, between 250 rpm and 300 rpm, the dye was rapidly mixed into the liquid contents of the well (Fig. 3.2). Heterogeneities (Fig. 3.2b) existed only briefly, before the dye was spread evenly through the liquid bulk (Fig. 3.2c).

From all the images collected it was apparent that heterogeneities will exist in the in the microwells, particularly at $N \leq 225$ rpm (Fig. 3.1). This would represent a

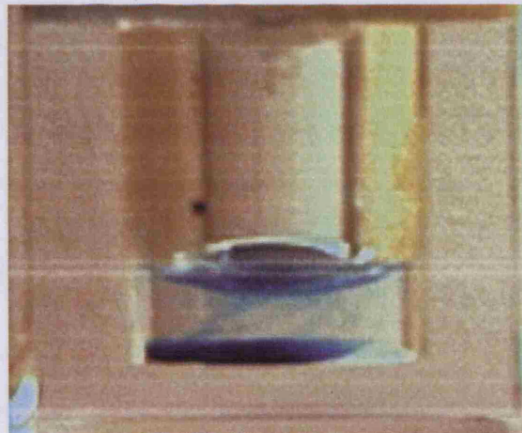
significant problem if the liquid additions are toxic to the cells being cultured at high concentrations. For example, if base additions were made to a microwell culture, initially a zone of high pH would exist at the bottom of the well. However, any adverse effects caused by the liquid additions would depend on the frequency and duration of the heterogeneities (Osman et al., 2001)(Osman et al., 2002). The duration of these heterogeneities is known as the mixing time and so was quantified in subsequent studies.

Mixing time in shaken 24-well (ULA) plates was quantified using the “iodine clock reaction”. As described in Section 2.5, this method utilises the decolourisation of a dark-orange iodine solution using a colourless sodium thiosulphate solution. Mixing time is defined by the complete decolourisation of iodine (Nienow et al., 1996). This method was chosen because the end-point is very distinct, furthermore, the hydrodynamics associated with mixing can be visualised, unlike many pH-based methods (Langheinrich et al., 1998). The hydrodynamics of the decolourisation of iodine, in 24-well plates, was visually similar to the patterns observed following the injection of blue food-dye. Initially, the sodium thiosulphate flowed to the bottom of the well (Fig. 3.3a). This was followed by decolourisation in the bottom region (Fig. 3.3b). Gradually the decolourisation progressed up the well as a continuous, horizontal front. The iodine solution at the gas-liquid interface was the last to clear (Fig. 3.3c). At the highest shaking speeds tested, 250 rpm and 300 rpm, the iodine decolourised rapidly (<1.6 s) and evenly (Fig. 3.4).

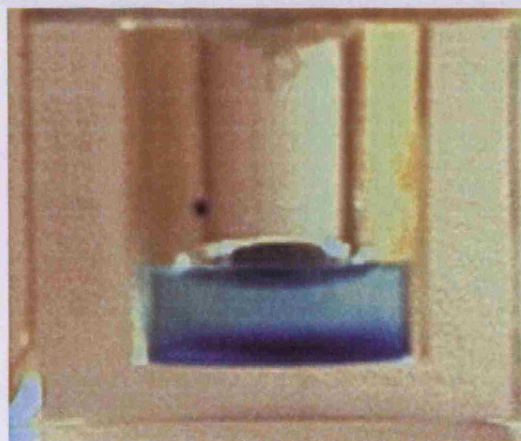
The measured mixing times in 24-well (ULA) plates decreased with increasing Re , and decreasing fill volume, as shown in Fig. 3.5. With no shaking, the mixing times varied from $3,600 \pm 849$ s ($V_L = 800 \mu\text{l}$) to $12,900 \pm 424$ s ($V_L = 2,000 \mu\text{l}$). When $Re = 1,830$, the mean mixing time was estimated at 1.7 ± 0.06 s for both $800 \mu\text{l}$ and $1000 \mu\text{l}$. For a $2,000 \mu\text{l}$ fill volume, the contents of the well rapidly splashed out at $Re = 1,830$ (300 rpm), hence measurements of the mixing time were not made. At $Re > 1,220$, a rapid decrease in the mixing time was observed for all fill volumes.



(a) $t = 0$ Injection



(b) $t = 13$ s after injection



(c) $t = 3$ minutes after injection

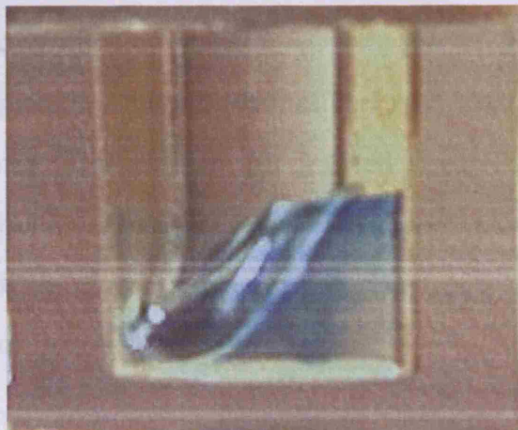
Figure 3.1: Mixing of a small liquid addition into the liquid contents of a single well from a 24-well (ULA) plate. Shaking speed = 120 rpm. $8 \mu\text{l}$ of inert blue food dye was injected into $800 \mu\text{l}$ of water and images were captured by high speed video as described in Section 2.5.

Table 3.4: Summary of published liquid phase mixing time data for various geometries of microfluidic well bioreactors.

Director (London)	2005
12,000-L STR	1000
8,000-L STR	1000
Wave bioreactor	1000
30-L Stirrer	1000
3-L STR, 50-200 rpm	1000
2-L STR	1000
24-Well Plate	1000



(a) $t = 0$ Injection



(b) $t = 0.7$ s after injection



(c) $t = 3.2$ s after injection

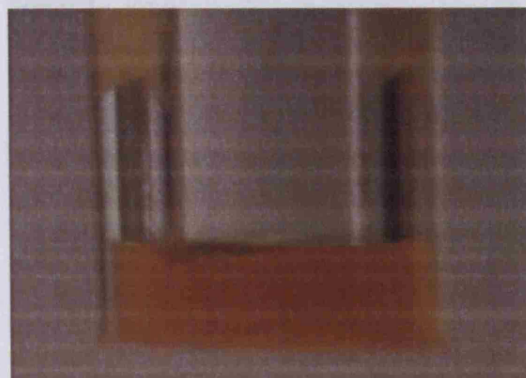
Figure 3.2: Mixing of a small liquid addition into the liquid contents of a single well from a 24-well (ULA) plate. Shaking speed = 300 rpm. $8 \mu\text{l}$ of inert blue food dye was injected into $800 \mu\text{l}$ of water and images were captured by high speed video as described in Section 2.5.

Table 3.4: Summary of published liquid phase mixing time data for various geometries of mammalian cell bioreactor.

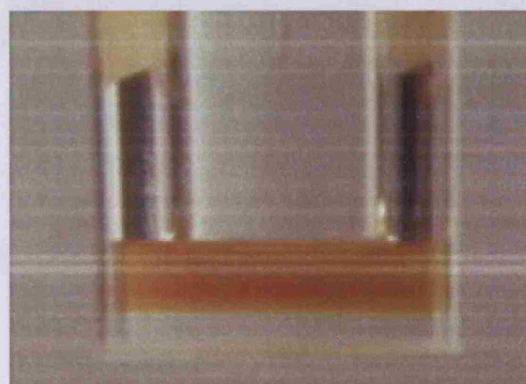
Bioreactor Configuration	Mixing time [s]	Reference
12,000-L STR	150	(Meier, 2005)
8,000-L STR	9-200	(Nienow et al., 1996)
Wave bioreactor	60 (100-L); 5-10 (10-L)	(Singh, 1999)
30-L Airlift	60-110	(Varley and Birch, 1999)
5-L STR, 50-200rpm	10-100	This work
2-L STR	≤60	(Osman, 2001)
24-Well Plate	12,900 - 2	This work

Compared to published data (Table 3.4), the majority of mixing times recorded in this work are long, particularly at $Re \leq 1,370$. Published mixing times are typically less than 200 s, even at production scale ($> 8,000$ -L) (Meier, 2005) and so it may be expected that the long mixing times measured here may have a negative impact on cell culture performance. Furthermore, the impact of very-long mixing times and “out of phase” conditions on the accuracy of K_La predictions from Equation 1.4 is unknown. It should be noted that a shaking speed of 200 rpm was the lowest reported in the work of Doig et al. (2005).

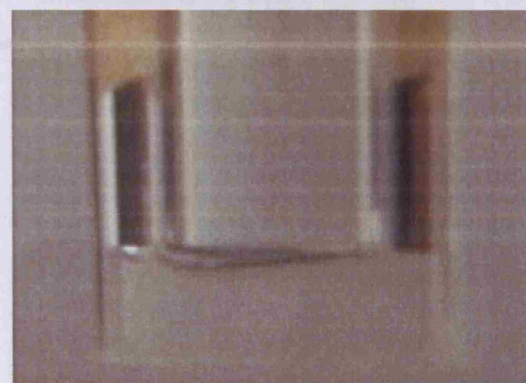
In an attempt to try and reduce the long mixing times measured in shaken microwells for $Re < 1,370$, two baffle configuration were designed. Both designs were based on the configurations commonly found in STRs: single- and double- wall baffles. Section 2.1.5 describes these configuration in more detail. All mixing times were assessed using a fill volume of 800 μ l and Re between 730 and 1,520. Fig. 3.6 presents the mixing times for these two baffle configurations. At the lowest Re investigated, the mixing time was found to be 996 ± 317 s and 1332 ± 188 s for the single- and double- wall baffles respectively. Compared to the mixing time estimated for the unbaffled wells, Fig. 3.6, introduction of baffles reduces the mixing time by 57% and 41% for the single- and double- wall configurations respectively. Greater reductions of 85% and 70% for the single-wall and double-wall configuration respectively were found at $Re = 1,370$. By introducing baffles, the mixing time was thus reduced significantly. However, between Re of 730 and 973, mixing times were still higher



(a) $t = \text{Injection}$

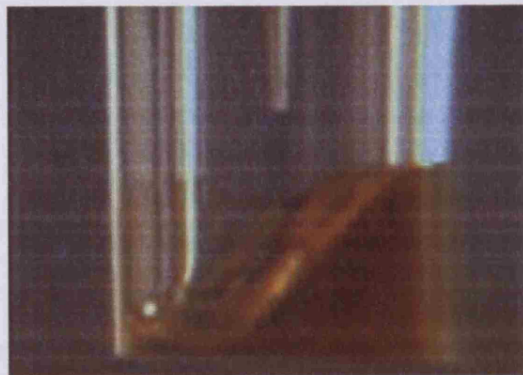


(b) $t = 8 \text{ minutes after injection}$

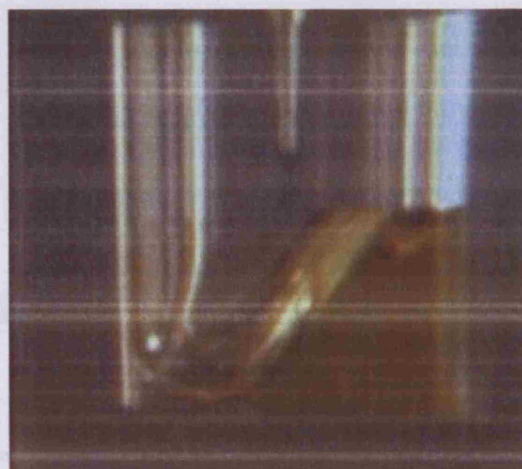


(c) $t = 41 \text{ minutes after injection}$

Figure 3.3: Mixing of a small liquid addition into the liquid contents of a single well from a 24-well (ULA) plate. Shaking speed = 120rpm. $8\mu\text{l}$ of 1.8 M sodium thiosulphate solution was injected into $800\mu\text{l}$ of 0.5 M iodine solution and images were captured by high speed video camera as described in Section 2.5.



(a) $t = \text{Injection}$



(b) $t = 0.8 \text{ s}$ after injection



(c) $t = 1.6 \text{ s}$ after injection

Figure 3.4: Mixing of a small liquid addition into the liquid contents of a single well from a 24-well (ULA) plate. Shaking speed = 300 rpm. $8\mu\text{l}$ of 1.8 M sodium thiosulphate solution was injected into $800\mu\text{l}$ of 0.5 M iodine solution and images were captured by a high speed video camera as described in Section 2.5.

than those typical of animal cell bioreactors (< 200).

3.4.2 Stirred-Tank Reactor

The mixing characteristics of a 5-L STR were assessed in the same manner as above. Coloured plates (green dye in first vial) having particles followed by iodine dye (decolouration) were added sequentially mixing time. Section 3.5 describes the methods. Experiments were performed at Re ranging from 100 to 2000. About 100

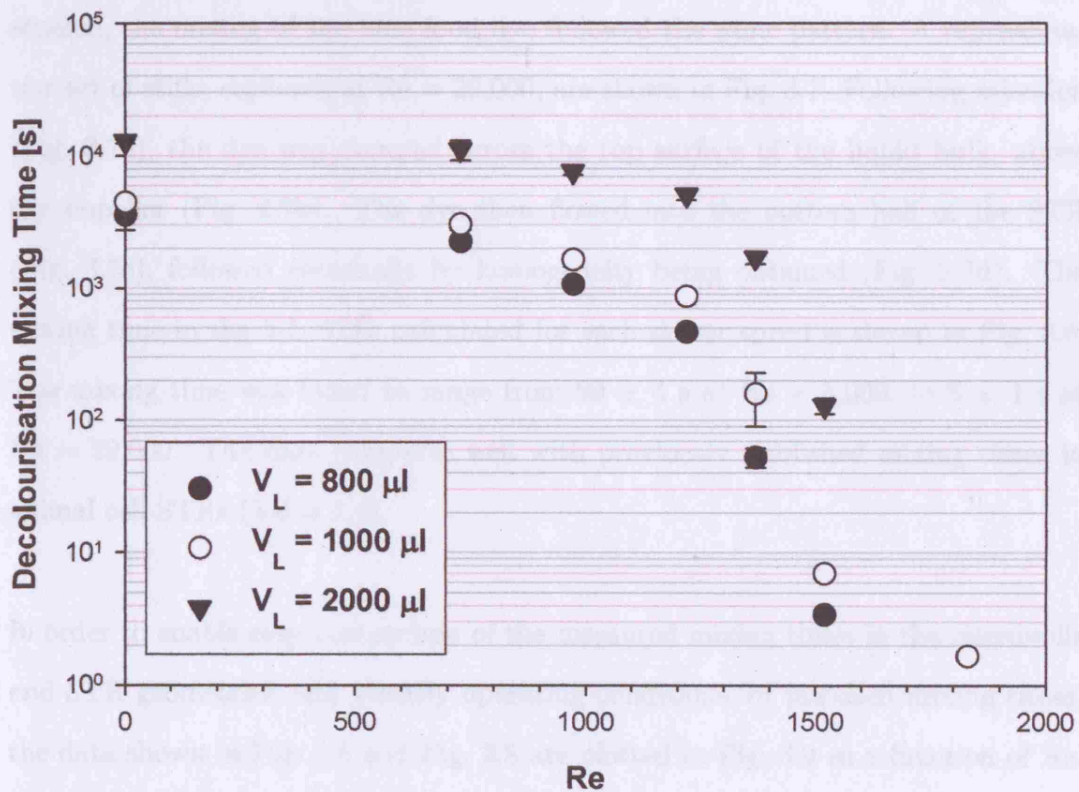


Figure 3.5: Mean mixing time measured in shaken 24-well (ULA) plates as a function of Reynolds number (Re) and liquid fill volume (V_L). Mixing times were estimated using the iodine clock reaction as described in Section 2.5. Error bars represent one standard deviation about the mean.

3.5 Characterisation of Energy dissipation rates

3.5.1 CFD Modelling of Shaken 24-Well Plates

All CFD models presented in this section were developed and analysed by Dr. Ben Wang.

than those typical of animal cell bioreactors (< 200 s).

3.4.2 Stirred-Tank Reactor

The mixing characteristics of a 5-L STR were assessed in the same manner as shaken microwell plates: tracer dye to first visualise mixing patterns, followed by iodine decolourisation experiments to quantify mixing time. Section 2.5 describes the methods. Experiments were performed at Re ranging from 5,900 to 29,000. At all Re studied, the mixing of the blue food dye followed the same pattern. A representative set of stills, captured at $Re = 29,000$, are shown in Fig. 3.7. Following injection (Fig. 3.7a), the dye was pumped across the top surface of the liquid bulk, above the impeller (Fig. 3.7b). The dye then flowed into the bottom half of the STR (Fig. 3.7c), followed eventually by homogeneity being obtained (Fig. 3.7d). The mixing time in the 5-L STR, calculated for each stirrer speed is shown in Fig. 3.8. The mixing time was found to range from 99 ± 4 s at $Re = 5,900$, to 8 ± 1 s at $Re = 29,000$. The data compares well with previously published mixing times in animal cell STRs (Table 3.4).

In order to enable easy comparison of the measured mixing times in the microwells and STR geometries, and identify operating conditions for matched mixing times, the data shown in Fig. 3.5 and Fig. 3.8 are plotted in Fig. 3.9 as a function of Re . Fig. 3.9 also shows that the 24-well plates would have to be shaken at $Re \geq 1,520$ in order to obtain mixing times equivalent to those found in the 5-L STR.

3.5 Characterisation of Energy dissipation rates

3.5.1 CFD Modelling of Shaken 24-Well Plates

All CFD models presented in this section were developed and analysed by Dr. Hu Zhang.

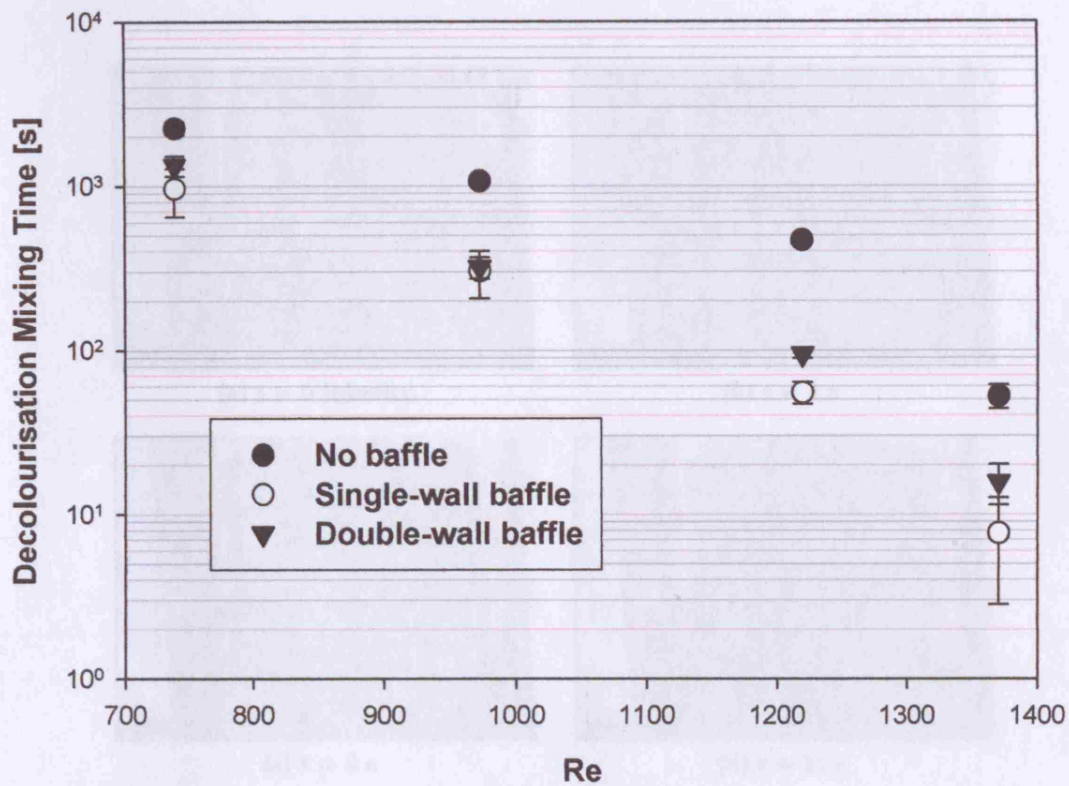
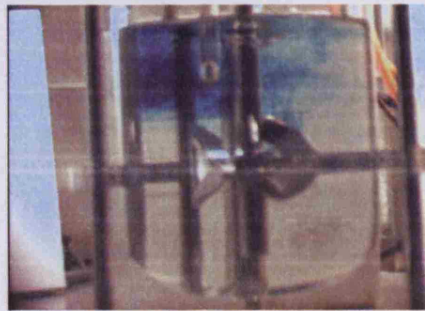


Figure 3.6: Mean mixing time measured in baffled shaken 24-well (ULA) plates as a function of Reynold's number (Re). Two baffle configurations were designed: single-wall and double-wall baffles, as described in Section 2.1.5. Mixing times were estimated using the iodine clock reaction as described in Section 2.5. Error bars represent one standard deviation about the mean.



(a) $t = 0$ Injection



(b) $t = 2$ s



(c) $t = 8$ s



(d) $t = 11$ s

Figure 3.7: Mixing of a small liquid addition into the liquid contents of a 5-L STR ($V_L = 3$ -L). Agitation speed = 200 rpm. 30 ml of inert blue food dye was injected into 3-L of water and images were captured by high speed video as described in Section 2.5.

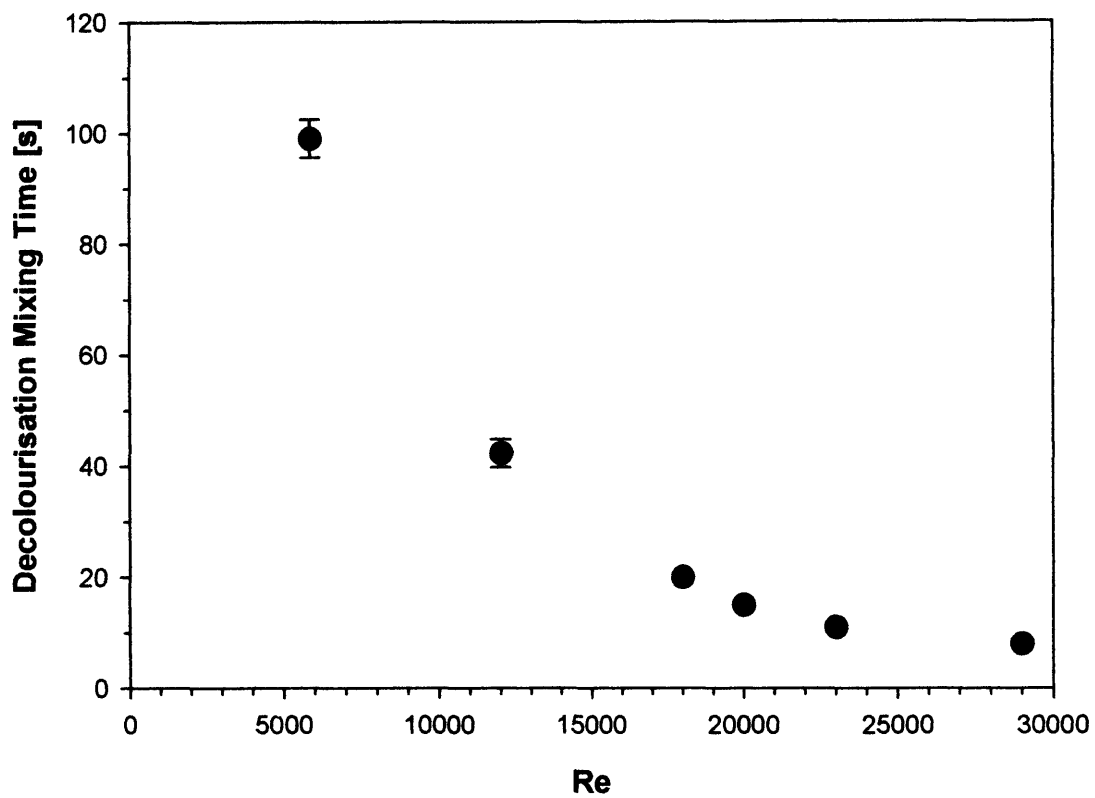


Figure 3.8: Mean mixing time measured in a 5-L STR ($V_L = 3$ -L) as a function of Re. Mixing times were estimated using the iodine clock reaction as described in Section 2.5. Error bars represent one standard deviation about the mean.

Mean energy dissipation rate (P/V) and shear rate are frequently used to assist in the evaluation of, scale-up, and scale-down of laboratory as described in Section 1.4.1. At present, there are two experimental methods to estimate P/V in shaken bioreactors: the torque method and the suspension method (described in Section 3.4.2). The first method requires a motorised assembly with a digital platform to enable the installation of a torque-meter on the drive shaft. Furthermore, the reported torque value may be low that long-term operation may be necessary for

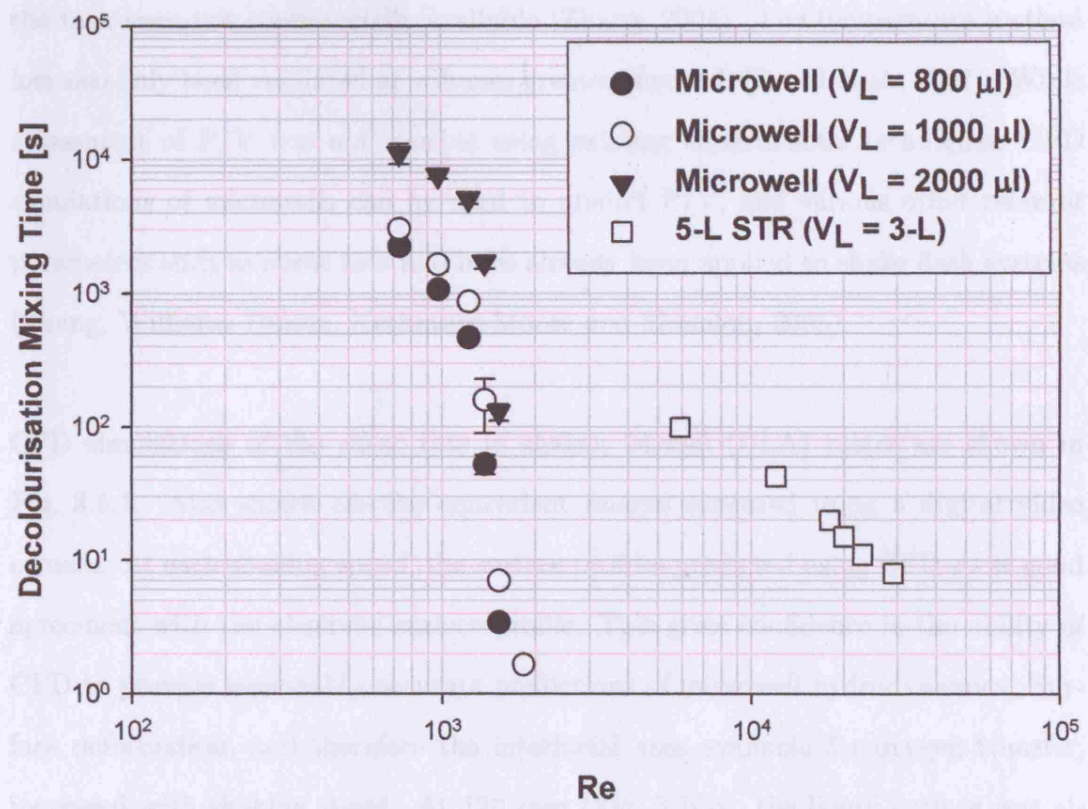


Figure 3.9: Comparison of the liquid phase mixing times for a shaken 24-well (ULA) plate and 5-L STR ($V_L = 3-L$). Mixing times were taken from Fig. 3.5 and Fig. 3.8. Error bars represent one standard deviation about the mean.

Hydrodynamic forces at 150 rpm are relatively mild compared to the 1000 rpm used in Heath and Kiss (2007). Using CFD, it is possible to make some initial conclusions regarding the suitability of shaken microwells for cell-culture applications. The maximum shear stress rate was approximately $2 \times 10^3 \text{ s}^{-1}$. This was found at the interface of the stirrer, performed at 150 rpm (Fig. 3.10a). Heath and Kiss (2007) investigated P/V depending to its effect on various animal cell lines.

Mean energy dissipation rate (P/V) and shear rate are frequently used to assist in the evaluation of, scale-up, and scale-down of bioreactors, as described in Section 1.4.1. At present, there are two experimental methods to estimate P/V in shaken bioreactors: the torque method and the temperature method (described in Section 1.4.3). The first method requires extensive modifications of the shaker platform to enable the installation of a torque-meter on the drive shaft. Furthermore, the expected torque levels were so low that torque-meters with sufficient sensitivity for the task were not commercially available (Zhang, 2004). The temperature method has also only been validated at volumes greater than 2-L (Raval et al., 2007). While assessment of P/V was not feasible using existing experimental techniques, CFD simulations of microwells can be used to predict P/V , and various other relevant parameters such as shear rate and have already been applied to shake flask systems (Zhang, Williams-Dalson, Keshavarz-Moore and Shamlou, 2005).

CFD simulations of the shear rate in shaken 24-well (ULA) plates are shown in Fig. 3.5.1. Also shown are the equivalent images captured using a digital video camera. At each shaking speed, the surface profiles predicted using CFD show good agreement with the observed surface profile. This gives confidence in the ability of CFD to provide reasonably accurate predictions of microwell hydrodynamics. Surface deformation, and therefore the interfacial area available for oxygen transfer, increased with shaking speed. At 120 rpm (Fig. 3.10b), the liquid surface was almost flat; by contrast, the liquid surface touched the bottom of the well when shaken at 300 rpm (Fig. 3.10j).

Hydrodynamic force, or “shear”, can adversely affect mammalian cells (Mollet et al., 2004) (Heath and Kiss, 2007). Using CFD, it is possible to make some initial conclusions regarding the suitability of shaken microwells for cell-culture applications. The maximum local shear rate was approximately $2 \times 10^3 \text{ s}^{-1}$. This was found at the interface of the simulation performed at 150 rpm (Fig. 3.10c). Heath and Kiss (2007) have classified P/V according to its effect on various animal cell-lines.

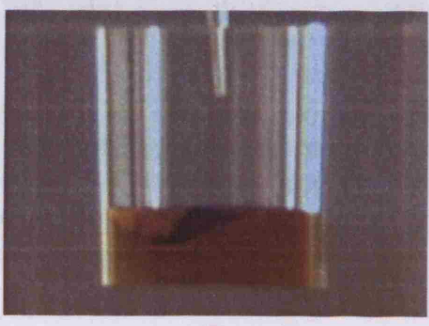
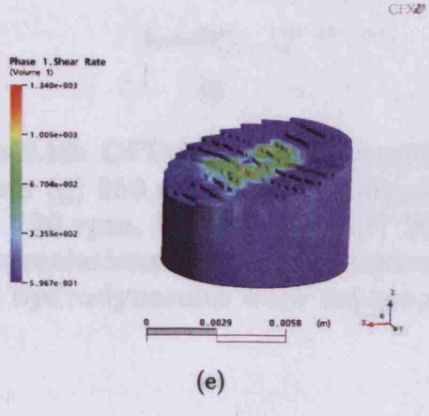
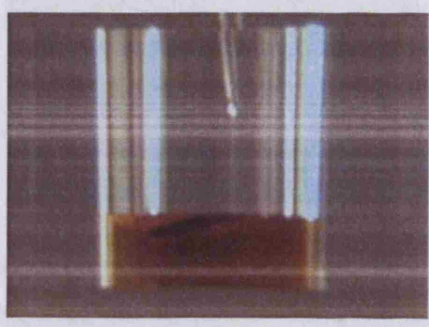
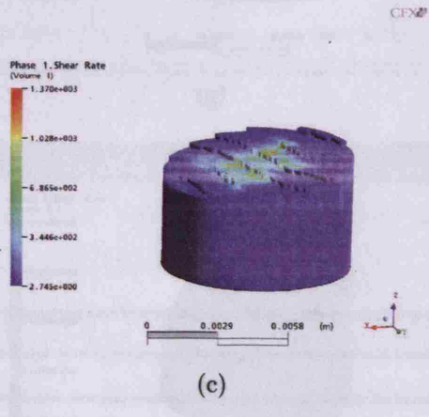
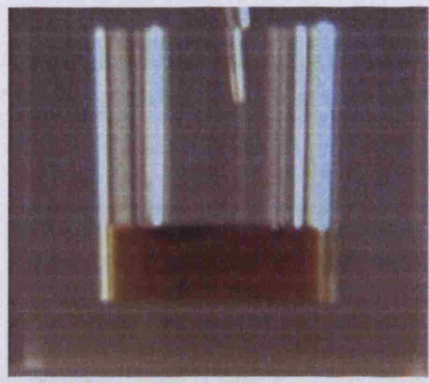
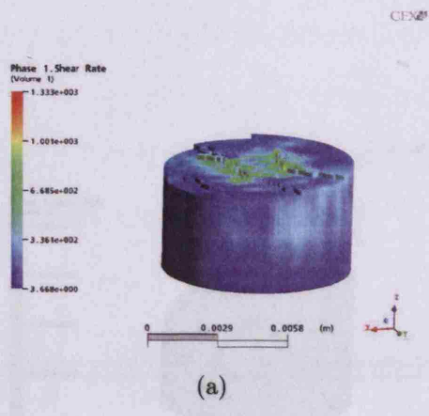


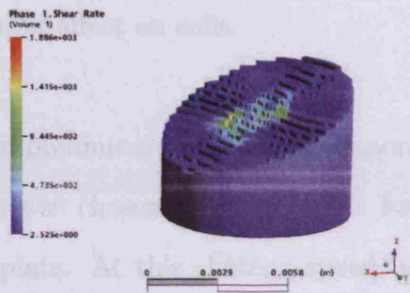
Figure 3.10

Fig. 3.9 compares the above results. Shear rate ($\dot{\gamma}$) and P/V can be directly related by the following equation (Eqn. 3.1):

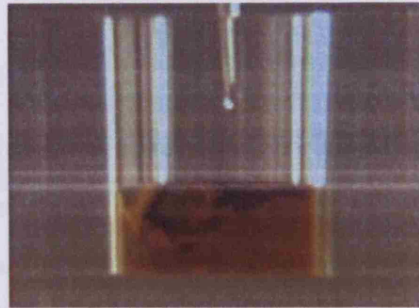
$$\dot{\gamma} = \sqrt{\frac{P}{V}} \quad (3.1)$$

Where $\rho = \text{viscosity}$. The maximum level of P/V at points are from 0.001 to 0.2 and 1.4 kW m⁻³. Comparing this result to the data depicted in Figure 3.9, suggests the predicted hydrodynamic conditions in a design 24-well TBA reactor are not

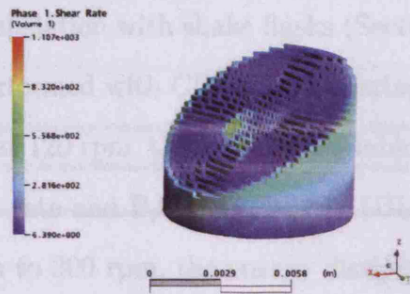
defining an cells.



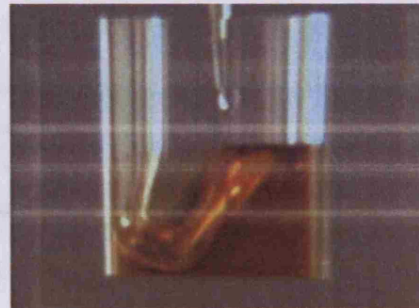
(g)



(h)



(i)



(j)

Figure 3.10: CFD Simulations performed at (a) 120 rpm, (c) 150 rpm, (e) 200 rpm (g) 250 rpm and (i) 300rpm, and fluid hydrodynamics visualised at (b) 120 rpm, (d) 160 rpm, (f) 200 rpm. (h) 250 rpm and (j) 300rpm. CFD simulations were performed as described in Section 2.6.2. Images of the hydrodynamics were captured as described in Section 2.5.

(Heymans et al., 2003). These data show a clear flow pattern in the wells, with

show N_{gr} there is a noticeable increase in flow rate. Using Equation 3.1 and the

parameters described in Section 3.3, N_{gr} for 24-well (TBA) plates was 25 rpm.

This is supported by the images shown in Fig. 3.10 where at the lowest speeds in-

vestigated, some disturbance of the surface was observed.

Fig. 1.2 summarises their main results. Shear rate ($\dot{\gamma}$) and P/V can be directly related by the following equation (Zhang, 2004):

$$\dot{\gamma} = \sqrt{\frac{P}{\mu V}} \quad (3.1)$$

Where μ = viscosity. The maximum local P/V, as predicted from Equation 3.1, was 1.4 KW m⁻³. Comparing this result to the data displayed in Figure 1.2 suggests the predicted hydrodynamic environment in shaken 24-well (ULA) plates has no detrimental affect on cells.

Based on preliminary cell-culture experiments [data not shown], a shaking speed of 120 rpm was chosen as a first basis for performing CFD simulations on a shaken 24-well plate. At this shaking speed, an average P/V of between 37 - 40 W m⁻³ was predicted using CFX 4. Given this was a theoretical prediction it was not clear if differences were real. Therefore it was decided to use 40 W m⁻³ as a basis for scale-translation with shake flasks (Section 3.7). Later, a wider range of simulations were performed with CFX 6. Comparing the results of the CFX 4 and CFX 6 simulations at 120 rpm, there was reasonable agreement in P/V values. Predicted values of shear rate and P/V for 24-SRW (ULA) plates are presented in Table 3.5. From 120 rpm to 300 rpm, the energy dissipation was predicted to decrease. Clearly this trend defies intuition and so experimental validation would be required to confirm this observation as correct.

Previous microwell studies have shown the presence of a critical shaking speed, N_{crit} (Hermann et al., 2003). Below N_{crit} , there is little fluid motion in the well, while above N_{crit} there is a noticeable increase in fluid flow. Using Equation 1.3 and the parameters described in Section 2.3, N_{crit} for 24-SRW (ULA) plates was 23 rpm. This is supported by the images shown in Fig. 3.10 where at the lowest speeds investigated, some deformation of the surface was observed.

Table 3.5: Energy dissipation per unit volume (P/V) and shear rate predicted using the CFD software package CFX 6 for shaken 24-Well plates.

	Shaking Speed [rpm]						
	120	150	200	225	250	300	400
Average Shear Rate [s ⁻¹]	190	130	98	99	84	73	150
Average P/V [W m ⁻³]	35	16	10	10	5	7	22

3.5.2 Power Input to a 5-L STR

Energy dissipation (P/V) in the 5-L STR, described in Section 2.1.6, was measured using an air-bearing and pressure transducer. Firstly, measurements of the power number (Po) of the 3-blade segment impeller were made over a range of conditions commonly used to cultivate mammalian cells. Using these measurements, P/V could be calculated from Equation 3.2. The full experimental procedure is detailed in Section 2.6.3.

Over the range of Re numbers 12,000 ($N = 100$ rpm) - 29,000 ($N = 250$ rpm), the measured Po numbers were very similar and varied from 0.35 to 0.41 (Fig. 3.11). At $Re = 35,000$, corresponding to a stirrer speed of 300 rpm, a significant increase in Po number was observed ($Po = 180$). At this operating point, vortexing of the STR's liquid content was observed and may explain the sharp rise in Po number.

Having established the Po number of the 3-bladed segment impeller, energy dissipation in the STR can be calculated by invoking Equation 3.2. Liquid properties were assumed to be those of water at 37°C.

$$\frac{P}{V_L} = \frac{Po \cdot \rho \cdot N^3 \cdot D_i^5}{V_L} \quad (3.2)$$

Energy dissipation in the 5-L STR ($V_L = 3\text{-L}$) increased with stirrer-speed from 0.93 W m^{-3} at 100 rpm, to 24 W m^{-3} at 300 rpm (Table 3.6). The energy dissipation values measured in this work compared well with literature values reported in Section 1.4.1.

3.6 Evaporation From Shaken Microwell Plates

Evaporation from microwell cultures is an unfortunate consequence of gas-exchange. For reasons of sterility and limiting evaporation, all microwell mammalian cell cultures must be covered; hence a trade-off between gas-exchange and evaporation can

Table 3.10: Mean energy dissipation in a 5-L STR ($V_i = 2-L$) as a function of stirrer speed. P/V was calculated using Equation 3.2, the power number measurements presented in Fig. 3.11 and the impeller diameter (D) is 7.0 cm. The density was assumed to 1000 Kg m^{-3} .

N [rpm]	Re_i	P/V [W m^{-3}]
120	12,000	7.0
150	15,000	7.1
200	20,000	8.0
300	30,000	14
360	36,000	24

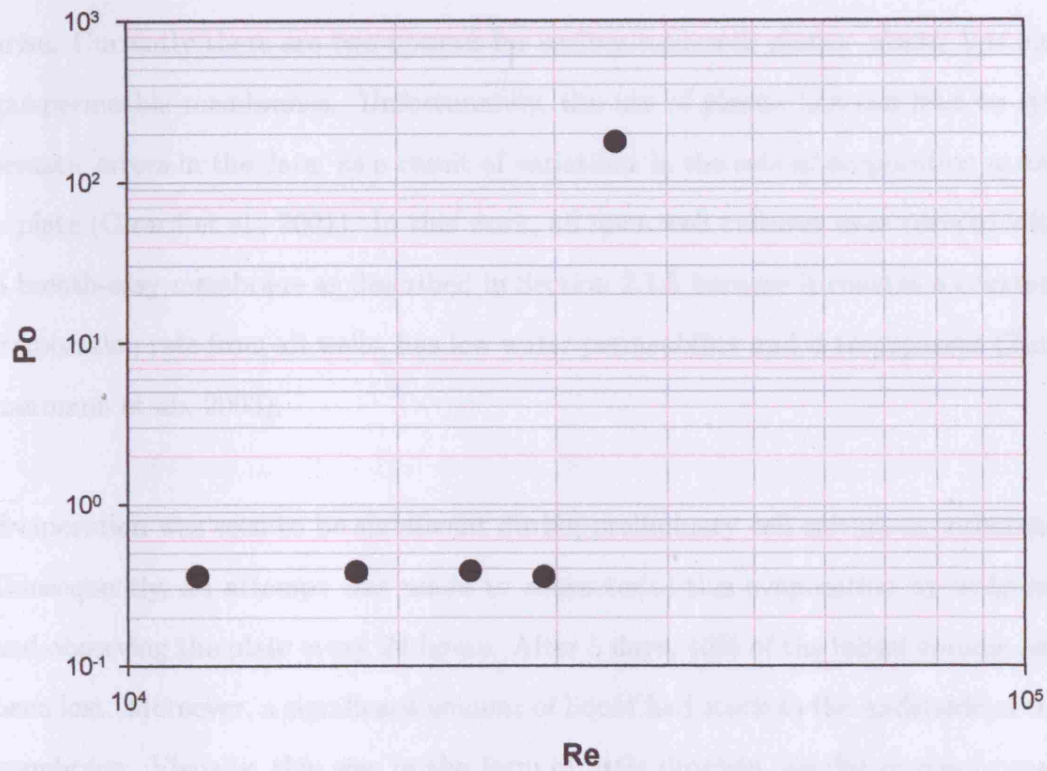


Figure 3.11: Mean power number of a 3-blade segment impeller as a function of Re_i . Po was measured in a 5-L STR using an air-bearing and pressure transducer as described in Section 2.6.3.

Table 3.6: Mean energy dissipation in a 5-L STR ($V_L = 3\text{-L}$) as a function of stirrer speed. P/V was calculated using Equation 3.2, the power number measurements presented in Fig. 3.11 and the impeller diameter (D_i) = 7.0 cm. The density was assumed to 1000 Kg m^{-3} .

N [rpm]	Re	P/V [W m^{-3}]
100	12,000	0.93
150	18,000	3.4
200	24,000	8.0
250	29,000	14
300	35,000	24

arise. Currently there are two options for sealing microwell plates: plastic lids and gas-permeable membranes. Unfortunately, the use of plastic lids can lead to systematic errors in the data, as a result of variations in the rate of evaporation across a plate (Girard et al., 2001). In this work, all microwell cultures were covered with a breath-easy membrane as described in Section 2.1.5 because it ensures a constant evaporation rate from all wells, has low water permeability and is transparent (Zimmermann et al., 2003).

Evaporation was seen to be significant during preliminary cell culture experiments. Consequently, an attempt was made to characterise this evaporation by weighing and observing the plate every 24 hours. After 5 days, 10% of the initial volume had been lost. Moreover, a significant amount of liquid had stuck to the underside of the membrane. Visually, this was in the form of little droplets, similar in size, spread over the entire surface. Attempts were made to return the liquid to the bulk by gently shaking and tilting the plate; however, the problem returned after a short period in the incubator. This evaporation was quantified by weighing the liquid *remaining in the bottom* of three separate wells, every 12-24 hours, over a period of 120 hours. Three shaking speeds: 120, 160 and 250 rpm and two fill volume: $800 \mu\text{l}$ and $2000 \mu\text{l}$ were investigated. At both fill volumes, the rate of evaporation from the liquid bulk was constant and independent of speed (Fig. 3.12). For $800 \mu\text{l}$, approximately 50% of the initial liquid had evaporated after 120 hours, while for $2000 \mu\text{l}$, just over 20% of the initial liquid bulk had evaporated over the same time-frame. Clearly, by

increasing the liquid fill volume, the extent of evaporation can be reduced. Larger fill volumes exhibit a lower specific surface area over which evaporation may occur.

The osmolality of the culture media can affect cell growth, metabolism and protein production (Ozturk and Palsson, 1991a)(Kimurat and Miller, 1996)(deZengotita et al., 1998)(Ryu and Lee, 1997)(Lin et al., 1999). To establish whether it impacts on culture performance in this case, samples were taken from microwell cultures and analysed using an osmometer as described in Section 2.8.4. Fig. 3.13 shows the measured changes in osmolality as a function of shaking speed and fill volume. At 120 rpm, the osmolality increased from 282 mOsm to 520 mOsm over 120 hours; at 250 rpm, the increase was 270mOsm to 455mOsm. In theory, both curves should be identical because of similar evaporation rates (Fig. 3.12). The difference in the two data sets may be due to differences in the dissolved CO₂, however the underlying reason is not clear at present.

To date, the literature in this area deals mainly with abrupt osmotic shocks (Ozturk and Palsson, 1991a)(Oh et al., 1993)(Ryu and Lee, 1997); by contrast, a gradual increase in osmolality was observed in this work. Reddy and Miller (1994) found for two hybridoma cell lines, that cell concentration, viability and specific antibody production rates remained at control levels until the osmolality was increased above 400 mOsm. Cherlet and Marc (1999) found no adverse effects on the cell growth and antibody production, using a gradual increasing osmolality, even up to 425 mOsm. For CHO cells, osmolalities above 400 mOsm should be avoided (Osman et al., 2002). From the literature data available, it seems that hybridoma cells will not be affected by osmolalities ≤ 400 mOsm until 84-96 hours into the culture which is during the death-phase of the cells.

Given the levels of evaporation described in Fig. 3.12, all microwell data presented subsequently in this thesis are corrected for evaporation over the time course of the culture. This will enable comparison to shake flask and STR data but it should be

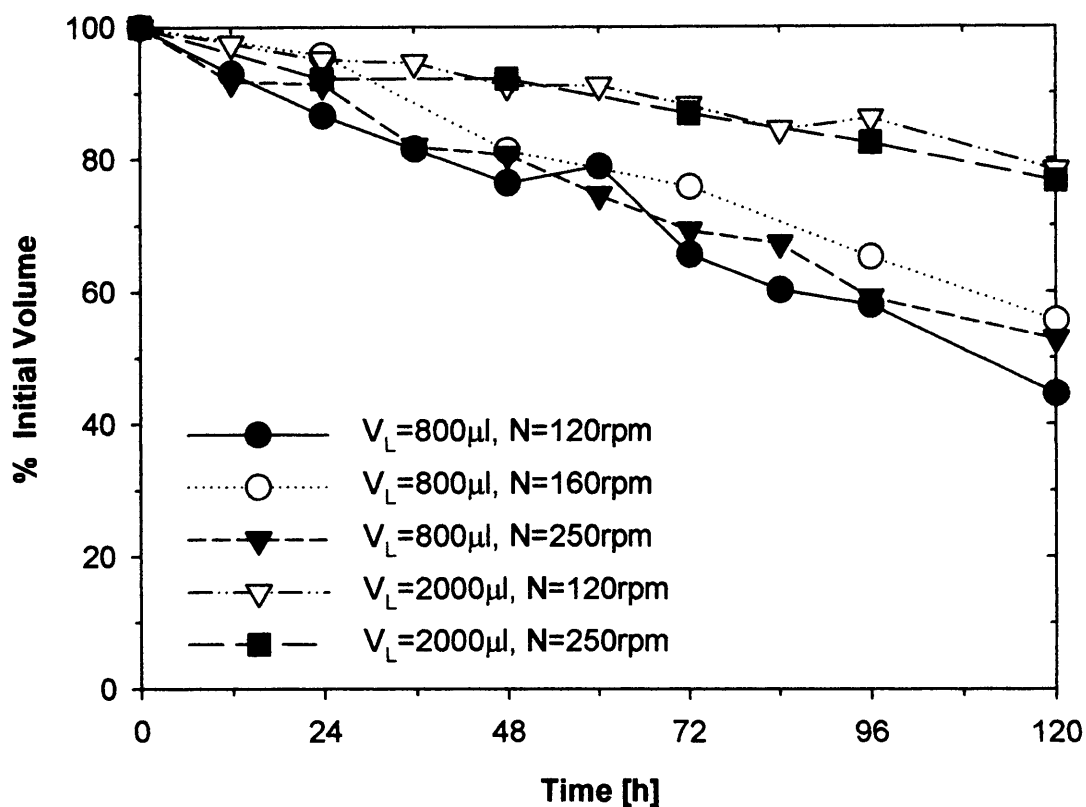


Figure 3.12: Evaporation from the liquid bulk of a 24-well (ULA) microplate at 37°C covered with a breath-easy membrane. The evaporation rate was determined gravimetrically as described in Section 2.1.5.

noted that all concentration values presented are under-estimates of the true value in the bulk liquid phase by a factor of up to 2.2.

3.7 Consideration of a Basis for Scale Translation From Shaken Microwell Plates to Shake Flasks and Bench-Scale STR

A variety of scale-down parameters have been proposed for mammalian cell-culture. These include: $k_L a$, aeration rate, impeller tip speed, fluid turnover rate, vessel geometry and P/V (Section 1.4.1). From the predictions made in Section 3.3, it seems unlikely that $k_L a$ will be a suitable scaling parameter as it is unlikely to be growth limiting. Other parameters such as aeration rate, geometry and impeller tip speed are not applicable to shaken microwells. P/V has a direct influence on both liquid phase mixing and gas-liquid mass transfer. Li et al. (2006) have shown the successful use of P/V for scaling a cell-culture process from 2-L to 2000-L scale. Therefore in this work P/V will be considered as an initial basis for scale-translation from microwell to conventional laboratory scales.

The CFD studies described in Section 2.6.2 predicted $P/V \approx 40 \text{ W m}^{-3}$ in a 24-well plate under the following conditions: $V_L = 800 \mu\text{l}$ and $N = 120 \text{ rpm}$. Using Equation (1.1) (Büchs et al., 2000a) and the properties of water at the working temperature of 37°C , it is possible to predict operating conditions for a 250ml shake flask where $P/V \approx 40 \text{ W m}^{-3}$.

Suitable conditions yielded from the analysis were $V_L = 100 \text{ ml}$ and $N = 120 \text{ rpm}$. These conditions enable the shake flask and microwell plate to be compared on the same shaker platform. Measurement of P/V in a 5-L STR was a factor of 10 lower at 8 W m^{-3} . As a initial basis for scale translation; growth kinetics, antibody production and metabolism in microwells and shake flask were compared at similar P/V

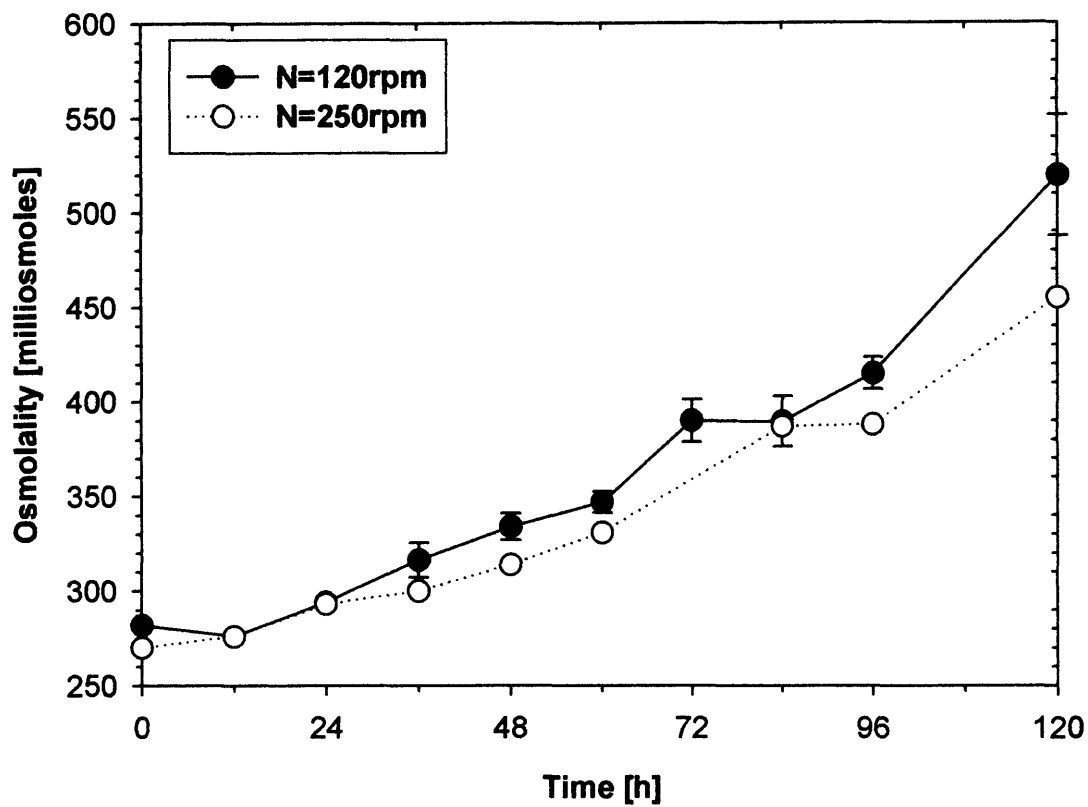


Figure 3.13: Variation of culture medium osmolality in shaken 24-well hybridoma cultures. Osmolality was measured using a Camlab freezing-point depression osmometer as described in Section 2.8.4. Hybridoma cultures were performed as described in Section 2.1.5. Error bars represent one standard deviation about the mean.

(40 W m³).

3.8 Summary

The engineering environment within the wells of a shaken 24-well plate has been investigated for cell-culture purposes. The key characteristics of liquid hydrodynamics, k_La , mixing, shear-rate, P/V , and liquid losses by evaporation have been quantified. Equivalent data from a typical 250 ml shake flask (100 ml, 120 rpm) and 5-L STR (3-L, 50 - 200 rpm) culture has been included for comparison and is summarised in Table 3.7 and Table 3.8.

To give some insight into the liquid phase hydrodynamics in the different bioreactor geometries, the Re , Ph , and Fr were calculated for various fill volumes and shaking speeds as described in Section 3.2. Transitional flow was predicted for the shake flask ($Re = 18,000$) and the STR. “In-phase” operation was predicted for both the shake flask ($Fr = 0.64$, $Ph = 2.68$) and microwells ($N \geq 200$ rpm).

Predictions of K_La in the microwell geometry were made using the correlation of Doig et al. (2005) as described in Section 3.3. All values were greater than the limiting value of 1 h^{-1} , suggesting oxygen transfer to the plates will be able to support cell densities of $10^7 \text{ cells ml}^{-1}$. Experimental measurements of k_La were made on the 5-L STR (Table 3.3) and again all values were greater than 1 h^{-1} .

The mixing of a small liquid addition to microwells was found to occur by two different mechanisms (Section 3.4.1). At $Re \leq 1,370$, the liquid addition passes to the bottom of the well, spreads along the bottom surface and then ascends the well as a continuous, horizontal front (Fig. 3.1). At $Re \geq 1,520$, the mixing was rapid and occurred evenly throughout the liquid bulk (Fig. 3.2). The majority of mixing times recorded in this work were lengthy, particularly at $Re \leq 1,370$. Published mixing times are typically less than 200 s, even at the production scale. An attempt was

made to reduce mixing time by employing baffles. A significant reduction in mixing time was observed (Fig. 3.6); unfortunately at Re between 730 and 1,220 many of the mixing times were still > 200 s. Mixing times measured in the 5-L STR were no longer than 100 s.

Evaporation from covered microwell plates was significant over the duration of a 120 hour culture . While only 10% of the initial volume leaves the plate, the vast majority sticks to the underside of the gas-permeable membrane. For an initial fill of $800 \mu\text{l}$, approximately 50% of the initial volume left the liquid bulk, while for $2000 \mu\text{l}$, only 20% had left the bulk. Due to this evaporation, osmolality gradually increased. However, this was not deemed significant until the death-phase.

CFD simulations were performed on 24-well plates to predict P/V and shear rate. P/V values were at least an order-of-magnitude less than those known to impact on cell performance. P/V has a direct influence on both hydrodynamics and gas-transfer. Moreover, it can be used successfully to scale mammalian cell -cultures (Li et al., 2006). As an initial basis for scale-translation between microwell and shake flasks, a P/V of 40 W m^{-3} was selected. Conditions were selected so both bioreactors could be cultured side-by-side on the same shaking platform. Unfortunately, P/V in the 5-L STR was somewhat less.

Having established a fundamental understanding of the hydrodynamics and oxygen-transfer in shaken 24-well plates, the influence of these on mammalian cell culture in shaken microwells will be examined in the following chapter.

Table 3.7: Summary of the main engineering parameters established for shaken 24-well (ULA) plates. Details of plate geometry and shaking conditions are given in Section 2.1.5.

Parameter	Section	N [rpm]							
		0	120	160	200	225	250	300	400
$V_L = 800 \mu\text{l}$									
Re_s	3.2	0	730	973	1220	1370	1520	1830	n/d
Fr	3.2	0	0.16	0.29	0.45	0.57	0.70	1.0	n/d
Ph	3.2	0	8.2	8.7	9.0	9.2	9.4	9.7	n/d
$K_{La} [\text{h}^{-1}]$	3.3	n/a	3.2	6.3	11	14	19	29	n/d
Mixing time [s]	3.4.1	3600 ± 848.5	2260 ± 210.7	1075 ± 9.240	468 ± 18.9	53 ± 8.7	3 ± 0.06	2 ± 0.06	n/d
Shear rate [s^{-1}]	3.5.1	0	190	n/d	98	99	84	73	147
P/V [W m^{-3}]	3.5.1	0	35	n/d	10	10	5	7	22
$V_L = 1000 \mu\text{l}$									
Re_s	3.2	0	730	973	1220	1370	1520	1830	n/d
Fr	3.2	0	0.16	0.29	0.45	0.57	0.70	1.0	n/d
Ph	3.2	0	8.8	9.2	9.6	9.8	10	10	n/d
$K_{La} [\text{h}^{-1}]$	3.3	n/a	2.5	5.1	8.6	12	15	23	n/d
Mixing time [s]	3.4.1	4483.3 ± 276.1	3048.3 ± 297.9	1650 ± 187.3	870 ± 30	159.5 ± 69.7	7.0 ± 0.1	1.7 ± 0.1	n/d
$V_L = 2000 \mu\text{l}$									
Re_s	3.2	0	730	973	1220	1370	1520	1830	n/d
Fr	3.2	0	0.16	0.29	0.45	0.57	0.70	1.0	n/d
Ph	3.2	0	11	11	12	12	12	n/d	
$K_{La} [\text{h}^{-1}]$	3.3	n/a	1.3	2.5	4.3	5.7	7.4	11	n/d
Mixing time [s]	3.4.1	$12,900 \pm 424$	$11,190 \pm 1,907$	$7,620 \pm 433$	$5,094 \pm 454$	$1,700 \pm 173$	129 ± 18	n/d	n/d

Table 3.8: Summary of the main engineering parameters established for a 5 L STR. Details of bioreactor geometry, agitation and aeration are given in Section 2.1.6.

Parameter	Section	N [rpm]					
		50	100	150	170	200	250
Re_i	3.2	5,900	12,000	18,000	20,000	23,000	29,000
k_{La} [h^{-1}]	3.3	4.35 ± 0.63	n/d	7.25 ± 0.92	n/d	9.30 ± 0.28	n/d
Mixing time [s]	3.4.2	99 ± 3.5	42.3 ± 2.5	20 ± 0.0	15.0	11.0 ± 1.0	8.0 ± 1.0
P/V [$W m^{-3}$]		0.13	1.0	3.4	5.0	8.0	16.0

Chapter 4

Kinetic Analysis of Shaken Microwell Cultures

4.1 Introduction and Aims

The culture of mammalian cells in static microwells is common practice during cloning and the initial stages of cell line selection (Wurm, 2004)(Tait et al., 2004). In these cases the aim is simply to identify high expressing clones and there is no intention to relate the data obtained to larger scales of operation. As described in Chapter 3 however, the use of microwell systems for the generation of bioprocess design data necessitates that the cells are cultured in suspension and the engineering environment the cells are exposed to is appropriately characterised. Given that the geometry of microwell plate is fixed in order to allow easy automation of experimental protocols, shaking of microtitre plates is the easiest and most efficient way to promote mixing of the liquid within each well. Shaking is necessary to ensure homogeneous cell suspension, the rapid blending of any liquid additions that might be used for pH control or in feeding strategies and also to promote gas-liquid mass transfer rates (Duetz et al., 2000)(Duetz and Witholt, 2001)(Elmahdi et al., 2003).

To date there are only two publications concerning shaken microwell cultures for mammalian cell culture process development (Girard et al., 2001)(Strobel et al., 2001). In the former, the use of shaken 12-well microtitre plates for the develop-

ment and optimisation of transient transfection processes was investigated. In the latter, the potential of replacing shake flask cultures with 96-DSW microtitre plate cultures for media development was studied. Although both studies showed comparable culture performance upon scale-up, no engineering basis for this translation was mentioned. This is likely to be caused by a lack of engineering analysis of the prevailing microwell hydrodynamics and gas-liquid mass transfer in both publications. As mentioned in Section 3.1, detailed understanding of the engineering environment in shaken microwells is vital for defining optimal operation of cell-cultures and a reliable basis for process scale-up. Moreover, the effect of this environment on culture performance is unknown.

The aim of this second chapter then is to more fully characterise hybridoma growth, antibody production and metabolism in batch shaken microwell cultures than has been previously reported. Experiments will be performed within the engineering environment that was extensively characterised in Chapter 3. This will allow the impact of the fluid hydrodynamics on culture performance to be understood and also help define optimal culture conditions. The specific objectives of this chapter are thus to:

- Study the effect of shaking speed and fill volume on hybridoma growth, antibody production and metabolism over the range of operating conditions used in Chapter 3, and attempt to relate culture performance to the prevailing engineering environment.
- Examine the influence of well geometry, well coating and the inclusion of various baffle configurations on culture performance.
- Experimentally measure dissolved oxygen tension in 24-well plate and shake-flask cultures, operating under the conditions described in Chapter 3, to establish if any gas-liquid mass transfer issues might be limiting culture performance (Section 3.3).

4.2 Initial Assessment of Well Geometry

The choice of microwell geometry for a particular cell culture application depends on a number of considerations including cell-line suitability, number and volume of samples required, applicability to automation, and compatibility with analytical equipment such as spectrophotometers.

The density of wells on a standard 96-well plate readily lends this design to high-throughput cell culture process development. In addition, they are compatible with liquid-handling robots allowing easy automation of experimental protocols (Lye et al., 2003). One major disadvantage is the small sample volume per well that may limit some analytical work, for example, flow cytometry. 24-well plates overcome this disadvantage due to the 1.4- to 1.6- fold increase in total well volume. However, as described in Section 3.6, the liquid evaporation rate is greater in 24-well than 96-well plates. In this section, the feasibility of culturing VPM 8 hybridoma cells in both 96- and 24- well plates was initially examined.

Two microwell formats, 24-SRW (ULA) and 96-DSW plates, as described in Section 2.1.5, were inoculated with VPM 8 cells. The well fill volumes were 800 μl for the 24-SRW (ULA) plate and 300 μl - 600 μl for the 96-DSW plate. The shaking speed was 120 rpm for the 24-SRW (ULA) plate and 200 rpm for the 96-DSW plate. The conditions selected for the 96-DSW plate were taken from Strobel et al. (2001).

The well geometry was found to have a pronounced effect on cell growth (Fig. 4.1). The peak viable cell concentration ($1.377 \times 10^6 \pm 1.873 \times 10^5$ cells ml^{-1}) obtained in the 24-SRW (ULA) plate was nearly 2.5 times that of the 96-DSW (300 μl) culture and over 3 times that of the 96-DSW (600 μl) culture. The viability of the 96-DSW cultures started to decline 12 hours post-inoculation. In contrast, the 24-SRW (ULA) culture maintained a high viability (> 90%) for the first 60 hours of culture before falling to 87% at 72 hours.

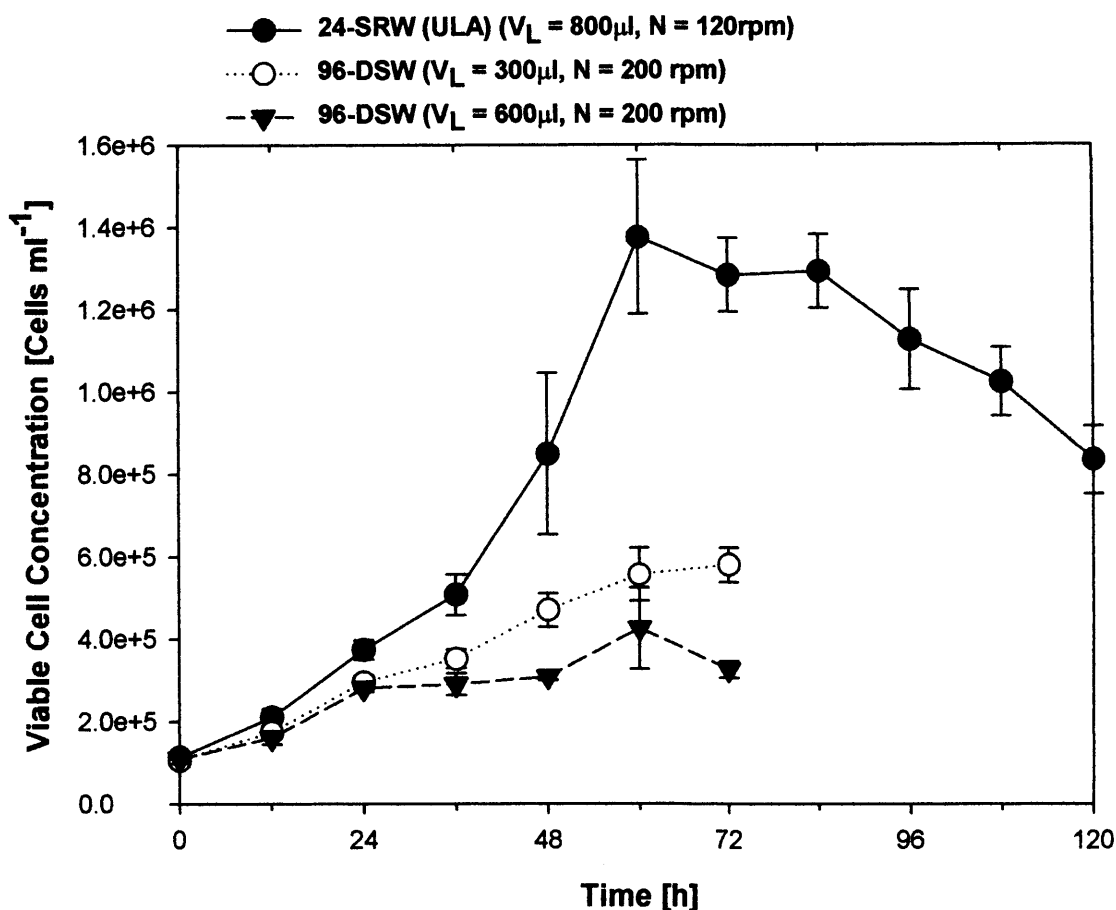


Figure 4.1: Effect of well geometry on VPM 8 hybridoma cell growth in shaken 24-SRW (ULA) and 96-DSW plates. Experiments were performed as described in Section 2.1.5. Hybridoma cells were initially taken from mid-exponential cultures and diluted to 1×10^5 viable cells ml^{-1} in RPMI-1640 media supplemented with 10% (v/v) fetal bovine serum. Diluted culture was inoculated into each well of a Corning 24-well ultra-low attachment plate or a 96-well ABgene 2.2 ml storage plate. Both plates were covered with a breathe-easy membrane and placed on an orbital shaker in a humidified incubator (37°C , 5% (v/v) CO_2). Every twelve hours, three wells were sacrificed for cell counts and metabolite analysis. All cell counts were conducted using a CASY TTC automated counter. Error bars represent one standard deviation about the mean.

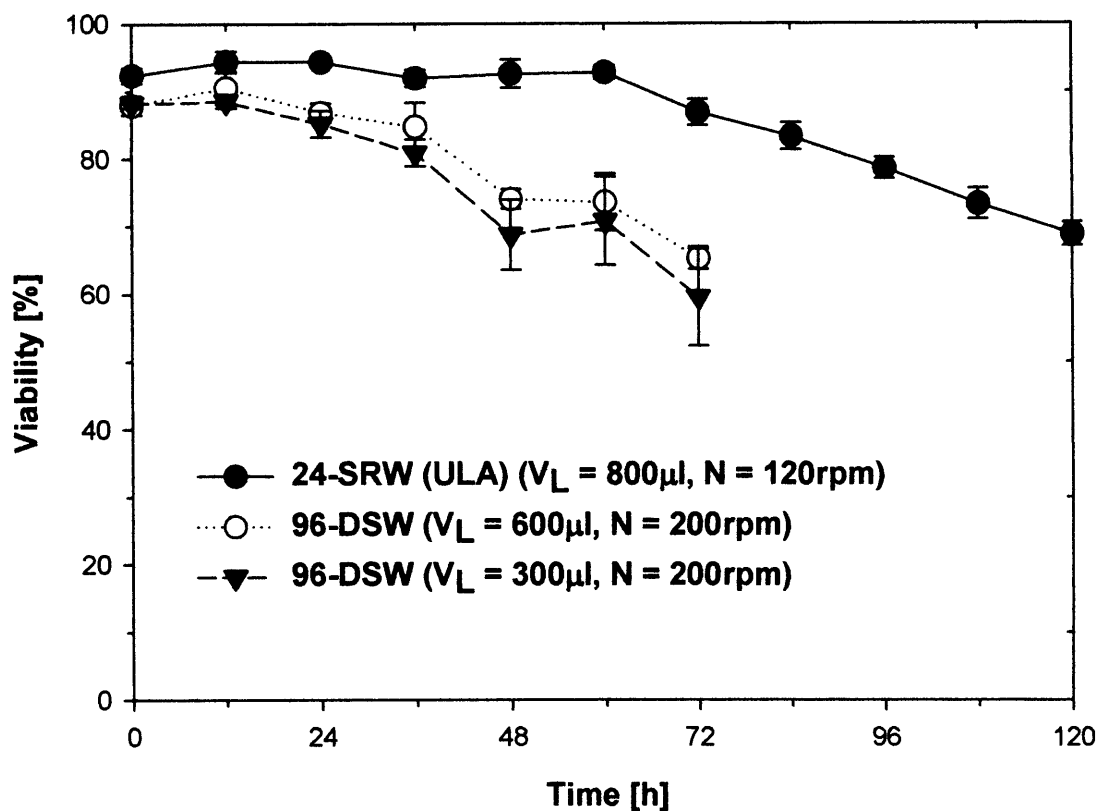


Figure 4.2: Effect of well geometry on VPM 8 hybridoma viability in shaken 24-SRW (ULA) and 96-DSW plates. Experiments performed as described in Fig. 4.1. Every twelve hours, three wells were sacrificed for cell counts and metabolite analysis. All viability assessments were conducted using a CASY TTC automated cell counter. Error bars represent one standard deviation about the mean.

It has previously been shown that it is possible to culture mammalian cells in shaken 96-well plates. Strobel et al. (2001) have demonstrated the successful cultivation of CHO DG44 cells in 96-deep well microplates. Likewise, Deshpande and Heinzle (2004) have also cultured CHO cells in 96-well format. Taken together with the data presented in Fig. 4.1, these reports suggest successful culture in 96-well plates is cell-line specific. To investigate this point further, a quick assessment of CHO-S growth in 96-DSW plates was made. The well fill volume used was 300 μl and the shaking speed was 200 rpm. No attempt was made to optimise the culture conditions.

Growth of CHO-S cells in shaken 96-DSW plates was found to be superior to the VPM 8 cell line under equivalent operating conditions (Fig. 4.3). The peak viable cell concentration ($1.075 \times 10^6 \pm 1.255 \times 10^5 \text{ cell ml}^{-1}$) was nearly twice as high as that achieved by the VPM 8 cells. The CHO-S cells maintained a high viability (> 90%) throughout the culture period. By contrast, the viability of the VPM 8 culture started to decline 12 hours after inoculation. These results support the hypothesis of successful culture in 96-well format being cell-line specific. In addition to the experiments performed in 96-DSW plates, hybridoma cultures in standard 96-well formats were attempted. The results were similar to those measured in 96-DSW: very little growth observed and a continuous decline in viability after inoculation [data not shown]. For further studies into the effect of microwell conditions on hybridoma cell growth and protein production, 24-SRW plates were selected.

4.3 Effect of Shaking Speed on Cell Growth and Antibody Production in Shaken 24-SRW (ULA) Microtitre Plates

As described in Chapter 3, the shaking speed used for microwell cultures can have a pronounced effect on engineering parameters such as mixing, $k_L a$ and P/V. In or-

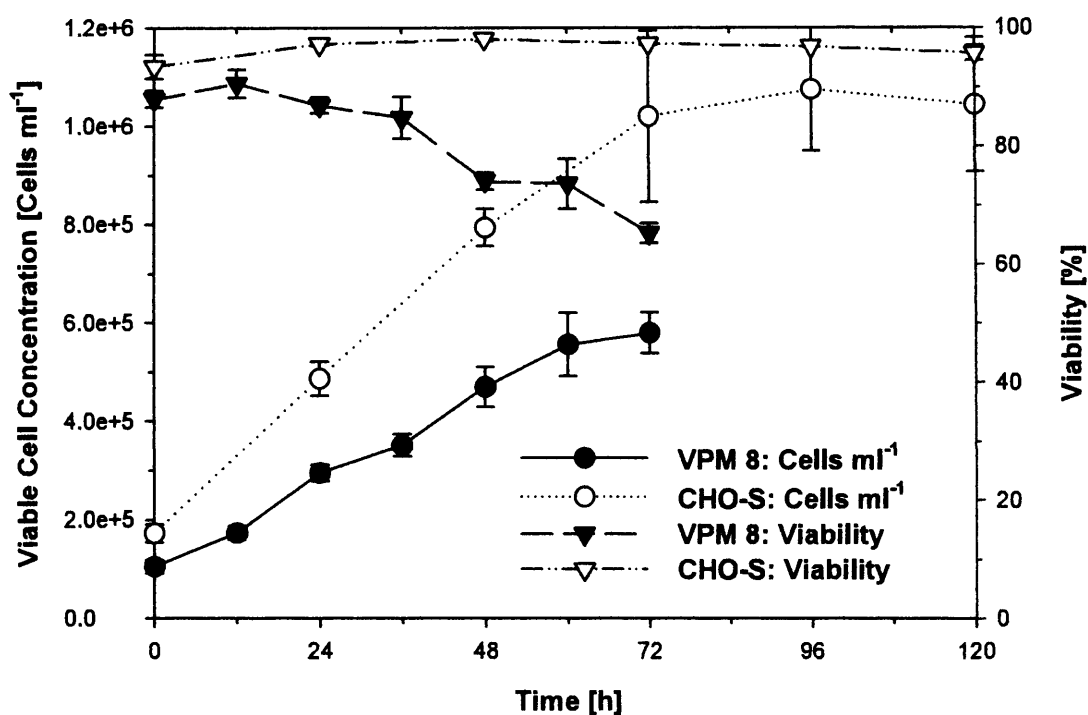


Figure 4.3: Comparison of the cell growth and viability of VPM 8 hybridoma and CHO-S cells in shaken 96-DSW microtitre plates. Experiments were performed as described in Section 2.1.5. Hybridoma cells were initially taken from mid-exponential cultures and diluted to 1×10^5 viable cells ml^{-1} in RPMI-1640 media supplemented with 10% (v/v) FBS. CHO-S cells were taken from mid-exponential cultures and diluted to 2×10^5 viable cells ml^{-1} in CHO-S-SFM II media. $300 \mu\text{l}$ of diluted culture was inoculated into each well of a 96-well ABgene 2.2 ml storage plate. Plates were covered with a breathe-easy membrane and placed on an orbital shaker in a humidified incubator (37°C , 5% (v/v) CO_2). Every 12-24 hours, three wells were sacrificed for cell counts and metabolite analysis. All cell counts and viability assessments were conducted using a CASY TTC automated counter. Error bars represent one standard deviation about the mean.

der to examine the effect of shaking speed on cell growth and antibody production, 24-SRW (ULA) plates were inoculated with VPM 8 hybridoma cells and shaken at speeds ranging from 120 to 250 rpm. The well fill volume was 800 μl . The culture kinetics are shown in Figs. 4.4, 4.5, 4.7, 4.8 and 4.6 while Table 4.1 summarises the calculated kinetics parameters and overall performance.

Better growth was observed at 120 and 160 rpm (Fig. 4.4)(Table 4.1) compared to all the other speeds tested. Mean viable cell concentrations at 120 rpm ($1.285 \pm 0.9019 \times 10^6 \text{ cell ml}^{-1}$) and 160 rpm ($1.291 \pm 0.8793 \times 10^6 \text{ cell ml}^{-1}$) were significantly greater than for the 200 rpm ($0.9360 \pm 0.01524 \times 10^6 \text{ cell ml}^{-1}$) and 250 rpm ($0.9698 \pm 0.07980 \times 10^6 \text{ cell ml}^{-1}$) after 72 hours of culture (ANOVA, $p < 0.005$). In addition, the integral viable cell concentrations (IVC) obtained at 120 rpm ($4.262 \times 10^9 \text{ cells.day.l}^{-1}$) and 160 rpm ($4.317 \times 10^9 \text{ cells.day.l}^{-1}$) were greater than those achieved at other speeds. Cells cultured at 120 rpm had the highest maximum specific growth rate (0.04 h^{-1}): between 15-25 % greater than that of the 160 rpm, 200 rpm and 250 rpm cultures. The growth results obtained at all shaking speeds (maximum viable cell concentrations between 0.9 and $1.4 \times 10^6 \text{ cells ml}^{-1}$) compare well with typical values reported for hybridoma cell growth in shake flasks [$(0.9 - 1.3) \times 10^6 \text{ cells ml}^{-1}$] (Schmid et al., 1990)(Ozturk and Palsson, 1991b)(Zhang, Szita, Boccazzi, Sinskey and Jensen, 2005).

All cultures maintained a high viability ($> 90 \%$) for the first 60 hours of culture (Fig. 4.5), after which the viability started to decline. The onset of the death phase coincided with the complete exhaustion of the main energy source L-glutamine (Fig. 4.8) suggesting it may be a limiting nutrient. Previous studies of hybridoma cell cultures operated in batch mode have reported L-glutamine as the limiting nutrient (Schmid et al., 1990)(Ozturk and Palsson, 1991b).

The shaking speed had no significant effect on antibody titre (Fig. 4.6). Unfortunately a trend could not be established that would allow any correlation of antibody

titre with shaking speed. The highest final titre ($49 \pm 6.2 \text{ mg l}^{-1}$) was achieved at 250 rpm, 20% higher than the lowest titre achieved at 120 rpm (Table 4.1). The highest specific production rate (SPR) ($14 \pm 1.4 \text{ mg}(10^9 \text{ cells.day})^{-1}$) was achieved at 200 rpm and was 60% higher than the lowest SPR achieved at 120 rpm. The results compare well with antibody titres reported for shake flask cultures of hybridoma cells ($40 - 50 \text{ mg l}^{-1}$)(Schmid et al., 1990)(Ozturk and Palsson, 1991b).

Glucose was never exhausted in any microwell culture so cannot be the limiting nutrient (Fig. 4.7). This has previously been reported for hybridoma cell culture performed in shake flasks (Schmid et al., 1990)(Miller et al., 2000)(Ozturk and Palsson, 1991b). Overall, the consumption of glucose was higher at 200 and 250 rpm (Table 4.1). These values were approximately 50% higher than the consumption rates at 120 rpm and 160 rpm. Lactate production occurred throughout the culture and increased with shaking speed from $0.16 \text{ g}(10^9 \text{ cells.day})^{-1}$ at 120 rpm, to $0.36 \text{ g}(10^9 \text{ cells.day})^{-1}$ at 250 rpm. The concentration of L-lactate measured in the study ($0.2 - 1.3 \text{ g l}^{-1}$) compared well with typical values reported for hybridoma cell cultures in the literature [$0.5 - 3 \text{ g l}^{-1}$] (Miller et al., 2000)(Ozturk and Palsson, 1991b)(Schmid et al., 1990).

The pH of the cultures in each well were analysed throughout the cultivation period. At inoculation, the offline pH measurements were in the range 7.8 - 8.0. By 84 hours, the pH of all cultures had decreased to between 6.8 and 7.3.

Limiting conditions were not found over the range of shaking speeds (120 - 250 rpm, 800 μl) tested in this study. It is believed that the agitation provided sufficient energy input to avoid limitations in oxygen supply and mixing. Firstly, theoretical K_La values were greater than the limiting value of 1 h^{-1} (Section 3.3), thus ensuring adequate oxygen supply; secondly, CFD predictions of P/V (Section 3.5.1) suggest hydrodynamic forces, or “shear”, will not be lethal to the cells; thirdly, it is believed that osmolality increases due to evaporation (Section 3.6) will not inhibit the culture

performance and finally, pH measurements during the growth phase, 7.0 - 8.1, are within a range not expected to impact on culture performance (Osman et al., 2002).

The reduction of hybridoma culture performance with increased shaking speed is thought to be the result of hydrodynamic stress impacting on the cells. From the work presented in this thesis, the engineering environment for optimum performance (120 rpm, 800 μ l) is very benign: "out of phase" conditions were predicted and mixing time experiments showed negligible axial flow. In light of CHO-S growth in 96 and 24 well formats, this work suggests the VPM 8 hybridoma cell-line is fragile and its suitability for large-scale culture questionable.

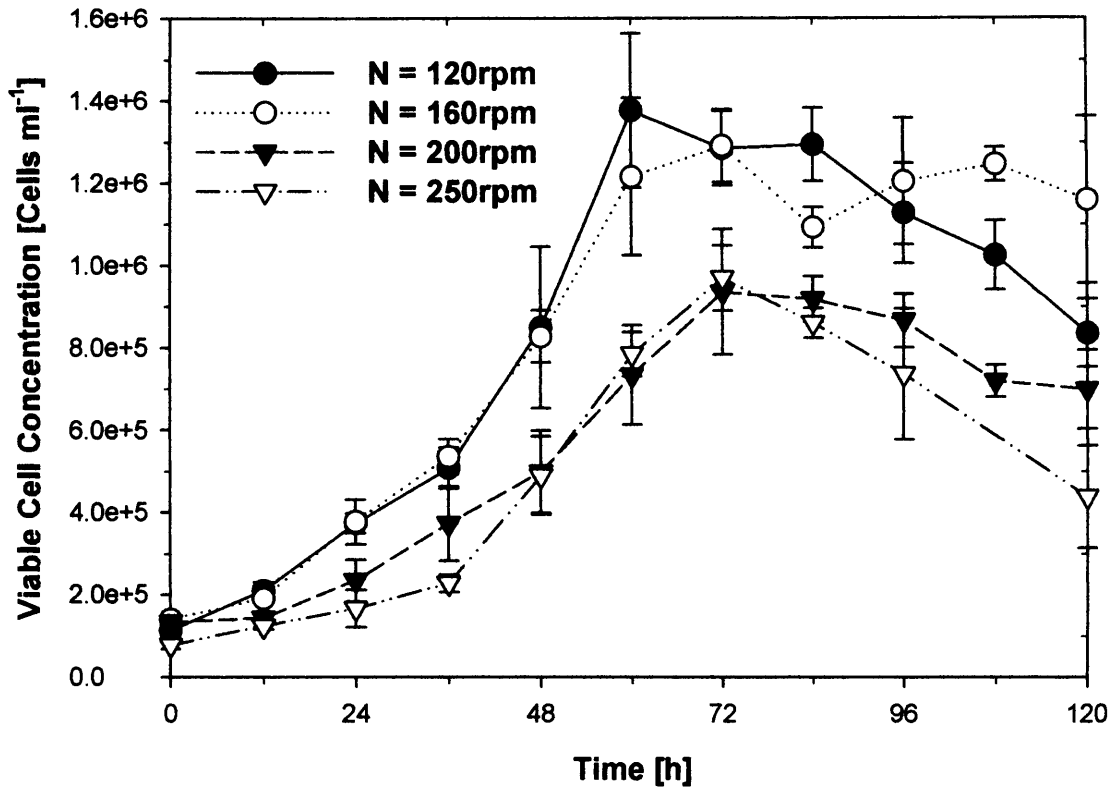


Figure 4.4: Effect of shaking speed On VPM 8 hybridoma cell growth in shaken 24-SRW (ULA) plates. Hybridoma cells were taken from mid-exponential cultures and diluted to 1×10^5 viable cells ml^{-1} in RPMI-1640 media supplemented with 10% (v/v) FBS. $800 \mu\text{l}$ of diluted culture was inoculated into each well of a Corning 24-well ultra-low attachment plate which was covered with a breathe-easy membrane and placed on an orbital shaker in a humidified incubator (37°C , 5% (v/v) CO_2). Every 12 - 24 hours, three wells per plate were sacrificed for cell counts and metabolite analysis. All cell counts were conducted using a CASY TTC automated counter. Error bars represent one standard deviation about the mean.

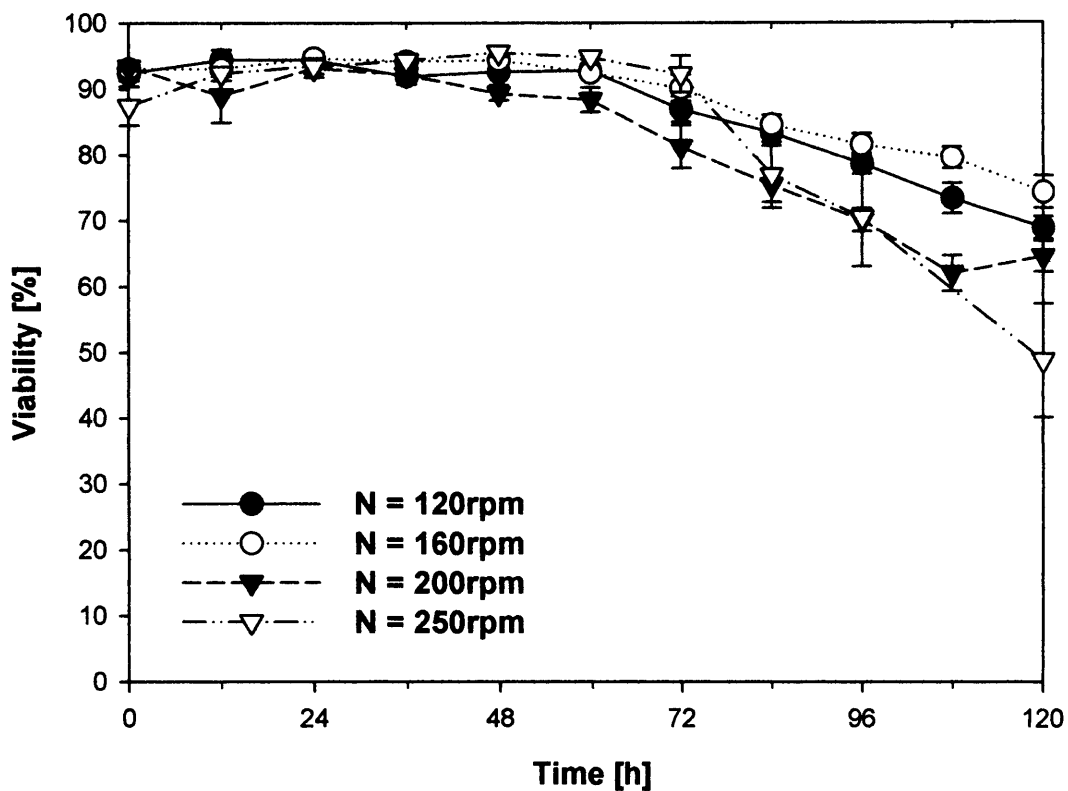


Figure 4.5: Effect of shaking speed on VPM 8 hybridoma viability in shaken 24-SRW (ULA) plates. Experiments were performed as described in Fig. 4.4. Every twelve hours, three wells per plate were sacrificed for cell counts and metabolite analysis. Viability assessment was conducted using a CASY TTC automated counter. Error bars represent one standard deviation about the mean.

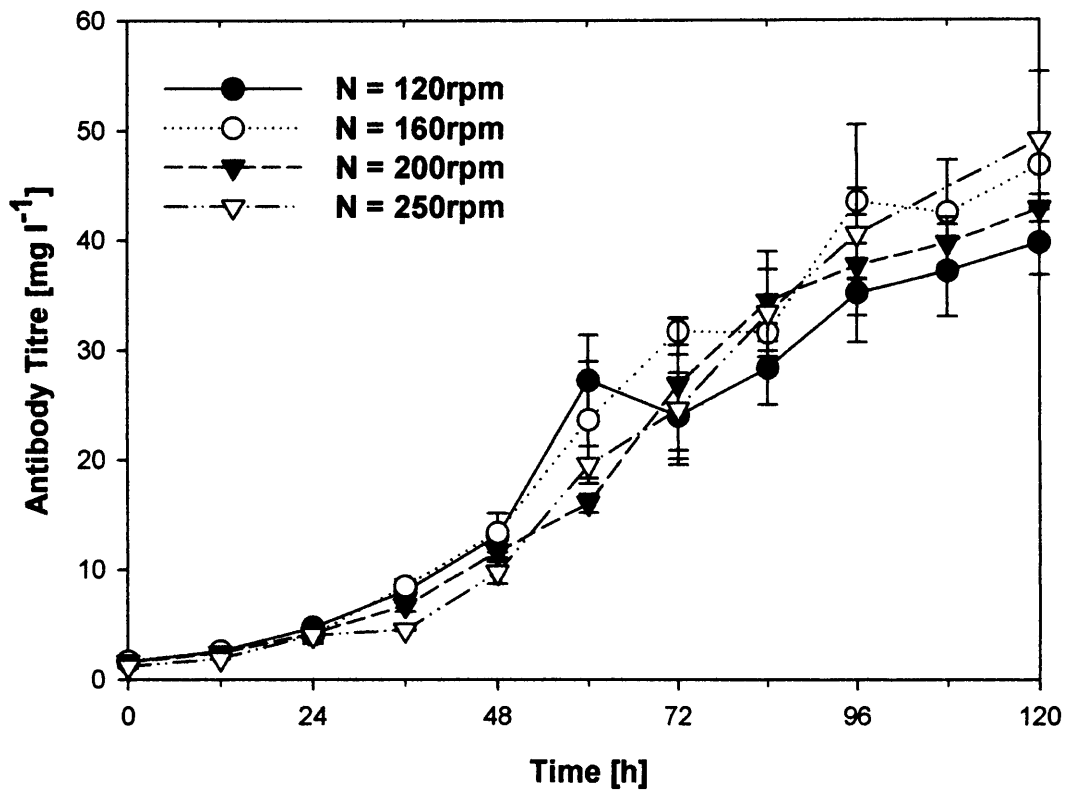


Figure 4.6: Effect of shaking speed on antibody concentration from VPM 8 hybridoma cells in shaken 24-SRW (ULA) plates. Experiments were performed as described in Fig. 4.4. Every twelve hours, three wells per plate were sacrificed for cell counts and metabolite analysis. Antibody concentration was determined using ELISA as described in Section 2.8.2. Error bars represent one standard deviation about the mean.

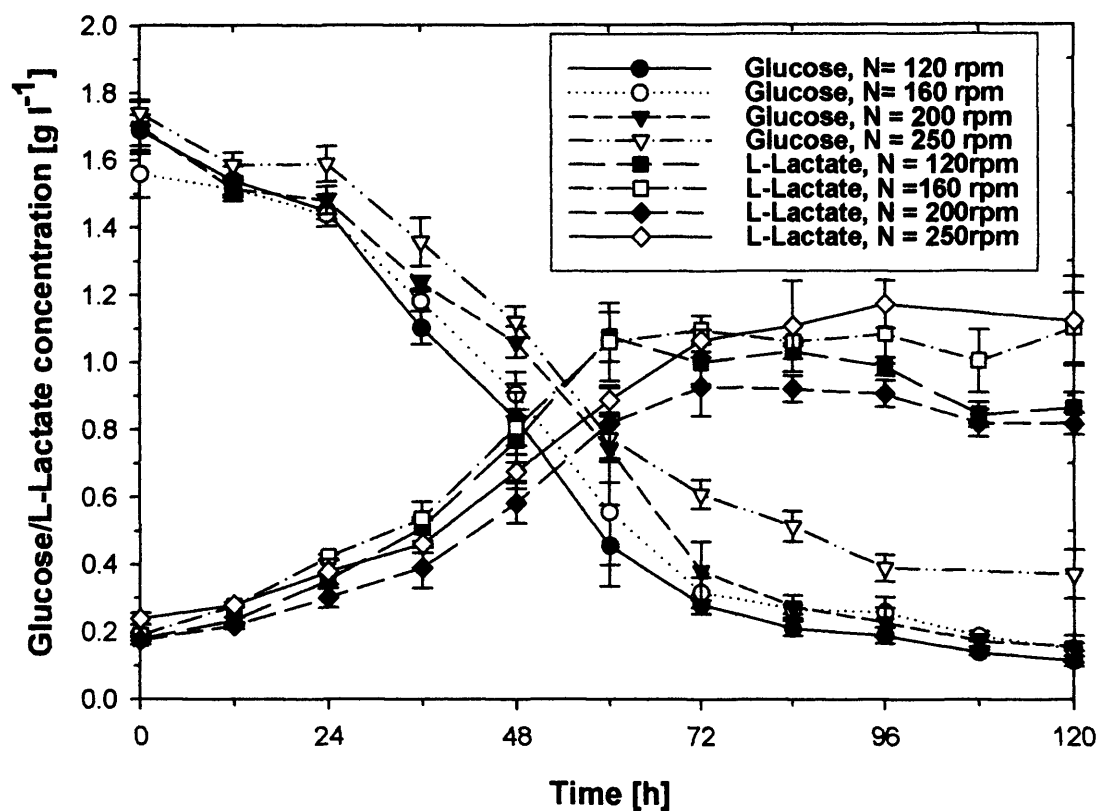


Figure 4.7: Effect of shaking speed on VPM 8 hybridoma glucose consumption and L-lactate production in shaken 24-SRW (ULA) plates. Experiments were performed as described in Fig. 4.4. Every twelve hours, three wells per plate were sacrificed for cell counts and metabolite analysis. Glucose and L-lactate concentrations were assessed using a YSI 2700 bioanalyser as described in Section 2.8.3. Error bars represent one standard deviation about the mean.

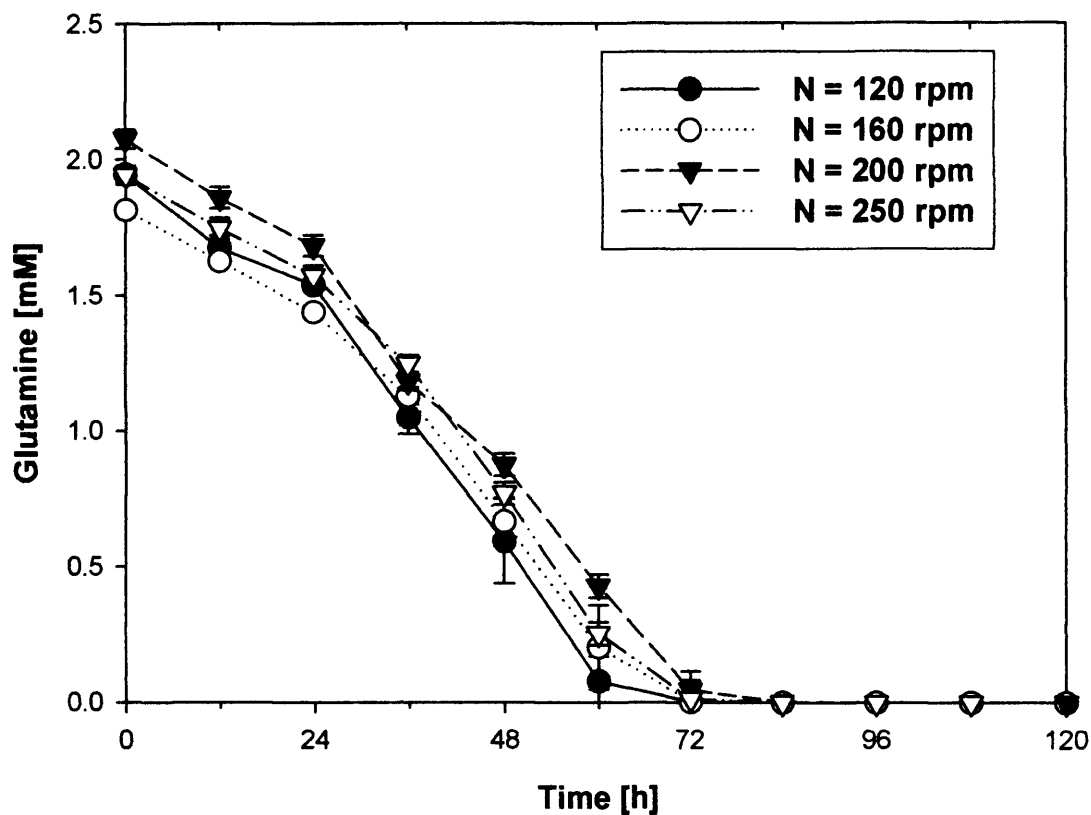


Figure 4.8: Effect of shaking speed on VPM 8 hybridoma L-glutamine consumption in shaken 24-SRW (ULA) plates. Experiments were performed as described in Fig. 4.4. Every twelve hours, three wells per plate were sacrificed for cell counts and metabolite analysis. Glutamine concentrations were assessed using a YSI 2700 bioanalyser as described in Section 2.8.3. Error bars represent one standard deviation about the mean.

Table 4.1: Effect of shaking speed on growth, antibody production and metabolism during the culture of VPM 8 hybridoma cells in shaken 24-SRW (ULA) plates. Experiments were performed as described in Fig. 4.4. Growth rate, integral viable cell concentration and average specific production/consumption rates were estimated from Figs.4.4, 4.5, 4.7, 4.8 and 4.6 as described in Section 2.7.

Culture parameter	N = 120 rpm		N = 160 rpm		N = 200 rpm		N = 250 rpm	
	Mean	CV [%]						
Final antibody concentration [mg l ⁻¹]	40	7	47	1	43	3	49	13
Integral of viable cell concentration [10 ⁹ cells.day.l ⁻¹]	4.262	3	4.317	7	2.915	10	2.629	8
Peak viable cell concentration [cells ml ⁻¹]	1.377x10 ⁶	14	1.291x10 ⁶	7	9.359x10 ⁵	16	9.009x10 ⁵	4
Maximum specific growth rate [h ⁻¹]	0.040	2	0.037	0	0.035	8	0.038	1
Specific antibody production rate [mg (10 ⁹ cells.day) ⁻¹]	9	4	11	0	14	10	13	15
Specific glucose consumption rate [g (10 ⁹ cells.day) ⁻¹]	0.37	3	0.33	1	0.54	16	0.52	4
Specific lactate production rate [g (10 ⁹ cells.day) ⁻¹]	0.16	11	0.21	7	0.22	4	0.36	21
Lactate produced / glucose consumed [g g ⁻¹]	0.43	8	0.65	8	0.42	11	0.70	25

4.4 The Effect of Well Fill Volume on Cell Growth and Antibody Production in Shaken 24-SRW (ULA) Microtitre Plates

For microbial systems grown in 96-DSW and 96-SRW plates it has previously been shown that fill volume has a significant impact on K_{La} (Hermann et al., 2003) and cell growth rate (Kensy, Zimmermann, Knabben, Anderlei, Trauthwein, Dingerdisen and Büchs, 2005). In general, both parameters decrease with an increase in fill volume. In the case of the 24-SRW geometry used here, the results in Section 3.3 showed that k_{La} is unlikely to be limiting for the vast majority of anticipated conditions. To investigate the influence of fill volume on hybridoma culture cell growth and antibody production were determined by inoculating a 24-SRW (ULA) plate with VPM 8 hybridoma cells in either 800 μl or 2000 μl of media. The microwell plates were then shaken at 120 or 250 rpm. The culture kinetics are shown in Figs. 4.9, 4.10, 4.12, 4.13 and 4.11 while Table 4.2 summarises the calculated kinetic parameters and overall performance.

In terms of growth (Fig. 4.9), the culture with the lowest fill volume and shaking speed (800 μl , 120 rpm) performed the best which is in agreement with literature findings for microbial systems. This culture achieved both the highest peak viable cell concentration (1.377×10^6 cells ml^{-1}) and IVC (4.262×10^9 cells.day.l $^{-1}$) (Table 4.2). The worst performance, in terms of cell growth, was observed for the 2000 μl fill volume shaken at 120 rpm. The peak viable cell concentration (6.832×10^6 cells ml^{-1}) and IVC (2.19×10^9 cells.day.l $^{-1}$) were the lowest of all experiments. Furthermore, the viability of this culture started to decline 36 hours after inoculation (Fig. 4.10).

In contrast to cell growth, the fill volume only had a small effect on the antibody titre (Fig. 4.11). The highest titre achieved was 50 ± 6 mg l $^{-1}$ (800 μl , 250 rpm), nearly 30% greater than that of the 2000 μl , 250 rpm culture. Fill volume also had a noticeable influence on the SPR. The highest SPR achieved was 18.3 ± 4.2 mg

$(10^9 \text{ cells.day})^{-1}$ ($2000 \mu\text{l}$, 120rpm) over twice that obtained in the $2000 \mu\text{l}$, 250 rpm culture.

Glucose was not exhausted in any experiment until 120 hours so cannot be the limiting nutrient (Fig. 4.12). The glucose consumption and lactate production rates (Table 4.2) were highest for the $2000 \mu\text{l}$, 120 rpm experiment ($0.79 \text{ mg}(10^9 \text{ cells.day})^{-1}$ and $0.65 \text{ mg}(10^9 \text{ cells.day})^{-1}$ respectively) and lowest for $800 \mu\text{l}$, 120 rpm culture ($0.37 \text{ mg}(10^9 \text{ cells.day})^{-1}$ and $0.16 \text{ mg}(10^9 \text{ cells.day})^{-1}$ respectively). L-lactate production by the $2000 \mu\text{l}$, 120 rpm culture was significantly higher than the other cultures studied (Fig. 4.12). L-glutamine was exhausted by all cultures after 72 hours except the $2000 \mu\text{l}$, 120 rpm experiment (Fig. 4.13). In this particular case, L-glutamine was not exhausted during the 120 hour culture period.

At inoculation, the pH of all experiments varied from 7.8 - 8.0, and thereafter remained in the range typical of those used to culture mammalian cells, 7.0 - 7.5. The pH for the $2000 \mu\text{l}$, 120 rpm experiment dropped to 6.8 after 84 hours.

In contrast to Section 4.3 where the shaking speed was shown to have little effect on culture performance, variations in fill volume had a more noticeable impact. This was particularly apparent at 120 rpm. With an $800 \mu\text{l}$ fill volume, the peak viable cell concentration and IVC were approximately double those achieved at $2000 \mu\text{l}$. At the higher fill volume, cell sedimentation was observed, along with higher glucose consumption, higher lactate production and higher antibody production rate suggesting an increase in the cellular metabolism at the expense of reduced growth. This phenomenon is thought to be the result of more cellular energy being diverted to make antibody rather than biomass (Miller et al., 2000)(Ozturk and Palsson, 1991b)(Muething et al., 2003)(Dinnis and James, 2005). It is likely that at the higher fill volumes inadequate oxygen transfer brought about this cellular response. In the next section, 24-SRW plates are instrumented to enable the non-invasive DOT measurement of cell cultures to test this hypothesis. A similar technique can

be invoked to measure pH.

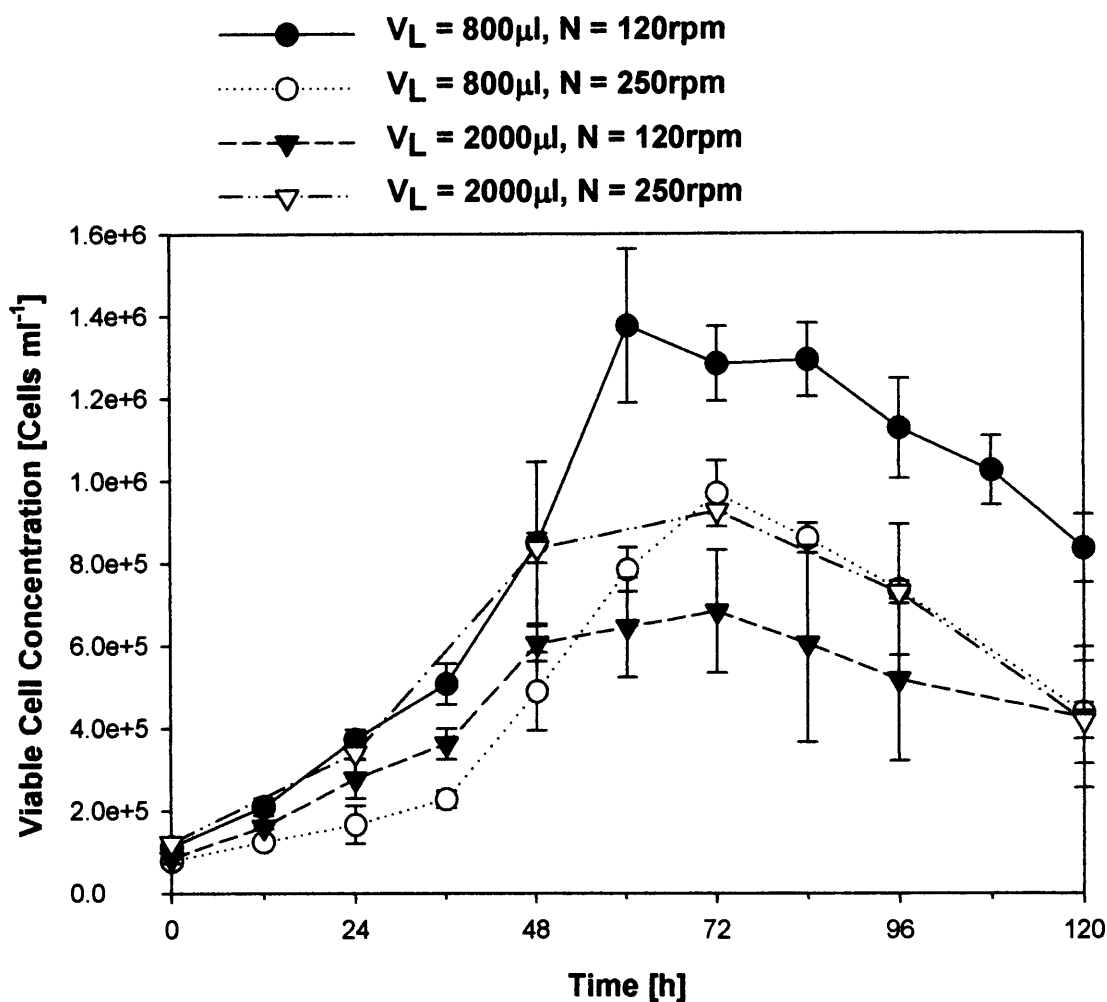


Figure 4.9: Effect of well fill volume on VPM 8 hybridoma growth in 24-SRW (ULA) microtitre plates. Hybridoma cells were taken from mid-exponential cultures and diluted to 1×10^5 viable cells ml^{-1} in RPMI-1640 media supplemented with 10% (v/v) FBS. Either $800 \mu\text{l}$ or $2000 \mu\text{l}$ of diluted culture was inoculated into each well of a Corning 24 well ultra-low attachment plate which was covered with a breathe-easy membrane and placed on an orbital shaker ($N = 120 \text{rpm}$ or 250rpm) in a humidified incubator (37°C , 5% (v/v) CO_2). Every 12 - 24 hours, three wells were sacrificed for cell counts and metabolite analysis. All cell counts were conducted using a CASY TTC automated counter. Error bars represent one standard deviation about the mean.

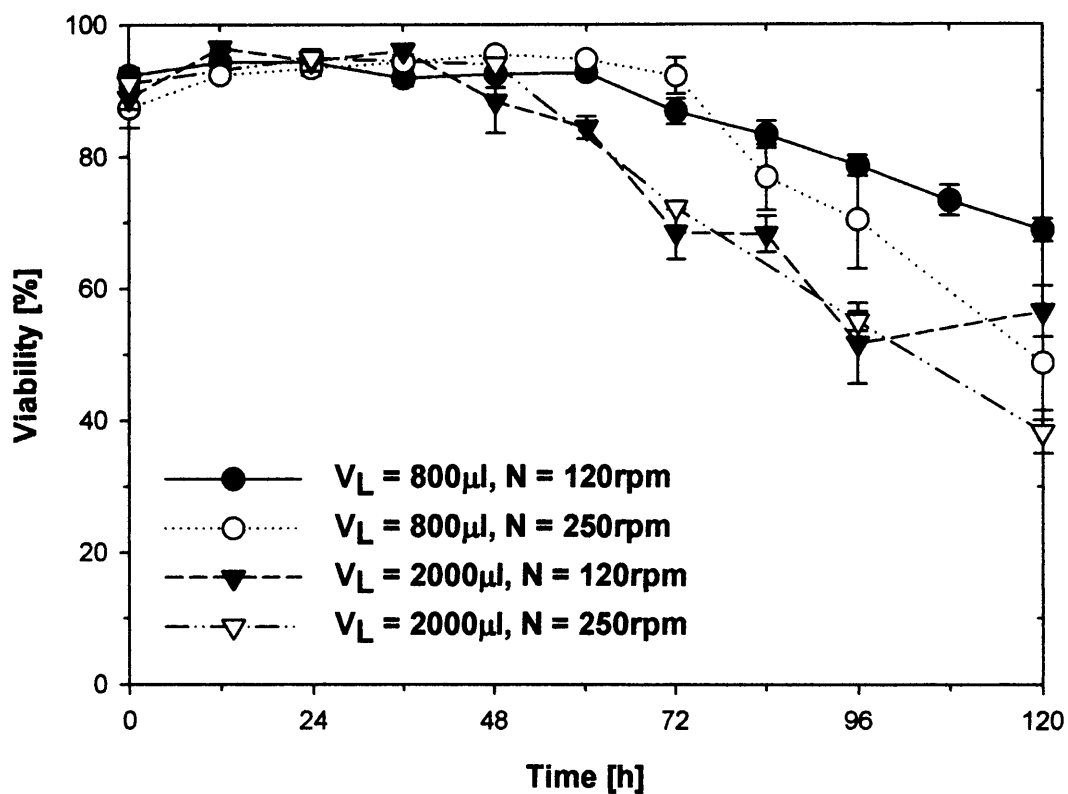


Figure 4.10: Effect of well fill volume on VPM 8 hybridoma viability in 24-SRW (ULA) microtitre plates. Experiments were performed as described in Fig. 4.9. Every 12 - 24 hours, three wells were sacrificed for cell counts and metabolite analysis. Viability was determined using a CASY TTC automated cell counter. Error bars represent one standard deviation about the mean.

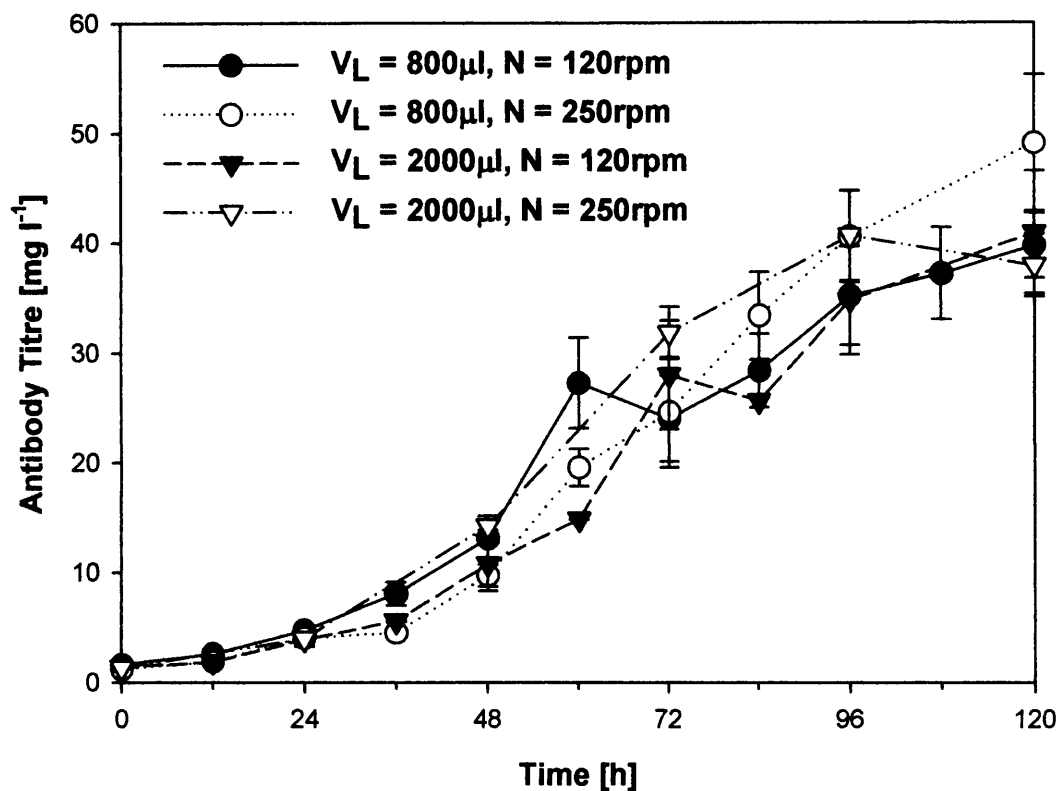


Figure 4.11: Effect of well fill volume on VPM 8 hybridoma antibody production in 24-SRW (ULA) microtitre plates. Experiments were performed as described in Fig. 4.9. Every 12 - 24 hours, three wells were sacrificed for cell counts and metabolite analysis. Antibody concentration was determined using ELISA as described in Section 2.8.2. Error bars represent one standard deviation about the mean.

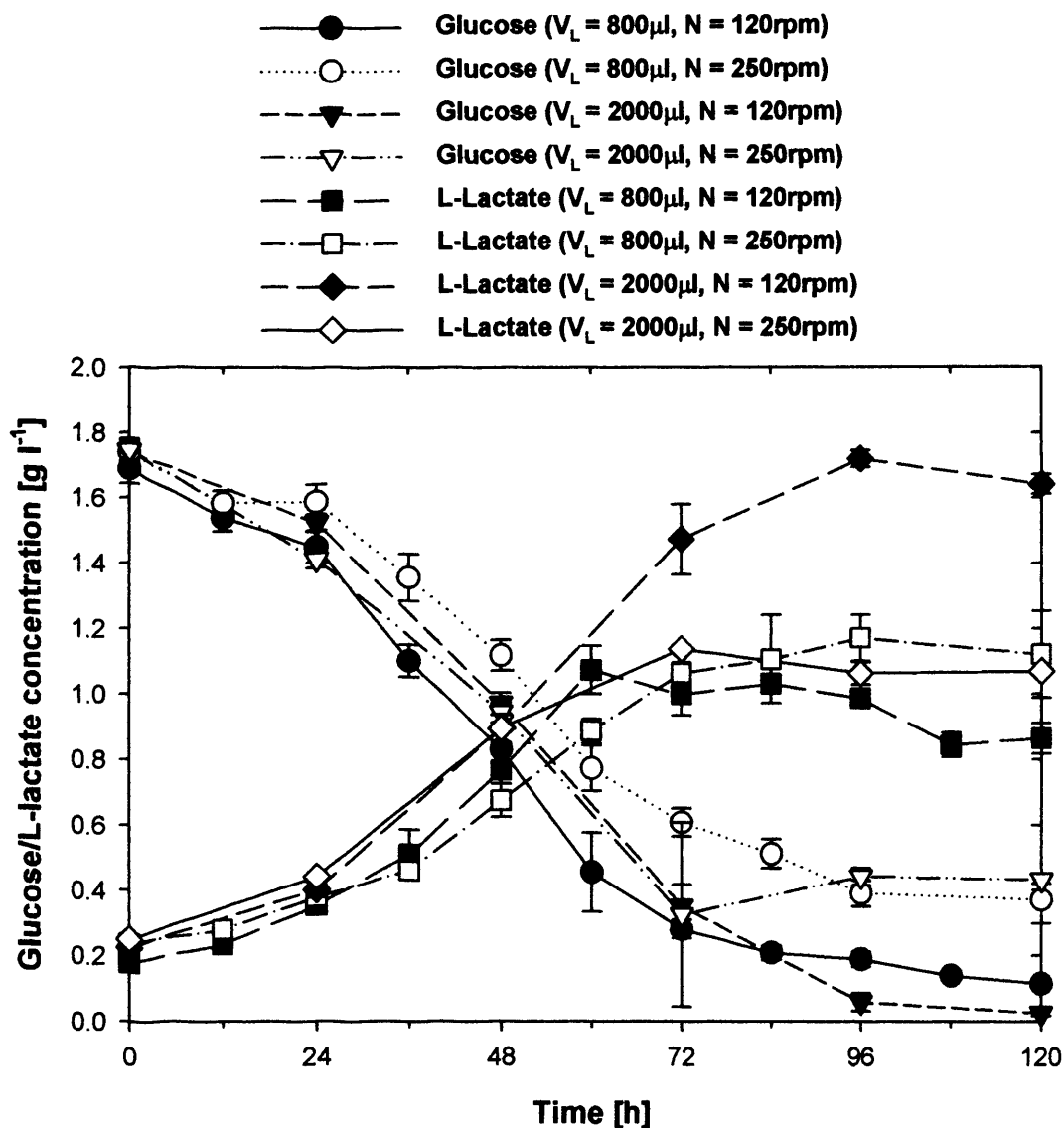


Figure 4.12: Effect of well fill volume on VPM 8 hybridoma glucose consumption and L-lactate production in 24-SRW (ULA) microtitre plates. Experiments were performed as described in Fig. 4.9. Every 12 - 24 hours, three wells were sacrificed for cell counts and metabolite analysis. Glucose and L-lactate concentrations were determined using a YSI 2700 bioanalyser. Error bars represent one standard deviation about the mean.

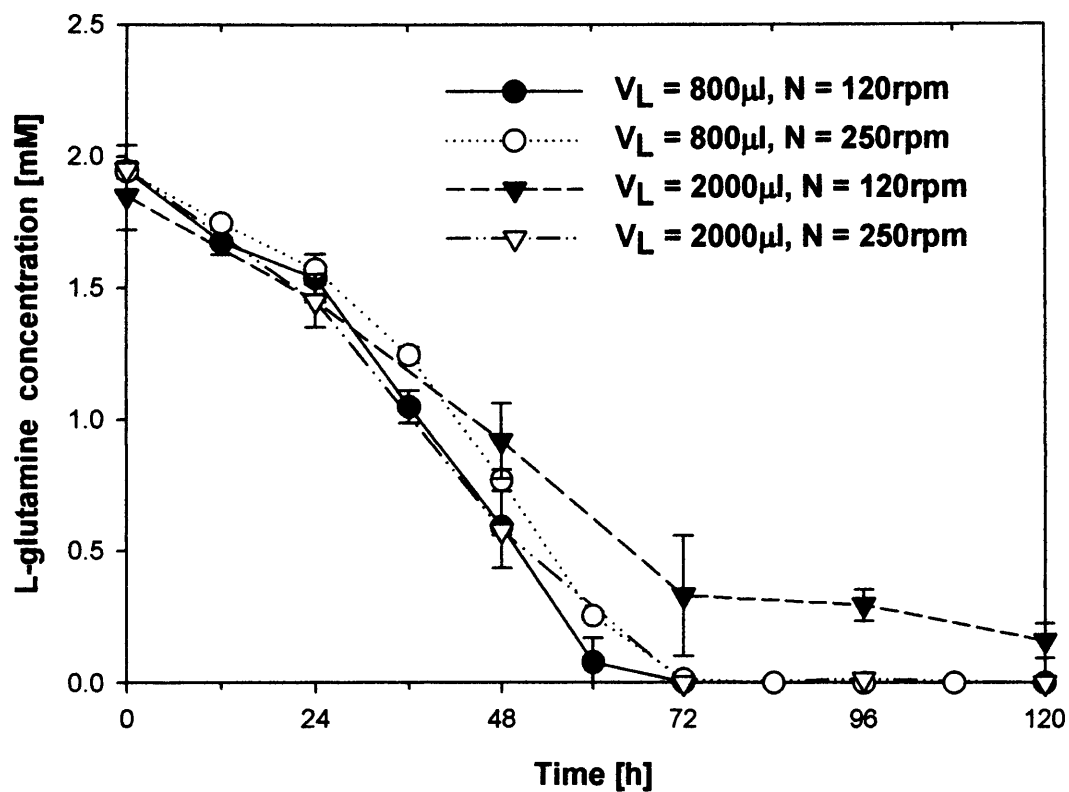


Figure 4.13: Effect of well fill volume on VPM 8 hybridoma L-glutamine consumption in 24-SRW (ULA) microtitre plates. Experiments were performed as described in Fig. 4.9. Every 12 - 24 hours, three wells were sacrificed for cell counts and metabolite analysis. The concentration of L-glutamine was determined using a YSI 2700 bioanalyser. Error bars represent one standard deviation about the mean.

Table 4.2: Effect of well fill volume on growth, antibody production and metabolism during the culture of VPM 8 hybridoma cells in 24-SRW (ULA) microtitre plates. Experiments were performed as described in Fig. 4.9. Growth rate, integral viable cell concentration and average specific production/consumption rates were estimated from Figs. 4.9, 4.10, 4.12 and 4.11, as described in Section 2.7.

Culture parameter	V = 800 μ l				V = 2000 μ l			
	N = 120 rpm		N = 250 rpm		N = 120 rpm		N = 250 rpm	
	Mean	CV [%]						
Final antibody Titre [mg l ⁻¹]	40	7	49	13	41	14	38	8
Integral of viable cell concentration [10 ⁹ cells.day.l ⁻¹]	4.262	3	2.629	8	2.188	8	3.103	n/d
Peak viable cell concentration [cells ml ⁻¹]	1.377x10 ⁶	14	9.009x10 ⁵	8	6.832x10 ⁵	22	9.270x10 ⁵	1
Maximum specific growth rate [h ⁻¹]	0.04033	2	0.03780	1	0.03675	16	0.04010	n/d
Specific antibody production rate [mg (10 ⁹ cells.day) ⁻¹]	9	4	13	15	18	23	12	n/d
Specific glucose consumption rate [g (10 ⁹ cells.day) ⁻¹]	0.37	3	0.52	4	0.79	6	0.42	n/d
Specific lactate production rate [g (10 ⁹ cells.day) ⁻¹]	0.16	11	0.36	21	0.65	7	0.26	n/d
Lactate produced / glucose consumed [g g ⁻¹]	0.43	8	0.70	25	0.82	1	0.62	n/d

4.5 DOT measurements During Cell Culture in Shaken 24-SRW (ULA) Microtitre Plates

Adequate supply of oxygen is crucial for successful microwell cultures. Insufficient oxygen has been shown to affect both growth and protein production (Ozturk and Palsson, 1991b). In Section 3.3, theoretical values of K_{La} were established for 24-SRW (ULA) plates using a variety of fill volumes and shaking speeds. As mentioned in that section, $10^6 - 10^7$ cells ml^{-1} require a K_{La} of around 1 h^{-1} to ensure sufficient oxygen transfer. Almost all K_{La} predictions were greater than 1 h^{-1} (Table 3.2), the exception was under the following conditions : 2000 μl , 120 rpm, where the K_{La} was estimated as $1.3 \pm 30\% \text{ h}^{-1}$. This suggested that oxygen transfer could become limiting. In order to confirm any oxygen mass transfer limitations a number of microwells were instrumented with fluorescent oxygen sensors as described in Section 2.2. Parallel cultures were also performed in shake flasks. Experiments were performed as described in Section 2.2.

The DOT measured in all microwell cultures with an 800 μl fill and the shake flask culture varied between 65 and 90 % (Fig. 4.14) and were in a range acceptable for cell culture (Fenge et al., 1993)(Singh, 1999)(Nienow, 2006). It was only with a 2000 μl fill in a microwell operated at the lowest speed that DOT dropped significantly. After 60 hours, the DOT measured in the bottom of the wells was $7.3 \% \pm 7.8 \%$.

24-well (ULA) plates filled with 800 μl of culture were not limited by oxygen at 120 rpm or above. Likewise, the shake flask culture was not limited by oxygen. In contrast, the DOT profile suggested oxygen limitations in a 24-SRW (ULA) plate with a 2000 μl fill, shaken at 120 rpm. These findings compare well with the predictions of K_{La} made in Section 3.3. In the microwell culture where DOT was not limiting, predicted K_{La} values were greater than 3.2 h^{-1} ; three times higher than the minimum value required to support $>10^6$ cells ml^{-1} . In contrast, for a 2000 μl fill shaken at 120 rpm, the predicted K_{La} was very close to the minimum

value of 1 h^{-1} . Taken together, these results show that Equation 1.4 can provide a good initial basis for predicting the oxygen transfer capability of the microwell plate.

4.6 Influence of Well Coating and Baffles on Cell Growth and Antibody Production in Shaken 24-SRW (ULA) Microtitre Plates

4.6.1 Effect of Well Coating

So far, Corning 24-well Ultra-low attachment (ULA) microwell plates have been used in all the previous studies. These plates have been designed to inhibit the attachment of mammalian cells to the surfaces; a hydrophilic, neutrally charged hydrogel layer coats each polystyrene well ¹. Since proteins and other biomolecules passively adsorb to surfaces through hydrophobic and ionic interactions, this surface naturally inhibits nonspecific cell immobilisation, thus inhibiting subsequent cell attachment. Because of this well treatment a single disposable plate is approximately £8 ². In contrast, an uncoated polystyrene plate is about 70p ³. Natural, unmodified polystyrene (PS) surfaces are hydrophobic and only bind cells and biomolecules through passive hydrophobic interactions. This can often lead to denaturation of the target protein molecule (Shmanai et al., 2001). A switch to PS plates would represent a significant financial saving given the potential high throughput applications of this work. However, the two surfaces may effect culture performance thorough differences in surface adsorption.

To assess the potential of a switch towards PS plates, cell growth and antibody production from cultures performed in a 24-SRW (ULA) plate and a 24-SRW (PS) plate were compared. In both cases, VPM 8 hybridoma cells were seeded at a den-

¹www.corning.com/Lifesciences/technical_information/techDocs/t_ultra_low_attachment_product_insert_cls_cc_009.pdf Cited: 14/07/2007

²Price as of May 2006. Quote from Sigma (Poole, Dorset UK)

³Price as of May 2006. Quote from Helena Biosciences (Gateshead, UK)

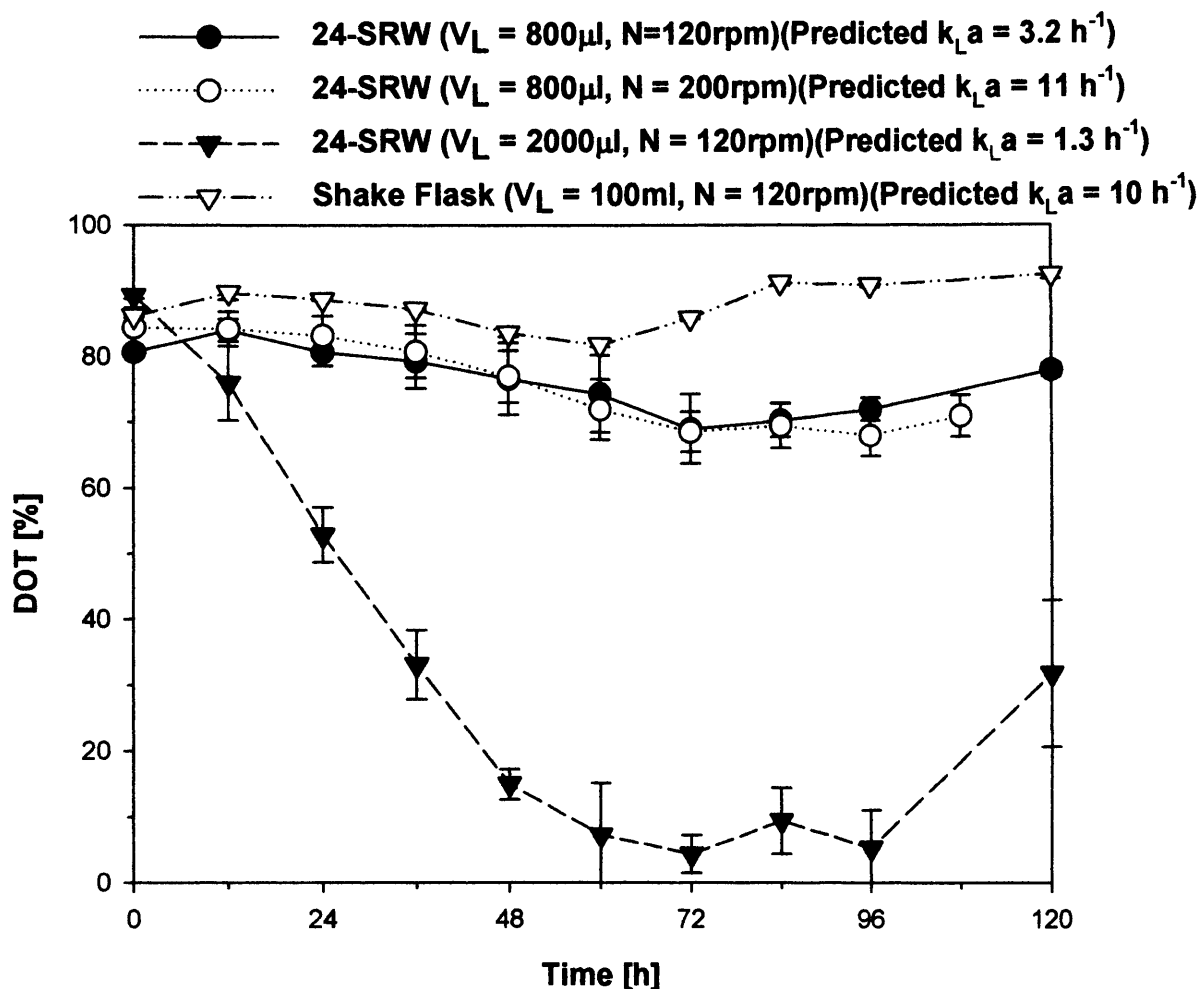


Figure 4.14: In-situ dissolved oxygen tension (DOT) measurements in a 24-SRW (ULA) microtitre plate and a 250 ml shake flask during the culture of VPM 8 hybridoma Cells. DOT was measured using PreSens oxygen sensor spots and the Fibox-3 single-channel fibre-optic oxygen meter, as described in Section 2.2. Hybridoma cells were taken from mid-exponential cultures and diluted to 1×10^5 viable cells ml^{-1} in RPMI-1640 media supplemented with 10% (v/v) FBS. $800 \mu\text{l}$ or $2000 \mu\text{l}$ of diluted culture was inoculated into each well of a Corning 24 well ultra-low attachment plate which was covered with a breathe-easy membrane. 100 ml of diluted culture was inoculated into a 250 ml shake flask. Both vessels were placed on an orbital shaker in a humidified incubator (37°C , 5% (v/v) CO_2). DOT was measured every 12h. Error bars represent one standard deviation about the mean.

sity of 1×10^5 cells ml^{-1} in 800 μl of RPMI-1640 media supplemented with 10% (v/v) FBS as described in Section 2.1.5. The agitation speed of the orbital shaker was set to 120 rpm. Both plates were covered with a breathe-easy membrane to prevent evaporation (Section 2.1.5).

The well coating was found to have had little effect on cell growth (Fig. 4.15) or antibody titre (Fig. 4.16). As mentioned earlier, PS passively adsorb both cells and proteins (antibody). Compared to the ULA plate, there was no consistent loss of cells or antibody on the PS surface. It is thought that fluid motion within the well was sufficient to ensure continuous cell suspension and prevent passive adsorption.

Well coating was found to have no significant effect on the concentrations of glucose, L-lactate and L-glutamine during culture [data not shown].

4.6.2 Effect of Baffles

In Section (3.4.1), baffles were introduced into 24-SRW (ULA) plates to help improve the liquid phase mixing. The idea being they would disrupt the largely radial flow of liquid and promote greater axial mixing. At all shaking speeds evaluated, a significant reduction in mixing time was achieved. However, over the range 0 - 160 rpm, the values of mixing time were still greater than those reported in typical mammalian cell bioreactors (< 200 s). This could impact on the future development of shaken 24-SRW (ULA) plates for fed-batch and pH controlled cultures since heterogeneities would exist for a longer period of time than at the pilot and production scales.

The purpose of this study was to assess the impact of the two baffle configurations described in Section 3.4.1 on the microwell environment in terms of culture performance. The two baffles configurations tested, single-wall and double-wall are described in Section 2.1.5. Each configuration was fitted into three wells of a 24-SRW

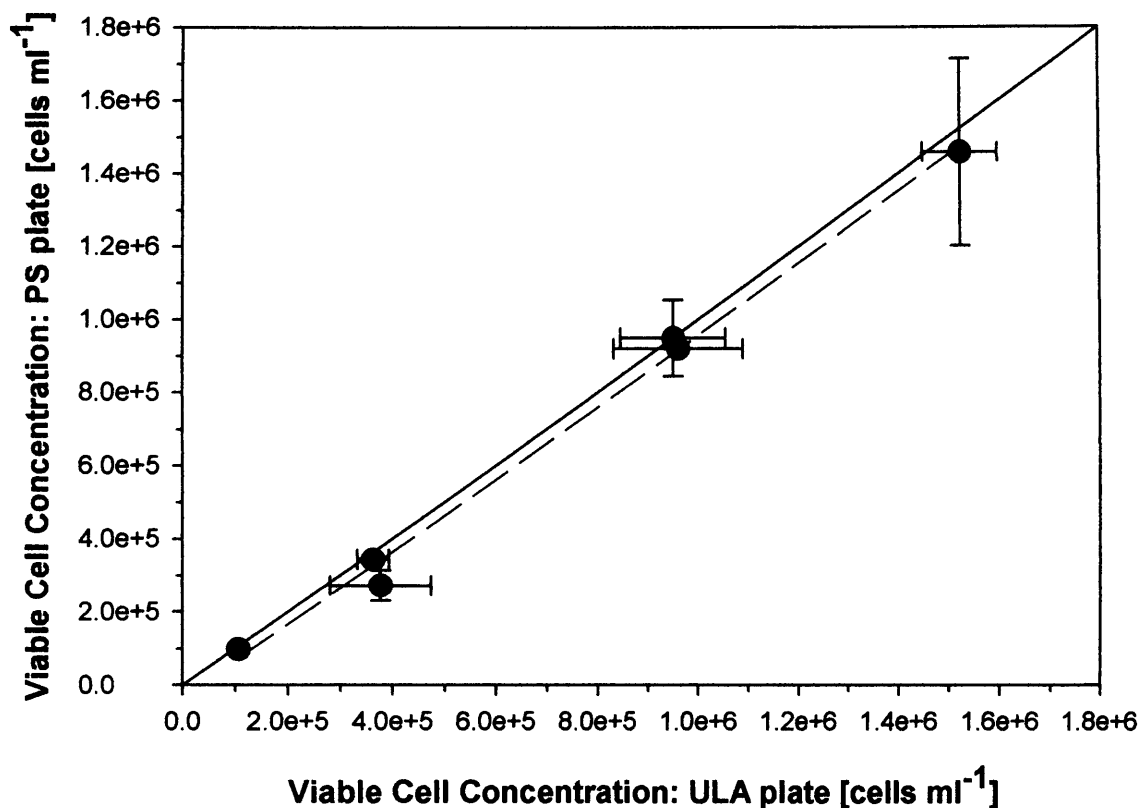


Figure 4.15: Effect of well coating on VPM 8 hybridoma growth in 24-SRW microtitre plates: parity plot of cell concentrations measured over a 5 day culture. Hybridoma cells were taken from mid-exponential cultures and diluted to 1×10^5 viable cells ml^{-1} in RPMI-1640 media supplemented with 10% (v/v) fetal bovine serum. 800 μl of diluted culture was inoculated into each well of a Corning 24 well ultra-low attachment plate (ULA) or a TPP 24 well polystyrene (PS) test plate which was covered with a breathe-easy membrane and placed on an orbital shaker (N = 120 rpm) in a humidified incubator (37°C, 5% (v/v) CO_2). Every 24 hours, three wells were sacrificed for cell counts and metabolite analysis. All cell counts were conducted using a CASY TTC automated counter. The solid line represents parity, while the dashed line represents a best-fit linear regression: $y = 0.988x - 31278$ ($r^2 = 0.994$). Error bars represent one standard deviation about the mean.

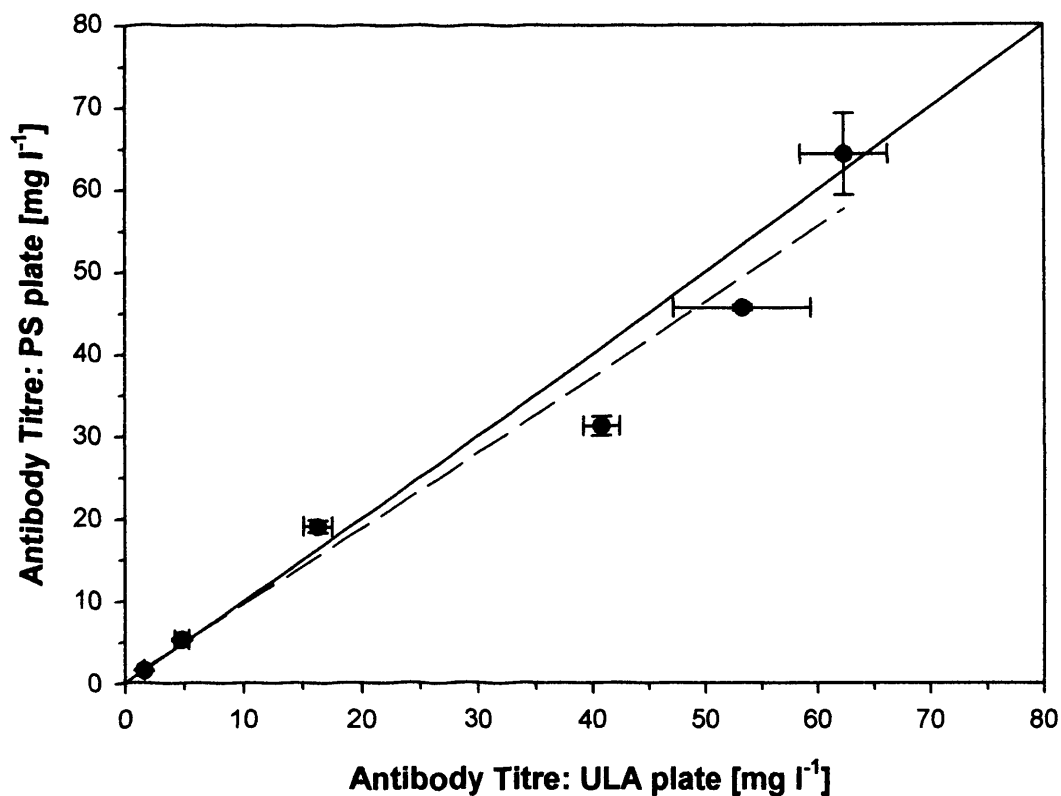


Figure 4.16: Effect of well coating on VPM 8 hybridoma antibody production in 24-SRW plates: parity plot of antibody titres measured over a 5 day culture. Experiments performed as described in Fig. 4.15. Every 24 hours, three wells were sacrificed for cell counts and metabolite analysis. Antibody concentration was determined using ELISA as described in Section 2.8.2. The solid line represents parity, while the dashed line represents a best-fit linear regression: $y = 0.9191x + 0.42399$ ($r^2 = 0.9606$). Error bars represent one standard deviation about the mean.

plate. All wells of the modified plate were inoculated with VPM 8 hybridoma cells at a density of 1×10^5 cells ml^{-1} in 800 μl of RPMI-1640 media supplemented with 10% (v/v) FBS. The plate was shaken at 120 rpm, on an orbital shaker platform with a shaker diameter (d_s) of 20 mm. The plate was covered with a breathe-easy membrane to minimise evaporation.

Over the first 48 hours of culture, the baffles had no positive effect on viable cell concentration compared to the unbaffled wells (Fig. 4.17). The viable cell concentration in the control was the highest after 72 hours (1.288×10^6 cells ml^{-1}), over 25% higher than in both the single-wall baffle and double-wall baffle wells. Furthermore, the IVC was found to be highest in the control experiment (2.50×10^9 cells.day.l $^{-1}$), nearly 20% higher than the single-wall baffled well and 14% higher than the double-wall baffled wells. The maximum specific growth rate was similar in all experiments. Cells cultured in both baffle configurations and the control maintained high viability (> 90 %) over the first 48h of culture; thereafter the viability declined. As with cell growth, the baffles did not enhance antibody titre (Fig. 4.18). The final titres and SPR (Table 4.3) were very similar to the control.

The addition of baffles had little effect on cell growth or antibody production. It is thought that the growth and protein production characteristics exhibited by the control culture (800 μl , 120 rpm) were the best obtainable using the VPM 8 cell-line and serum-supplemented RPMI-1640 media, and so the addition of baffles would not required to remove or minimise a limiting condition associated with the liquid hydrodynamics.

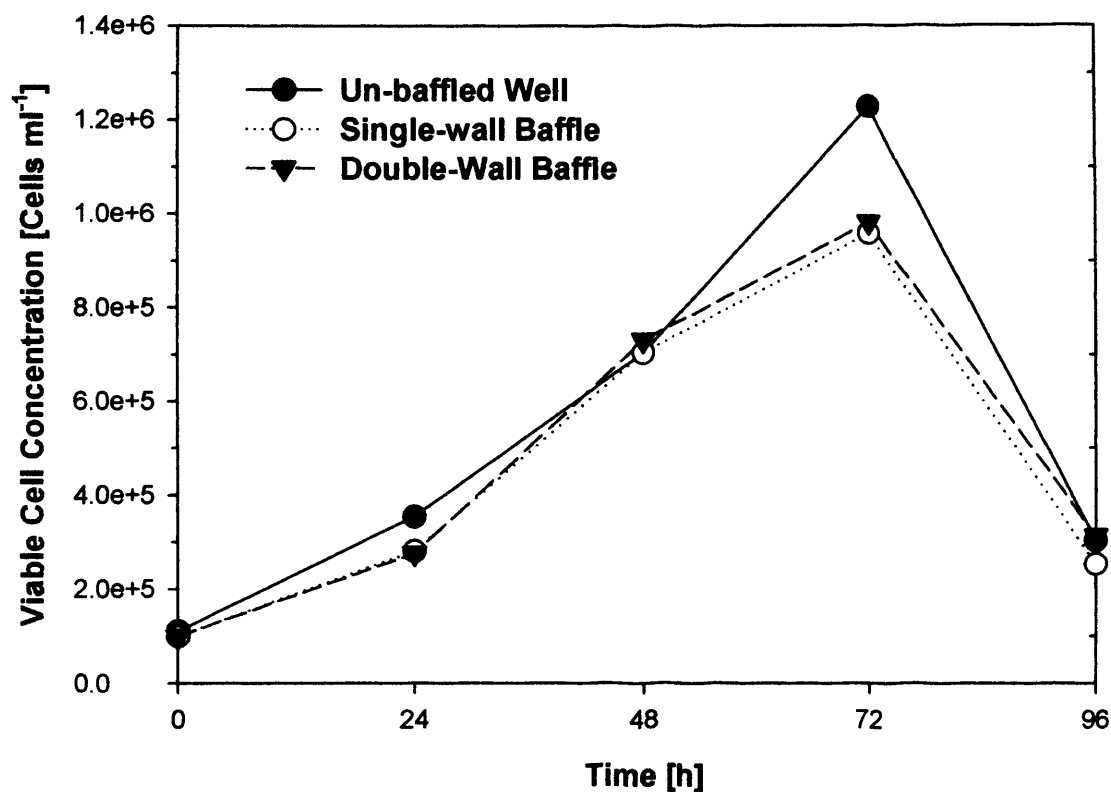


Figure 4.17: Effect of baffles on the growth of VPM 8 hybridoma cells cultured in 24-SRW plates. Two baffles configurations were designed and tested: single-wall and double-wall. Both are described in Section 2.1.5. Hybridoma cells were taken from mid-exponential cultures and diluted to 1×10^5 viable cells ml^{-1} in RPMI-1640 media supplemented with 10% (v/v) fetal bovine serum. $800 \mu\text{l}$ of diluted culture was inoculated into each well of a baffled Corning 24 well ultra low attachment plate which was covered with a breathe-easy membrane and placed on an orbital shaker ($N = 120 \text{ rpm}$) in a humidified incubator (37°C , 5% (v/v) CO_2). Cell count were conducted using a CASY TTC cell counter.

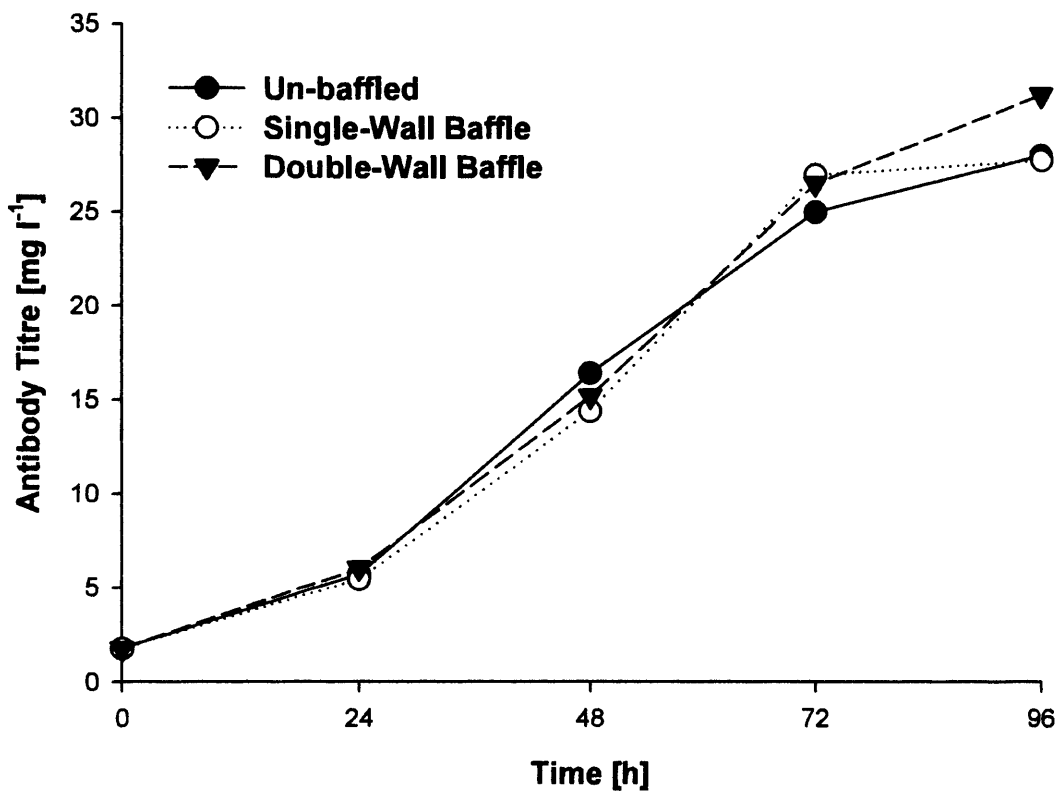


Figure 4.18: Effect Of baffles on the antibody production of VPM 8 hybridoma cells cultured in 24-SRW plates. Two baffles configurations were designed and tested: single-wall and double-wall. Experiments performed as described in Fig. 4.17. Antibody concentration was determined using ELISA as described in Section 2.8.2.

Table 4.3: Effect of baffles on the growth and antibody production of VPM 8 hybridoma cells cultured in 24-SRW (ULA) plates. Two baffles configurations were designed and tested: single-wall and double-wall. Experiments performed as described in Fig. 4.17. Growth rate and integral viable cell concentration were estimated as described in section 2.7.

Culture parameters	No-Baffle	Single-Wall Baffle	Double-Wall Baffle
Final antibody titre [mg l ⁻¹]	28	28	31
Integral of viable cell concentration [10 ⁹ cells.day.l ⁻¹]	2.50	2.12	2.20
Peak viable cell concentration [cells ml ⁻¹]	1.228x10 ⁶	9.579x10 ⁵	9.818x10 ⁵
Maximum specific growth rate [h ⁻¹]	0.03845	0.04067	0.04145
Specific antibody production rate [mg (10 ⁹ cells.day) ⁻¹]	10	12	13

4.7 Summary

Building on the engineering characterisation of microwell systems described in Chapter 3, the results presented in this chapter have begun to relate the importance of these to cell culture growth kinetics and antibody production.

Shaking speed was found to have a significant but not marked influence on microwell hybridoma culture. A slight decrease in growth was observed at 200 - 250 rpm, along with an increase in both glucose consumption and lactate production rates (Section 4.3). It is believed to be the result of sufficient energy dissipation in the system helping to avoid limitations in oxygen supply and hydrodynamics.

Fill volume had a more noticeable effect on cell performance, particularly at lower shaking speeds (Fig. 4.9). A combination of low shaking speed and high well fill volume (2000 μl , 120 rpm) was found to result in cell sedimentation and anaerobic conditions (Fig. 4.14). This last point confirms the accuracy of k_{La} predictions from Equation 1.4. To supply adequate oxygen to support 10^6 cells ml^{-1} , a K_{La} of around 1 h^{-1} is required (Fenge et al., 1993). A K_{La} of 1.3 h^{-1} was predicted for a 24-well plate operating with a 2000 μl fill, shaken at 120 rpm; allowing for the reported accuracy of 30% in the equation of (Doig et al., 2005) and the known cell concentrations of the hybridoma cell-line used suggested that insufficient oxygen transfer may occur. This was confirmed by making DOT measurements during a microwell culture (Fig. 4.14).

An attempt was made to culture VPM 8 hybridoma cells in both 24-SRW and 96-DSW plates (Section 4.2). While successful in 24-SRW plates, culture in 96-DSW plates proved unsuccessful under various operating conditions (shaking speed, fill volume and well geometry). This was believed to be related to the cell-line rather than an unfavorable environment: a CHO cell-line grew and maintained a high viability over a week-long culture period. Therefore, 24-SRW plates were chosen to perform all subsequent hybridoma cultures.

Overall, the use of baffles was shown to have some positive effect on the blending of liquid additions made to microwell cultures even if they did not enhance culture performance (Figs. 4.17, 4.18)(Table 4.3). Future automation of these cultures will inevitably involve liquid additions however and so in such situations the use of baffles to reduce the mixing time may still prove to be advantageous.

A comparison of growth and antibody titre in ultra-low attachment (ULA) wells and polystyrene (PS) plates was made to investigate the possibility of switching to the cheaper PS plates. However, it is known that cells and protein can adsorb to PS surfaces. Cell counts and antibody titre were comparable in both cases (Figs. 4.15 and 4.16). Therefore it would be sensible to switch to the cheaper PS plates for high throughput experimentation.

Based on the characterisation of the engineering environment in Chapter 3 and the variables in this chapter found to influence cell culture kinetics, it is now possible to specify initial design principles for the successful operation of microwell cell cultures:

1. Prior knowledge of cell line: growth rates, peak viable cell concentrations, antibody titre, antibody production rates
2. Define array/data requirements - specify minimum fill volume and well type
3. CFD - surface deformation and general hydrodynamics local energy dissipation rates < lethal ones.
4. Use correlation to estimate $k_L a$ for given conditions - redefine RPM_{min} if necessary
5. Check for cell sedimentation at RPM_{min} - if sedimentation occurs then shaking speed must be increased.
6. Define operating conditions - check initial batch culture of chosen cell line(s).

Having shown that suspension culture of mammalian cells is feasible in shaken microwell plates and established some initial experimental design criteria, in the next chapter a first attempt at scaling-up a cell culture process from shaken microwell plate to a lab-scale stirred-tank reactor (STR) is made. An understanding of the relationship between microwell generated data and larger scale culture performance will be vital if the microwell approach is to be used to inform bioprocess design.

Chapter 5

Scale Translation of Hybridoma Cultures Based on Energy Dissipation¹

Dissipation¹

5.1 Introduction and Aims

Cell culture data generated in shaken microwell plates must be reproducible and predictive of performance at larger scales before this cheap, automatable, high-throughput platform technology can provide a useful alternative to shake flasks and bench-scale STRs in process evaluation and optimisation (Micheletti et al., 2006). This approach was discussed in detail in Section 1.4.4. Upon scale-up from microwells it would be expected to reproduce, at larger scales, similar product yield and quality (Varley and Birch, 1999).

To enable predictive scale-up of microwell processes, knowledge of the engineering fundamentals (Chapter 3) and their effect on culture performance (Chapter 4) is important. Previous studies on the scale-up of mammalian cell culture have used the following scale-up bases: fluid turnover rate (Chisti, 1993); superficial gas velocity (Xie et al., 2003); aeration rate (vvm)² and impeller tip speed (Marks, 2003) and,

¹Some of the results in this chapter have been previously published as Micheletti et al. (2006)

²Volumetric flow rate per minute per unit volume

most recently, power input per unit volume (Li et al., 2006). The utility of P/V as a basis for scale translation has been previously described in Section 3.7

The aim of this chapter is to make an initial attempt at scaling-up microwell cultures using matched average energy dissipation (P/V) as a basis for scale translation. The specific objectives of this chapter are to:

- Culture VPM 8 hybridoma cells at non-matched energy dissipation rates to demonstrate how differences in P/V lead to variations in culture performance.
- Scale-up a VPM 8 hybridoma culture from shaken 24-well plates to shake flasks and a 5-L STR using matched P/V.

5.2 Cell Culture Performance Under Non-Matched P/V

Shake flasks are currently one of the standard geometries used for early stage development of mammalian cell culture conditions along with spinner flasks and bench-scale STR (Girard et al., 2001)(Balcarcel and Clark, 2003)(Muller et al., 2005). In order to understand the influence of average energy dissipation rate on hybridoma growth and antibody production in this culture geometry, shake flask cultures operated at 0, 40 and 810 W m⁻³ were assessed. These operating conditions were determined based on the correlation of Büchs et al. (2000a) shown in Equation 1.1.

Power dissipation was found to have a pronounced effect on cell growth (Fig.5.1). Cells cultured at 40 W m⁻³ achieved the highest peak viable cell concentration (1.472x10⁶ cells ml⁻¹), over twice that of the static culture. In the culture performed at 810 W m⁻³, the cells did not grow to any measurable degree. The IVC (10⁹ cells.day⁻¹.l⁻¹) of the cultures at 0, 40 and 810 W m⁻³ were 2.050, 4.100 and 0.2400 respectively. Cell sedimentation was visible in the static cultures, while trypan-blue inspection of the cells cultured at 810 W m⁻³ showed unusually high levels of cellular debris throughout the culture period suggesting cellular damage.

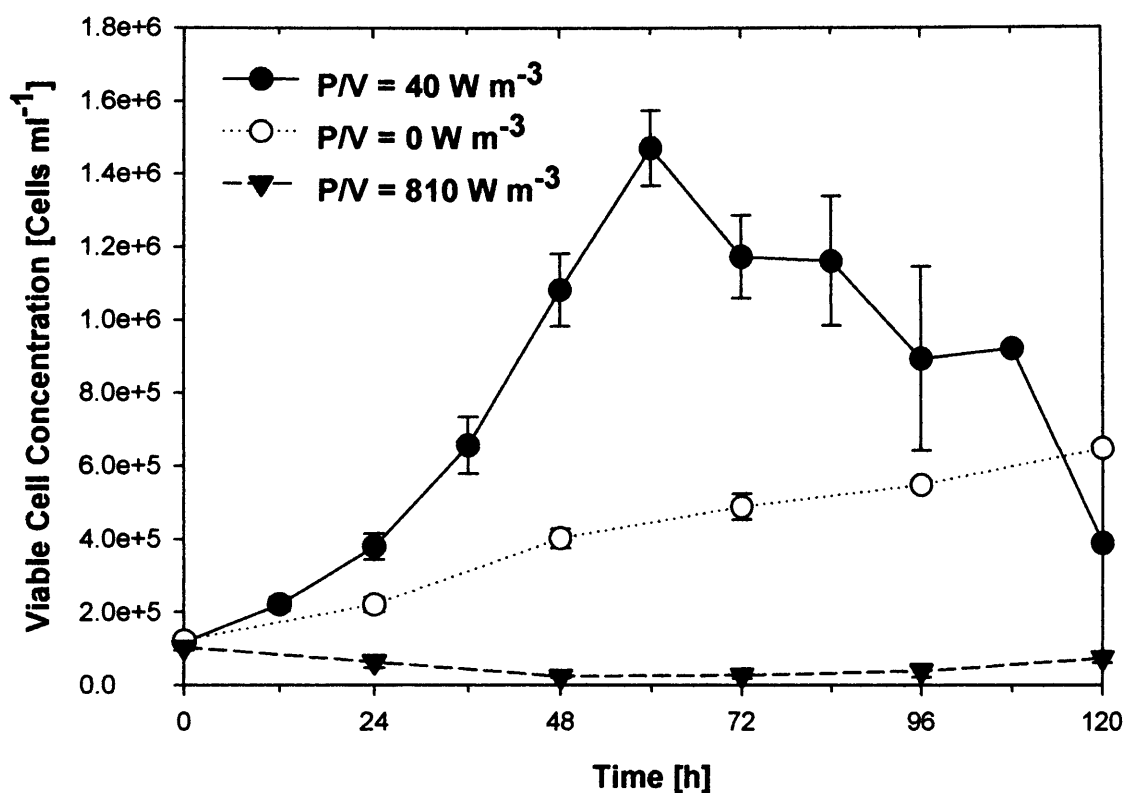


Figure 5.1: Effect of average energy dissipation (P/V) on VPM 8 hybridoma cell growth in 250 ml shake flasks. Hybridoma cells were taken from mid-exponential cultures and diluted to 1×10^5 viable cells ml^{-1} in RPMI-1640 media supplemented with 10% (v/v) FBS. The average P/V values in shake flasks were calculated using Equation 1.1. To produce an average P/V of 0, 40 and 810 W m^{-3} the following conditions were used: (fill volume = 100 ml, shaking speed = 0 rpm), (100 ml, 120 rpm) and (25 ml, 250 rpm) respectively. Following inoculation, cultures were placed on an orbital shaker in a humidified incubator (37°C , 5% (v/v) CO_2) as described in Section 2.1.4. Cell counts were conducted using a CASY TTC automated cell counter as described in Section 2.8.1. Error bars represent one standard deviation about the mean.

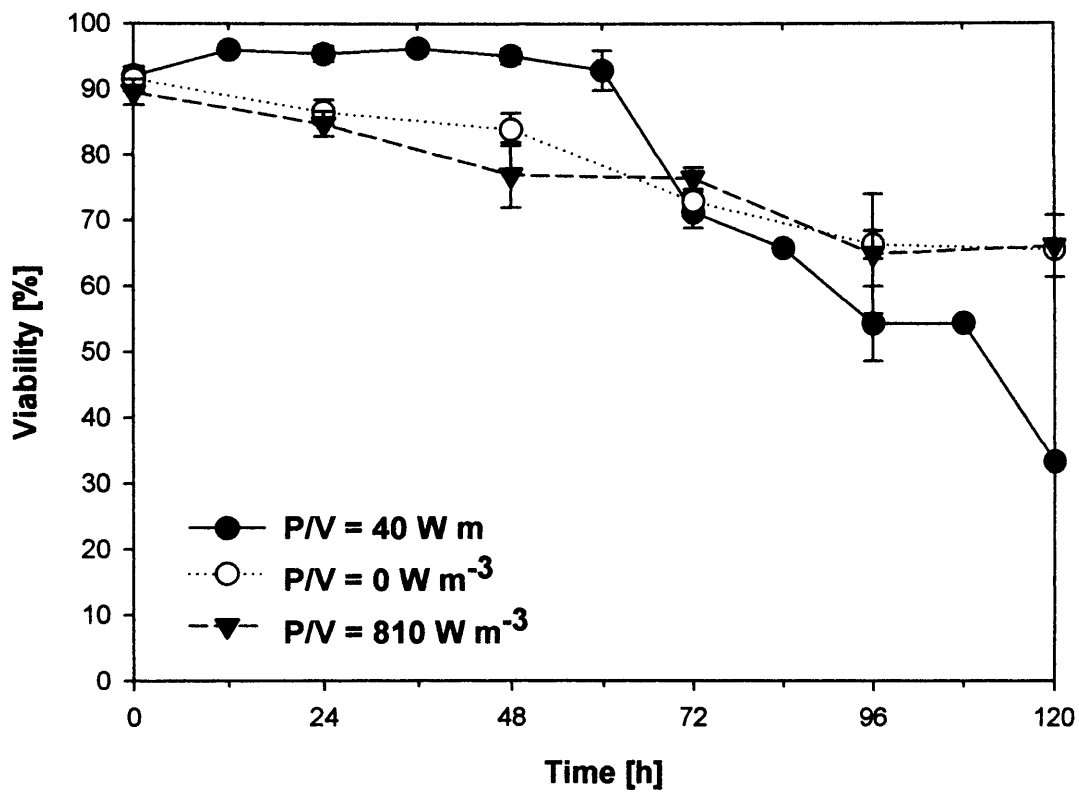


Figure 5.2: Effect of average energy dissipation (P/V) on VPM 8 hybridoma viability in 250 ml shake flasks. Experiments were performed as described in Fig. 5.1. Viability assessments were made using a CASY TTC automated cell counter as described in Section 2.8.1. Error bars represent one standard deviation about the mean.

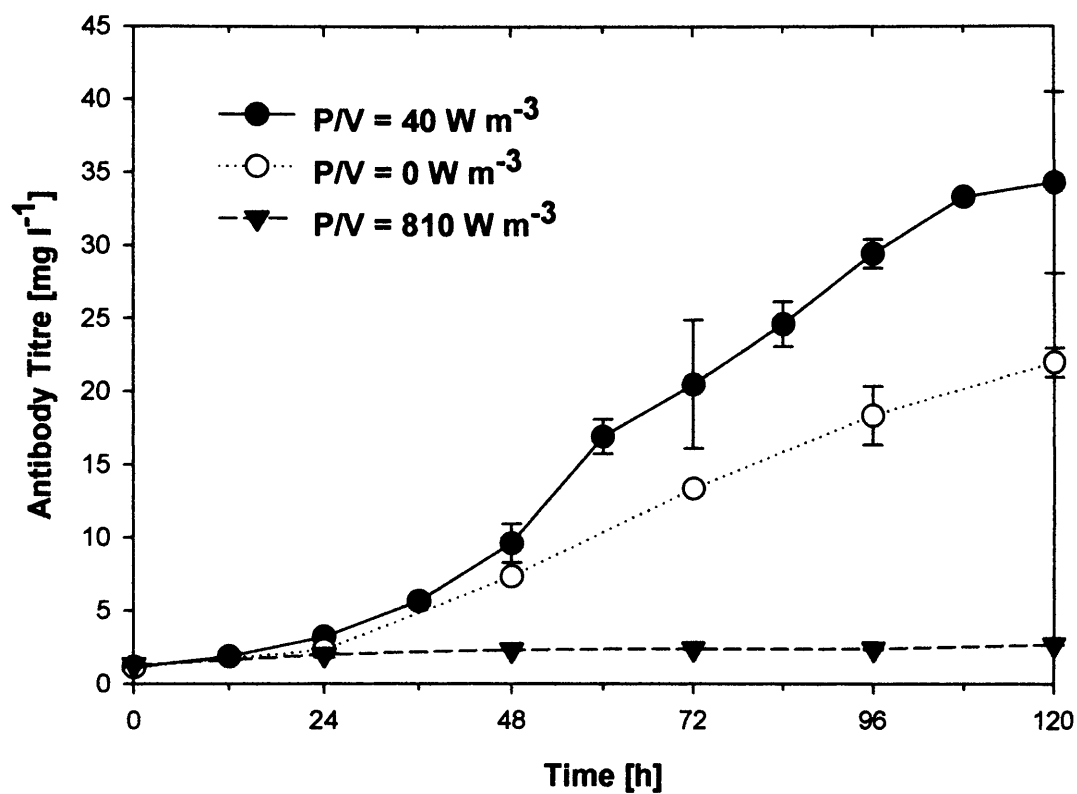


Figure 5.3: Effect of average energy dissipation (P/V) on VPM 8 hybridoma antibody production in 250 ml shake flasks. Experiments were performed as described in Fig. 5.1. Antibody titres were quantified using ELISA as described in Section 2.8.2. Error bars represent one standard deviation about the mean.

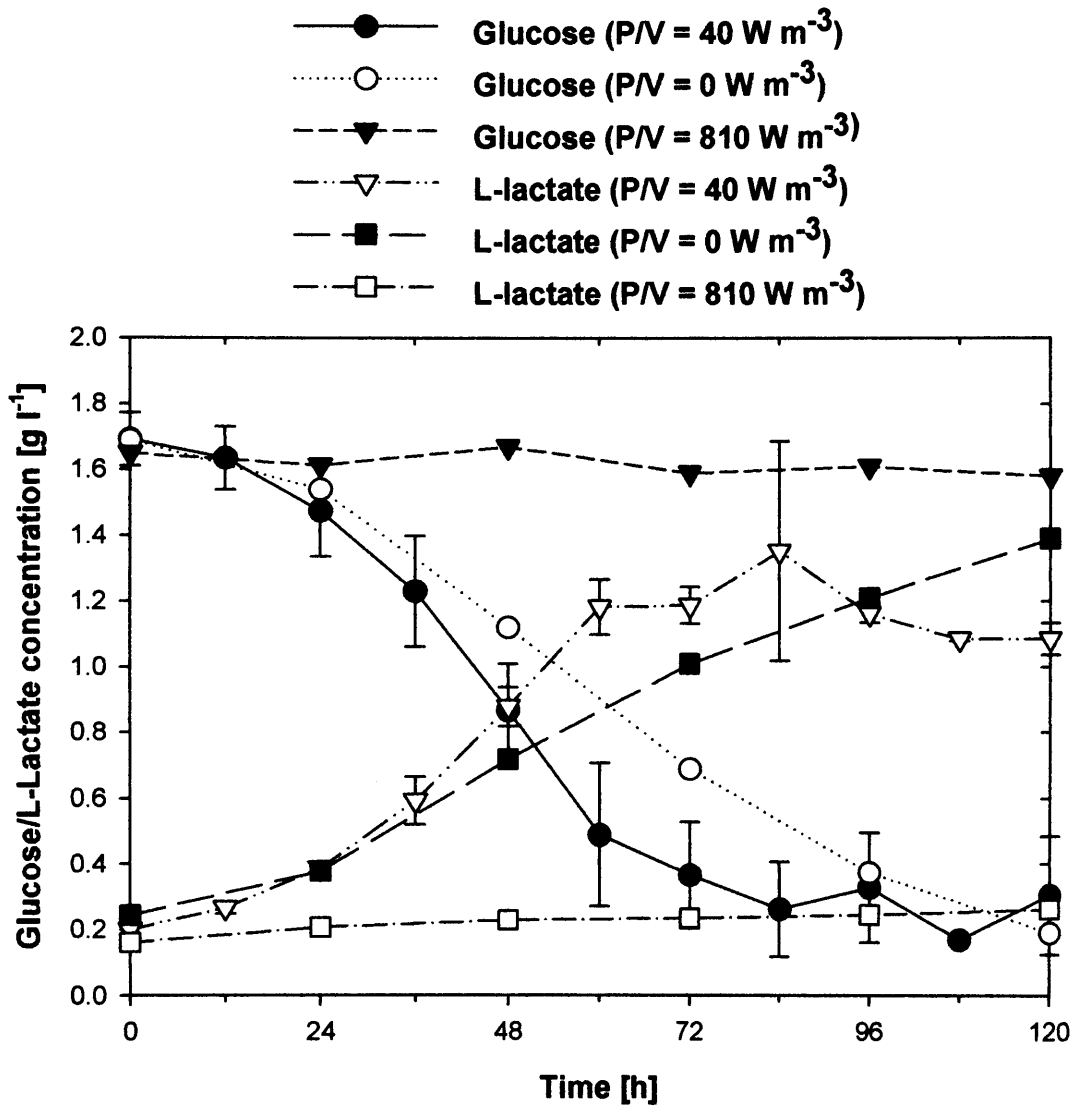


Figure 5.4: Effect of average energy dissipation (P/V) on VPM 8 hybridoma glucose consumption and L-lactate production in 250 ml shake flasks. Experiments were performed as described in Fig. 5.1. Glucose and L-lactate concentrations were measured as described in Section 2.8.3. Error bars represent one standard deviation about the mean.

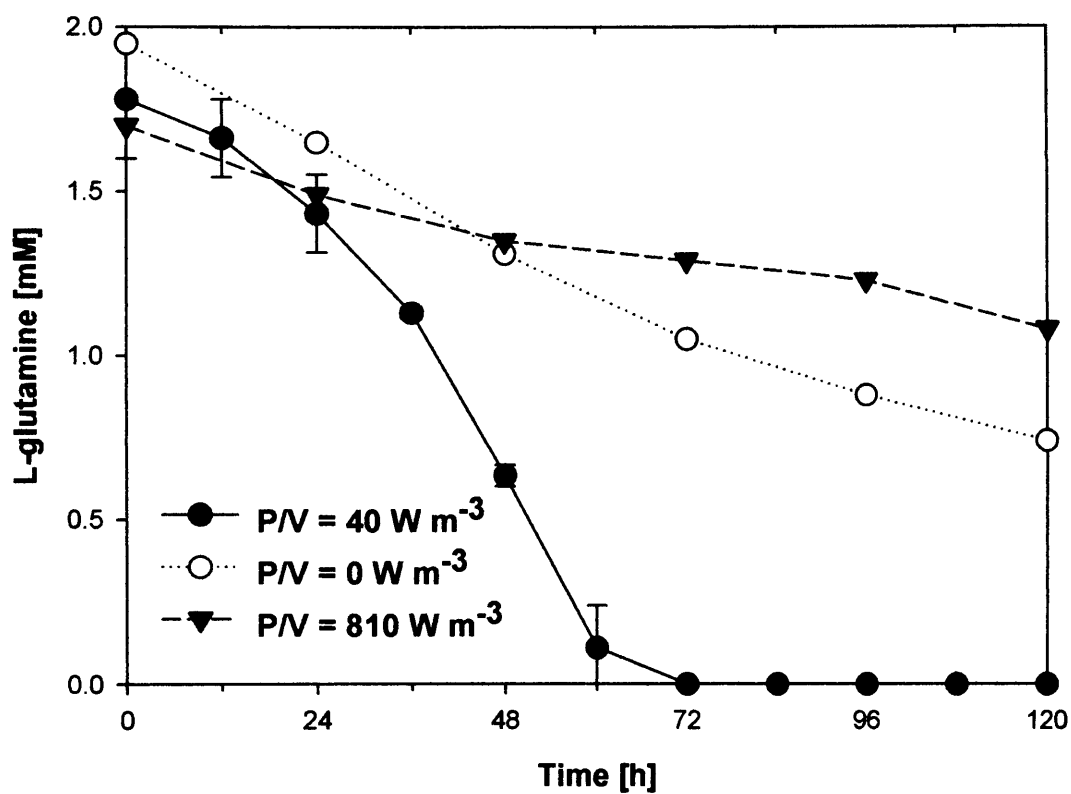


Figure 5.5: Effect of average energy dissipation (P/V) on VPM 8 hybridoma L-glutamine consumption in 250 ml shake flasks. Experiments were performed as described in Fig. 5.1. L-glutamine concentration was measured as described in Section 2.8.3. Error bars represent one standard deviation about the mean.

The results obtained at 40 W m^{-3} (maximum viable cell concentration = 1.472×10^6 cells ml^{-1}) compare well with typical values reported for hybridoma cell growth in shake flasks [$(0.9 - 1.3) \times 10^6$ cells ml^{-1}] (Schmid et al., 1990)(Ozturk and Palsson, 1991a)(Zhang, Williams-Dalson, Keshavarz-Moore and Shamlou, 2005). In these cases it is estimated that the average energy dissipation rates used by these other cultures were in the range $10 - 60 \text{ W m}^{-3}$.

The viability of the static and 810 W m^{-3} cultures declined continuously throughout the culture period (Fig. 5.2). In contrast, the viability of the shake flask performed at 40 W m^{-3} maintained a constant high viability ($> 90\%$) over the first 60 hours of culture before rapidly decreasing.

The highest final antibody titre (Fig. 5.3) was achieved in the culture performed at 40 W m^{-3} (34.3 mg l^{-1}). This was 1.6 times that of the static culture and 12.8 times that of the 810 W m^{-3} culture. The results at 40 W m^{-3} compared well with antibody titres reported for shake flask cultures of hybridoma cells ($40 - 50 \text{ mg l}^{-1}$) (Schmid et al., 1990)(Ozturk and Palsson, 1991a) under conditions described above.

There was no significant consumption of glucose or production of lactate by cells cultured at 810 W m^{-3} (Fig. 5.4). Although, some consumption of L-glutamine was measured at this operating condition (Fig. 5.5).

The inferior growth and antibody titres achieved by cells cultured at extremely low or high energy dissipation rates (0 and 810 W m^{-3}), compared to a value (40 W m^{-3}) similar to those used in previous small scale culture studies (Zhang, Williams-Dalson, Keshavarz-Moore and Shamlou, 2005), suggest two important points. Firstly, for each vessel there is likely to be an optimal value of P/V as clearly demonstrated in Fig. 5.1. Second, in relation to scale-up the P/V values need to match at the two different scales unless one of the two P/V values is far from optimum at that particular scale. At each stage, the energy dissipation rate must avoid being too

low so as to induce cell sedimentation, poor mixing or even anaerobic conditions. Conversely, the energy dissipation must avoid being too high so as to be detrimental to the cell growth and antibody production (Li et al., 2006).

In the next section, an initial attempt at scaling-up a cell culture process from microwell plate to shake flask and a 5-L STR is made.

5.3 Scale-up of Cell Culture Performance at Matched P/V

Scale translation of a VPM 8 hybridoma culture from 24-SRW plates to a 250 ml shake flask and a 5-L STR was performed, where possible, using matched P/V values or optimal conditions for a particular geometry. The average P/V in both the microwell and shake flask was set to 40 W m^{-3} . In Section 4.3, this magnitude of average P/V was shown to be optimal for microwells; therefore optimal culture conditions prevail in both microwell and shake flask cultures. Data from a 5-L STR run, operated under typical conditions for STR operation at this scale (Miller et al., 2000)(Varley and Birch, 1999)(Li et al., 2006), was included for comparison. In this case, the P/V value for the STR was estimated to be 8 W m^{-3} (Section 3.5.2). A 24-SRW plate, 250 ml plastic shake flask and 5-L STR were inoculated with cells at $1 \times 10^5 \text{ cells ml}^{-1}$ in 800 μl , 100 ml and 3-Litre respectively of RPMI-1640 media supplemented with 10% (v/v) FBS. The microwell plate and the shake flask were shaken at 120 rpm as described in Section 2.1.5. The STR was agitated at 200 rpm as described in Section 2.1.6. All cell growth, antibody and metabolic data were corrected for the effect of evaporation by the method described in Section 2.1.5.

Cell growth was found to be comparable in all three bioreactor geometries (Fig. 5.6). However, a one-way ANOVA of the peak viable cell concentrations, described in Section 2.9, revealed significant differences between the three geometries ($p < 0.05$). In

Fig. 5.6, it appears that the peak viable cell concentration in the 5-L STR was statistically different from the other two geometries. This was confirmed by a t-test, described in Section 2.9, performed on the peak viable cell concentrations obtained in the shake flask and microwell cultures. Significant differences were not found at the 95% level.

Cell viability was maintained at a high value ($> 90\%$) for the first 60 h of culture (Fig. 5.7) in all three geometries. After which it started to decline with the most rapid and extensive decline seen in the shake flask culture. This decrease in viability coincided with the complete exhaustion of L-glutamine (Fig. 5.10), suggesting it was either the sole or one of the main limiting nutrients.

The mean final antibody titres were also similar between the three scale (Fig. 5.8): the antibody titre achieved in the 24-SRW plate was the highest ($40 \pm 2.8 \text{ mg l}^{-1}$) approximately 20% greater than in the shake flask and the STR. Likewise, the SPR achieved in the three geometries were very similar (Table 5.1).

Overall, the glucose concentration profiles for the three geometries were very similar throughout the 120 hour culture period (Fig. 5.9). Glucose was exhausted in the STR after 72 hours of culture, contrasting to the shake flask and microwell cultures where $\approx 0.2 - 0.4 \text{ g l}^{-1}$ remained after 120 hours. Previous studies reporting the metabolism of hybridoma cells have never found glucose to be a limiting nutrient (Miller et al., 2000)(Ozturk and Palsson, 1991a)(Schmid et al., 1990). The lactate concentrations over the first 60 hours of culture were similar in all three geometries (Fig. 5.9) thereafter all plateaued out at significantly different values. The concentration of L-lactate measured in the study ($0.2 - 1.6 \text{ g l}^{-1}$) compared well with typical values reported for hybridoma cell cultures in the literature ($0.5 - 3 \text{ g l}^{-1}$) (Miller et al., 2000)(Ozturk and Palsson, 1991a)(Schmid et al., 1990). In all three geometries, the L-glutamine was exhausted after 72 hours of culture (Fig. 5.10). As mentioned in previous sections, L-glutamine is a common limiting nutrient in

hybridoma culture and its exhaustion correlates with the onset of the death phase.

The calculated glucose consumption rates and lactate production rates were similar in the microwell and shake flask culture (Table 5.1). However, both of these parameters were somewhat higher in the STR culture: the glucose consumption rate was approximately 4 times higher and the lactate consumption rate was ≈ 10 times higher.

The findings presented in this section are in agreement with the findings of Strobel et al. (2001) who showed that CHO performance in a shaken 96-DSW plate was equivalent to that in shaken flasks. However, the findings of the current study do not support the previous research of Girard et al. (2001) whom found a two-fold increase in antibody titre from CHO cells cultured in shaken 12-well plates when compared to equivalent data from a spinner flask and 3-Litre STR. The observed increase in titre in the work of Girard et al. (2001) could be attributed to evaporation from the wells.

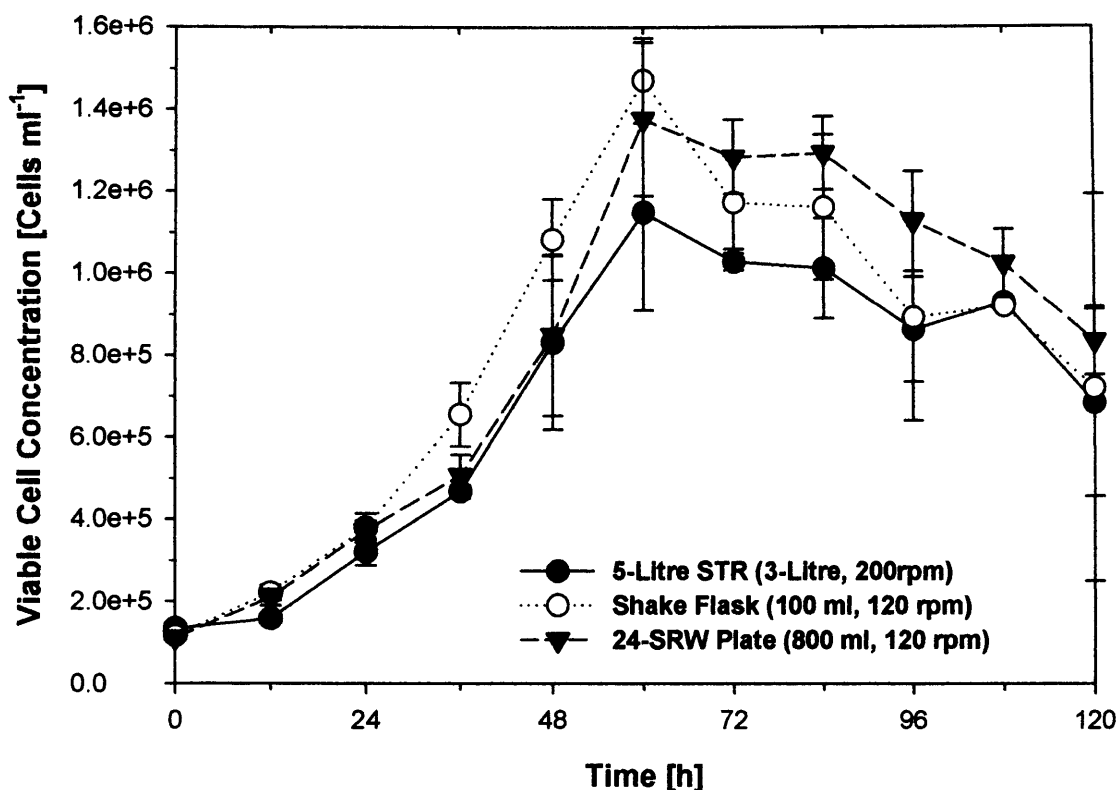


Figure 5.6: Scale-up of VPM 8 hybridoma cells based on matched average energy dissipation per unit volume: cell growth in shaken 24-SRW plates, 250 ml shake flasks and a 5-L stirred-tank reactor. Hybridoma cells were taken from mid-exponential cultures and diluted to 1×10^5 viable cells ml^{-1} in RPMI-1640 media supplemented with 10% (v/v) FBS. The STR culture was further supplemented with 1 g l^{-1} pluronic F68 and 60 ppm silicone A antifoam after 48h of culture. $800 \mu\text{l}$ of diluted culture was inoculated into each well of a Corning 24-well ultra low attachment plate which was covered with a breathe-easy membrane as described in Section 2.1.5. 100 ml of diluted culture was inoculated into a plastic, vent-capped, 250ml shake flask as described in Section 2.1.4. Both the microwell plate and shake flasks were placed on an orbital shaker (120 rpm) in a humidified incubator (37°C , 5% (v/v) CO_2). 3-L of diluted culture was inoculated into the 5-L STR. The following set-points were used: 200rpm (agitation speed), $30\% \pm 1\%$ (DOT) and 7.2 ± 0.1 (pH). The aeration ($100 \text{ cm}^3 \text{ min}^{-1}$; air supplemented with nitrogen or oxygen on demand) was provided in the headspace for the first 48 hours, followed by intermittent sparging. pH was controlled using CO_2 as described in Section 2.1.6. All cell counts were conducted using a CASY TTC automated cell counter as described in Section 2.8.1. Error bars represent one standard deviation about the mean.

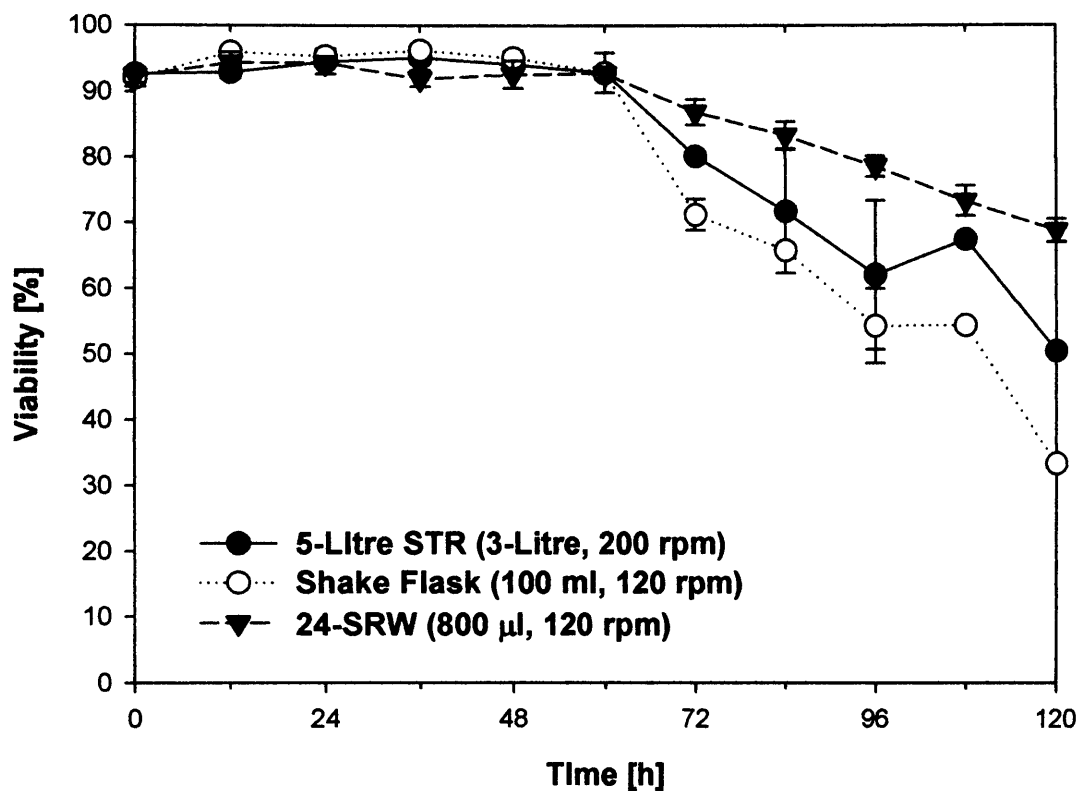


Figure 5.7: Scale-up of VPM 8 hybridoma cells based on matched average energy dissipation per unit volume: cell viability in shaken 24-SRW plates, 250 ml shake flasks and a 5-L stirred-tank reactor. Experiments performed as described in Fig. 5.6. All viability assessments were made using a CASY TTC automated cell counter as described in Section 2.8.1. Error bars represent one standard deviation about the mean.

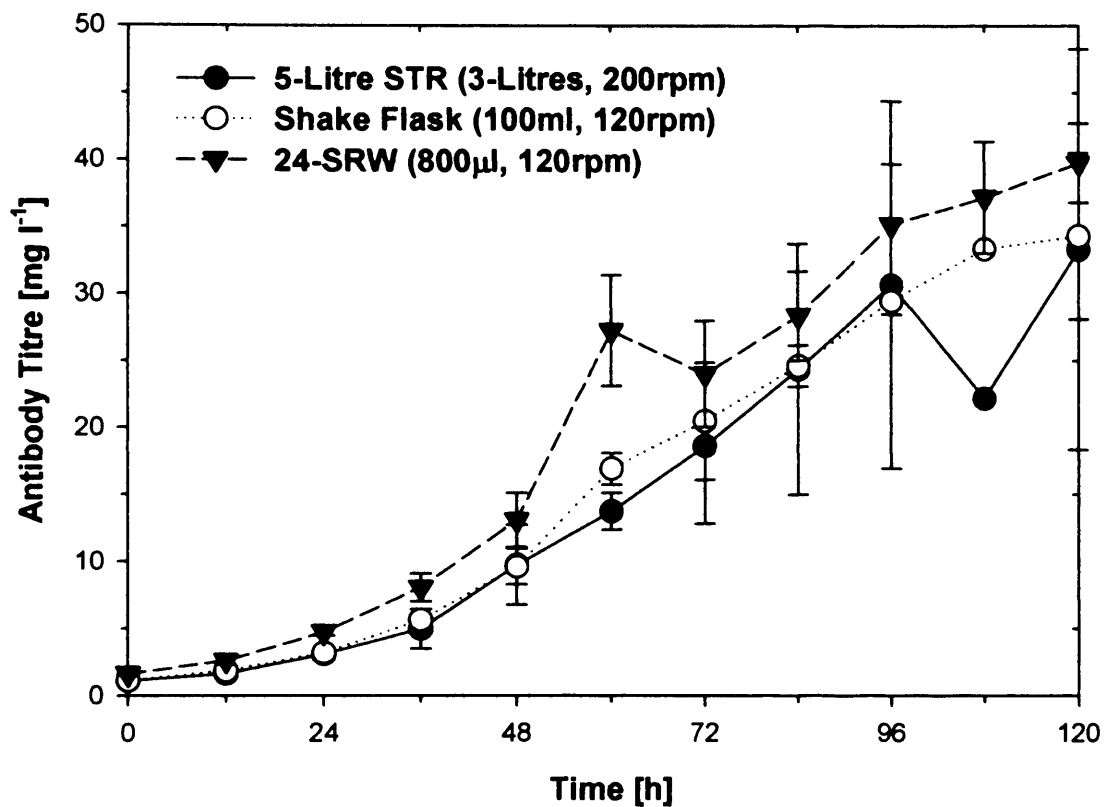


Figure 5.8: Scale-up of VPM 8 hybridoma cells based on matched average energy dissipation per unit volume: antibody titre in shaken 24-SRW plates, 250 ml shake flasks and a 5-L stirred-tank reactor. Experiments performed as described in Fig. 5.6. Antibody titres were quantified using ELISA as described in Section 2.8.2. Error bars represent one standard deviation about the mean.

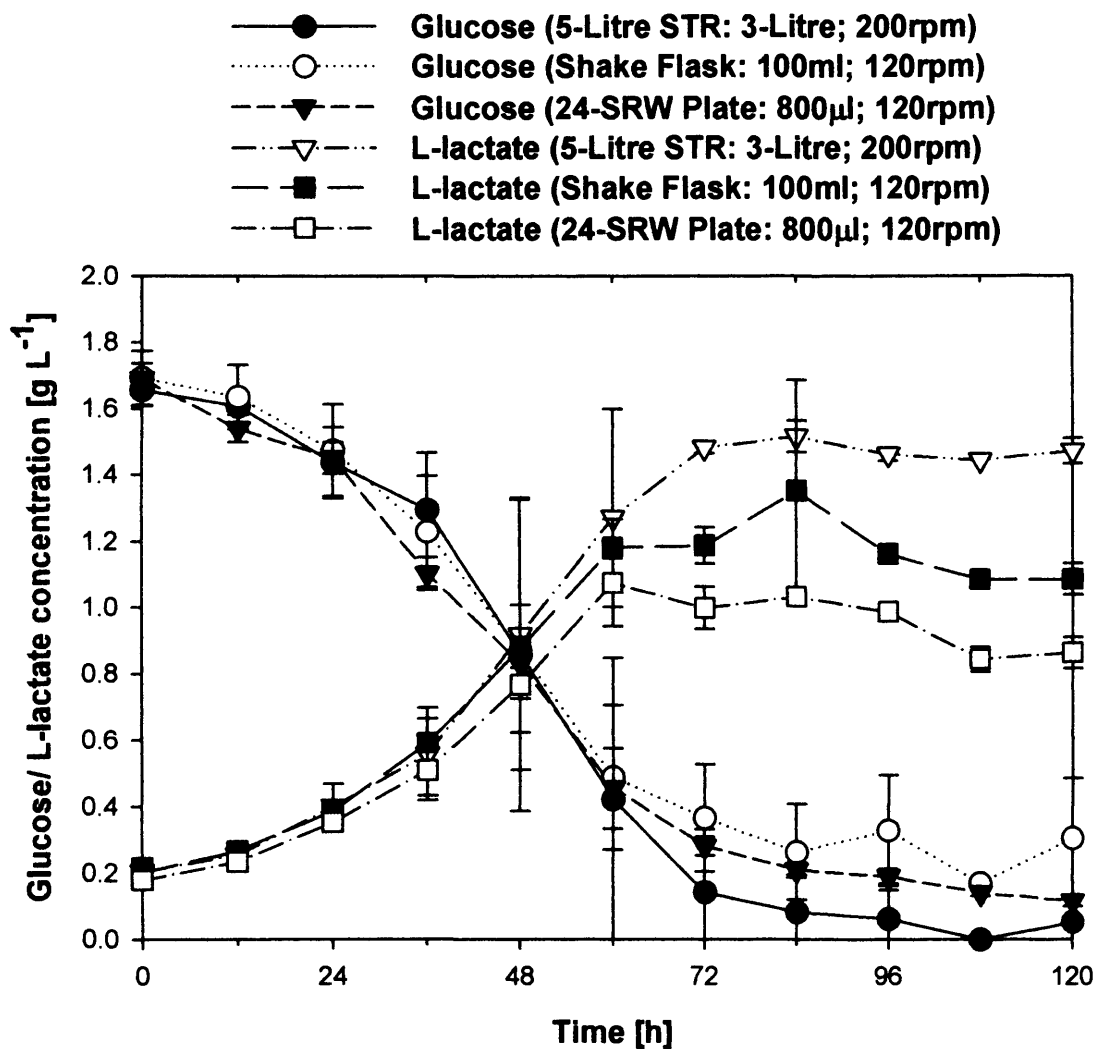


Figure 5.9: Scale-up of VPM 8 hybridoma cells based on matched average energy dissipation per unit volume: glucose and lactate concentrations in shaken 24-SRW plates, 250 ml shake flasks and a 5-L stirred-tank reactor. Experiments performed as described in Fig. 5.6. Glucose and L-lactate concentrations were measured as described in Section 2.8.3 Error bars represent one standard deviation about the mean.

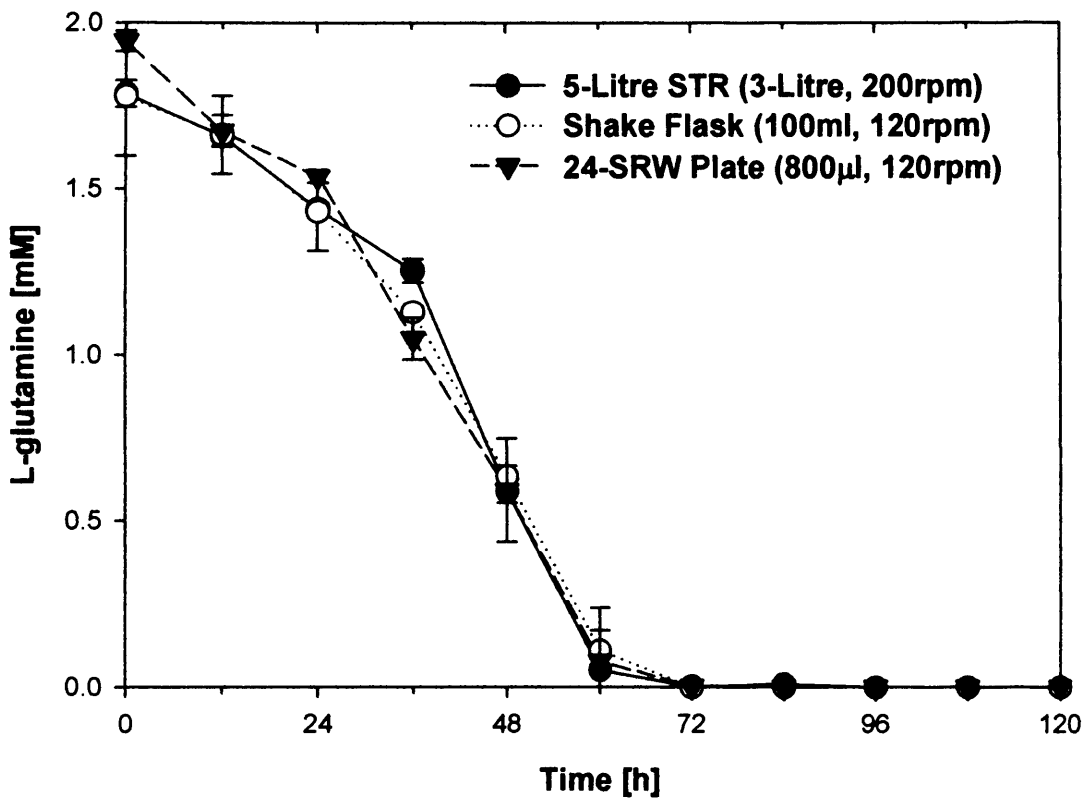


Figure 5.10: Scale-up of VPM 8 hybridoma cells based on matched average energy dissipation per unit volume: L-glutamine concentration in shaken 24-SRW plates, 250 ml shake flasks and a 5-L stirred-tank reactor. Experiments performed as described in Fig. 5.6. Glutamine concentration was measured as described in Section 2.8.3 Error bars represent one standard deviation about the mean.

Table 5.1: Scale-up of VPM 8 hybridoma cells based on matched average energy dissipation per unit volume: cell growth, antibody production and metabolism in shaken 24-SRW plates, 250 ml shake flasks and a 5-L stirred-tank reactor. Experiments performed as described in Fig. 5.6. Data taken from Fig.5.6,5.7,5.8,5.9,.

Parameter	24-SRW Plate		250ml Shake Flask		5-L STR	
	Mean	CV [%]	Mean	CV [%]	Mean	CV [%]
Final antibody concentration [mg l^{-1}]	40	7	34	18	33	45
Integral of viable cell concentration [$10^9 \text{ cells.day.l}^{-1}$]	4.262	3	4.100	17	3.518	16
Peak viable cell concentration [cells ml^{-1}]	1.377×10^6	14	1.472×10^6	7	1.167×10^5	18
Maximum specific growth rate [h^{-1}]	0.04033	2	0.04280	5	0.03800	7
Specific antibody production rate [$\text{mg (}10^9 \text{ cells.day)}^{-1}$]	9	4	8	0.5	10	59
Specific glucose consumption rate [$\text{g (}10^9 \text{ cells.day)}^{-1}$]	0.37	3	0.34	7.7	1.41	90
Specific lactate production rate [$\text{g (}10^9 \text{ cells.day)}^{-1}$]	0.16	11	0.22	18	2.03	113
Lactate produced / glucose consumed [g g^{-1}]	0.43	8	0.640	13	1.20	47

5.4 Summary

In this chapter, a first attempt has been made at scaling-up a hybridoma-based cell culture process from shaken microwell plates to shake flasks and a 5-L lab-scale STR using matched average energy dissipation rate (P/V) as a basis for scale translation. The utility of P/V as a scaling parameter was first introduced in Section 3.7, where it was discussed how average P/V can be matched in the case of microwells and shake flask but not for STRs. In addition, experiments performed in the chapter have studied how variations in average P/V lead to variations in culture performance.

Energy dissipation was first shown to have a significant affect on culture performance in shaken flasks (Section 5.2). At low energy dissipation rates (0 W m^{-3}), cell sedimentation was observed, along with reduced growth and antibody titre. At high energy dissipation rates (810 W m^{-3}), a reduction in growth and antibody titre were observed along with evidence of cellular damage. For each bioreactor geometry, there is likely to be an optimal value of P/V (approximately 40 W m^{-3} for shake flasks) and secondly, for scale-up, the P/V values need to match at the two different scales unless one of the two P/V values is far from optimum at that particular scale.

A first attempt at scaling-up a microwell cell culture process to 250 ml shake flasks and a 5-L STR proved very successful (Section 5.3). Similar growth and antibody production data at all three scales suggest microwell culture can provide informed bioprocess data for cell culture process development. Combined with automation, microwell plates could provide a cheaper, higher-throughput tool for process development than shake flasks and lab.scale STRs.

Chapter 6

Conclusions and Future Work

Optimisation of suspension cell-culture is traditionally carried out in spinner flasks, shake flasks, and small bench-scale stirred-tank reactors (STR) as previously described in Chapter 1. The current need to reduce process development time necessitates the adoption of high throughput experimentation, however, the labour and material costs involved render this almost impractical at conventional scales (Lye et al., 2003)(Girard et al., 2001)(Micheletti and Lye, 2006). In contrast, experimentation in microwell formats offers a potential new platform technology to obtain key process design data early and cost effectively (Lye et al., 2003). The use of a microwell format readily lends itself to automation (Doig et al., 2002)(Nealon et al., 2005), and the implementation of advanced operating strategies such as liquid addition for pH control (Elmahdi et al., 2003) and fed-batch operation. To date, just two studies have been published on the development and optimisation of suspension mammalian cell culture in shaken microwell plates (Girard et al., 2001)(Strobel et al., 2001). These previous studies have reported reasonable to excellent correlation of microwell data with larger bioreactor geometries such as spinner flasks, shake flasks and bench-scale STR. However, both overlooked characterisation of the engineering environment in the microwells and its influence on scale translation. For the microwell approach to be reliably implemented, it is first necessary to understand the influence of the engineering environment in microwells on cell-cultures. This will be vital for defining optimal operation for cell-cultures and ultimately a reliable basis for process scale-up.

In this study, the engineering environment in shaken microwell plates, under conditions relevant to the culture of suspension-adapted mammalian cells, was extensively characterised in terms of liquid hydrodynamics and gas-liquid mass transfer. Further, the impact of this engineering environment on hybridoma cell performance in batch shaken microwells cultures was assessed in terms of cell growth, antibody production and metabolism. From this, optimal culture conditions were established. Finally, it has been shown possible to scale-up a hybridoma microwell culture to 250 ml shake flasks and 5-L stirred-tank reactors using average energy dissipation rate as a basis for scale-translation.

In the initial stages of the project it was important to establish reliable techniques for cell culture in microwells. Evaporation losses from membrane covered shaken microwell plates were found to be significant over the 120 hour culture period. While only 10 % of the initial weight was lost to the surrounding environment, a significant proportion of the wells' liquid content evaporated and then adhered to the underside of the breathe-easy membrane used to cover the wells. This was measured to be nearly 50% of the initial well fill volume when operating with an initial fill volume of 800 μ l and shaken at 120 rpm (Section 3.6). Further studies found that evaporation from the wells was independent of shaking speed but dependent on the initial fill volume. Further research might explore the possible use of more hydrophobic membranes to help reduce the adherence of evaporated liquid to the underside of the membrane. Consequently all microwell data was corrected for evaporation losses to allow direct comparison with shake flask and stirred-tank reactor data. As a direct consequence of evaporation, the culture osmolality increased. Measurements made over the first 84 hours of culture were found to be less than those known to impact on culture performance.

Successful culture in 96-well plates was found to be cell-line specific (Section 4.2). While attempts to culture VPM 8 hybridoma cells in this format proved unsuccess-

ful, this work plus that of other (Strobel et al., 2001)(Deshpande and Heinzle, 2004) have all demonstrated successful culture of various CHO cell-lines in 96-well plates.

Initial experiments in shaken 24-well plates showed that under normal incubator temperature for cell culture, 37°C. the fluid in the well was almost 39°C. Using the methods described in Section 2.1.5, the incubator set-point has to be reduce to typically 35°C to avoid excessive well temperatures.

In order to provide an engineering basis for later scale translation, one of the initial objectives of this work (Section 1.5) was to characterise the engineering environment in shaken microwell under conditions that are relevant to the culture of suspension-adapted mammalian cells. The liquid phase hydrodynamics in shaken 24-SRW plates was predicted using the Reynolds (Re), Froude (Fr) and Phase number (Ph) (Section 3.2). Although a Re number was calculated for microwells, information on how it relates to flow regime is still lacking. Further work needs to be done to establish this relationship. Possible techniques to determined this relationship could be microparticle image velocimetry (PIV), to predict local fluid velocities or computational approaches such as direct numerical simulation to model the flow (Michieletti and Lye, 2006). A transitional flow regime was predicted in a shake flask and 5-L stirred-tank reactor (STR), operating under conditions to act as an experimental comparison. At shaking speeds between ≤ 160 rpm, a large fraction of fluid was predicted to remain in contact with the base of the 24-SRW plate and not follow the motion of the shaker platform resulting in reduced mixing intensity and oxygen transfer. This is known as “out-of-phase” operation (Büchs et al., 2000b). By contrast, at shaking speeds ≥ 200 rpm and in the shake flask, all the fluid was predicted to be “in-phase” and follow the orbit of the shaking platform.

The volumetric oxygen mass transfer coefficient (k_La) in shaken 24-SRW (ULA) wells was predicted using Equation 1.4. In general, the k_La values predicted, 1.3 - 29 h^{-1} , suggest that oxygen transfer should not limit VPM-8 hybridoma cell culture

in shaken 24-SRW plates (Section 3.3). Furthermore, with considered selection of shaking speed and well fill volume, this well geometry should support the oxygen demand of current industrial production cell-lines with maximum viable cell concentrations up to 1×10^7 cells ml^{-1} (Wurm, 2004). $k_L a$ values predicted for the shake flask and 5-L STR suggest oxygen transfer will not limit culture performance in these two geometries either under comparable conditions.

The mixing of small liquid additions to shaken 24-well plates was found to occur by two distinct routes dependent on the Re number (Section 3.4.1). At lower values of Re (≤ 1370), the liquid addition was mixed from the bottom of the well to the top (Fig. 3.3), heterogeneities were clearly visible and mixing times were long when compared to typical values for cell culture (Table 3.4). Clearly this would impact on culture performance if the additions are cytotoxic at high concentration, for example, addition of alkali for pH control. At higher values of Re (≥ 1520), the additions were incorporated rapidly into the liquid contents of the wells (Fig. 3.4) and mixing times were typical of those published for cell-culture bioreactors. An attempt was made to reduce the mixing times in 24-SRW (ULA) plates using a novel well design incorporating baffles (Section 2.1.5). Although a significant improvement in mixing was measured at all speeds, the mixing times at the lower values of Re were still longer than 200 s (Fig. 3.6). A small liquid addition made to the 5-L STR was found to spread out over the top portion of the liquid; above the level of the impeller, before passing into the bottom portion and restoring homogeneity (Fig. 3.7).

The performance of VPM 8 hybridoma cell cultures in shaken 24-SRW plates operated over a wide range of shaking speeds and well fill volumes were assessed for cell growth, antibody production and metabolism. Shaking speed was found to have a significant but not marked affect on performance (Section 4.3). This was thought to be the result of an adequate supply of energy to suspend cells and provide adequate oxygen transfer, but not too high to be detrimental to culture performance.

Well fill volume had a more pronounced affect on culture performance particularly during operation at high fill volumes and low shaking speed (Fig. 4.9). Under extreme operating conditions, cell sedimentation was observed and anaerobic conditions measured. Furthermore, DOT measurements at this condition verified the $k_L a$ prediction, suggesting Equation 1.4 can provide accurate predictions of the oxygen transfer capability of shaken microwell systems for cell culture applications.

Further experiments using the hybridoma cell-line and 24-SRW plates were conducted looking at the affect of baffles and well coating on cell culture performance. Baffles were found to have no affect on culture performance although they will have positive affect on the blending of liquid additions to microwell cultures as described previously. Future automation of these cultures will inevitably involve liquid additions so the use of baffles to reduce mixing time will be advantageous. Likewise, the affect of a low attachment coating to reduce cell and protein adsorption was shown to have no positive affect compared to standard polystyrene wells, however, PS wells are considerable cheaper so for high-throughput applications this cost saving will prove to be beneficial.

A study looking at the influence of P/V on culture performance in 250 ml shake flasks found a significant affect (Section 5.3). At low P/V values, cell sedimentation and anaerobic conditions due to limited mixing were observed. By contrast, high P/V resulted in visible cellular damage, poor growth and reduced antibody production. This study suggested an optimal range of P/V for shake flask cultures of suspension-adapted mammalian cells.

CFD simulations performed on 24-SRW (ULA) plates predicted average energy dissipation rates (P/V) between 5 and 40 $W m^{-3}$ (Section 3.5.1). Furthermore the maximum hydrodynamic stress predicted was at least two orders of magnitude lower than that known to negatively impact on mammalian cells (Heath and Kiss, 2007).

Initial attempts at scaling-up a cell culture process from shaken microwell plates to shake flasks and bench-scale STR using matched P/V as a basis were successful. This basis was chosen since it has a direct impact on both hydrodynamics and oxygen mass transfer; further, a recent study has shown its successful use in the scale-up of a recombinant CHO cell line in stirred-tank reactors (Li et al., 2006). The comparable data obtained at each scale suggest that microwells can provide data that is both reproducible and representative of shake flasks and STRs. Although P/V was selected in this, other basis for translation could be used depending on the application. For example, matched $k_L a$ might prove successful for cell-lines with high oxygen uptake rates.

What is now needed is the ability to automate microwell cultures and then use this platform to perform advanced microscale cultivation strategies such as feeding, pH control and temperature jumps (Nealon et al., 2006)(Elmahdi et al., 2003)(Ferreira-Torres et al., 2005)(Doig et al., 2002). These strategies are commonly used in the development of cell culture processes but their development and optimisation is time consuming, labour intensive and costly due to the low throughput and manual nature of the bioreactors currently used (Girard et al., 2001).

Automation of parallel microwell experimentation using laboratory liquid-handling robots, such as the Tecan platforms ¹ previously used in studies from this laboratory (Fig. 1.5) would significantly reduce labour requirements while increasing throughput. Steps performed by a typical robot include incubation, shaking, liquid handling, centrifugation, and detection using plate readers. Furthermore, suppliers of automation equipment like Tecan now offer customised applications to allow existing liquid handling robots to perform more complex tasks including ELISA and cell-based assays². There are already publications that describe the automation of whole bioprocessing steps including fermentation (Ferreira-Torres et al., 2005) and primary recovery (Jackson et al., 2006) in which cell culture steps might be imple-

¹ www.tecan.com

² www.tecan.com

mented. These are described in more detail in Section 1.4.4.

Once the basic routines such as inoculation, incubation and detection are automated it will then be possible to focus attention on using the platform to aid the development and optimisation of feeding strategies. Indeed, it has been shown that design of experiment techniques can be combined with existing software controlling the robots to aid the selection of appropriate feed compositions (Heath and Kiss, 2007).

pH control in shaken microwell is another area that deserves further study: differences in the pH profiles between a microwell cultivation and an instrumented, controlled STR culture may affect the success of scale-up. As mentioned in Section 1.4.4, Elmahdi et al. (2003) made a successful first attempt at controlling pH of *S. erythraea* culture in shaken 24-well plates. However, the culture pH was measured using standard polarimetric probes that are invasive but quick enough for the culture times involved. For high-throughput, automated cultures; a quick, non-invasive measurement technique would be essential. Girard et al. (2001) describe a method to correlate the culture pH with the light adsorption of phenol red contained within the media. Another method would be to use microtitre plates with integrated optical pH sensors³. pH sensitive fluorescent dye are embedded at the bottom of each well; using a commercial fluorescence plate reader the pH can be rapidly measured.

Temperature jumps within a culture, typically 37°C to between 30°C and 33°C, are often used in fed-batch or transient transfection processes to increase product formation rates (Dinnis and James, 2005)(Yoon et al., 2003). By lowering the temperature, the growth rate is suppressed and thus nutrient are direct towards production. The small volumes used in microwells lend themselves to rapid changes in temperature compared to larger vessels like shake flask and STRs.

Another area that deserves further investigation is using microwell cultures to study how cells respond physiologically to expected changes in the culture environment at

³www.presens.de

larger scales and then use the microscale data to make informed decisions during process design. At large scale, apoptosis is the most common reason for the termination of a culture and is the result of one or more of the following: nutrient depletion, metabolic by-product accumulation, excessive shear forces or hypoxia (Butler, 2005)(Laken and Leonard, 2001). To prevent or inhibit apoptosis two strategies are used: manipulation of the cellular environment through nutrient supplementation or genetic manipulation (Butler, 2005)(Laken and Leonard, 2001). Microwell plates offer a potential high throughput platform to study apoptosis in cell cultures and then develop and optimise feeding strategies or indeed genetic manipulations to extend the time of high viability and prolong protein production. The stage of a cell in its cycle can be vital for defining the optimal time to make changes to a culture environment particularly the addition of drug treatments or transfection agents (Tait et al., 2004)(Lloyd et al., 1999). Both of these studies are commonly conducted using a flow-cytometer (Simon and Karim, 2002). As mentioned above, suppliers of liquid handling robots are offering customer the option of integrating cell-based assays, that is a flow cytometer, into the automation platform. As well as studying the physiological response to changes in culture conditions, it is crucial to understand the influence of the culture changes on product synthesis and structure. For example, microwells could be used to study how changes in pH affect the glycosylation of antibodies (Osman et al., 2001).

The hybridoma and CHO-S cell line used in this work are focused more towards research rather than production. By challenging the microwell platform with other suspension adapted mammalian cell lines particularly those used by industry such as PER-C6, NSO, CHO, baby hamster kidney (BHK), human embryonic kidney (HEK 293) and human retinal cells would confirm the general applicability of this platform technology for process development and optimisation within an industrial setting (Xie et al., 2002)(Wurm, 2004).

Finally, microscale techniques could be applied for the development and optimisation

of other unit operations particularly downstream processes (DSP). To date, most studies published on microscale unit operations have dealt with upstream operations, such as fermentation (Duetz et al., 2000)(Duetz and Witholt, 2001)(Elmahdi et al., 2003)(Micheletti et al., 2006) and bioconversion (Doig et al., 2002)(Ferreira-Torres et al., 2005). Very few have dealt with DSP operations. Jackson et al. (2006) have developed a microscale depth filtration technique to study the filtration characteristic of *E. coli* broth and the interaction between fermentation and primary recovery. Some work has already been published on chromatography, in particular looking at the sequence of events involved (Chandler and Zydney, 2004)(Mazza et al., 2002)(Rege et al., 2004)(Rege et al., 2006).



Bibliography

- Altmann, F., Staudacher, E., Wilson, I. B. and Marz, L.: 1999, Insect cells as hosts for the expression of recombinant glycoproteins, *Glycoconj J* **16**(2), 109–123.
- Aunins, J., Woodson, B., Hale, T. and Wang, D.: 1989, Effects of paddle impeller geometry on power input and mass transfer in small-scale animal cell culture vessels, *Biotechnol Bioeng* **34**(9), 1127–1132.
- Bahia, D., Cheung, R., Buchs, M., Geisse, S. and Hunt, I.: 2005, Optimisation of insect cell growth in deep-well blocks: development of a high-throughput insect cell expression screen, *Protein Expres Purif* **39**, 61–70.
- Balagadde, F. K., You, L., Hansen, C. L., Arnold, F. H. and Quake, S. R.: 2005, Long-term monitoring of bacteria undergoing programmed population control in a microchemostat, *Science* **309**(5731), 137–140.
- Balcarcel, R. R. and Clark, L. M.: 2003, Metabolic screening of mammalian cell cultures using well-plates, *Biotechnol Prog* **19**(1), 98–108.
- Battersby, B. J. and Trau, M.: 2002, Novel miniaturized systems in high-throughput screening, *Trends Biotechnol* **20**(4), 167–173.
- Betts, J. I., Doig, S. D. and Baganz, F.: 2006, Characterization and application of a miniature 10 mL stirred-tank bioreactor, showing scale-down equivalence with a conventional 7 L reactor, *Biotechnol Prog* **22**(3), 681–688.
- Brandt, B., Hidalgo, A. and Bornscheuer, U.: 2006, Immobilization of enzymes in microtiter plate scale, *Biotechnol J* **1**(5), 582–587.

- Brody, J. A. and Huntley, B.: 1965, Human lymphocytes cultured in microplates, *Nature* **208**, 1232–1233.
- Büchs, J.: 2001, Introduction to advantages and problems of shaken cultures, *Biochem Eng J* **7**(2), 91–98.
- Büchs, J., Lotter, S. and Milbradt, C.: 2001, Out-of-phase operating conditions, a hitherto unknown phenomenon in shaking bioreactors, *Biochem Eng J* **7**(2), 135–141.
- Büchs, J., Maier, U., Milbradt, C. and Zoels, B.: 2000a, Power consumption in shaking flasks on rotary shaking machines: I. Power consumption measurement in unbaffled flasks at low liquid viscosity, *Biotechnol Bioeng* **68**(6), 589–593.
- Büchs, J., Maier, U., Milbradt, C. and Zoels, B.: 2000b, Power consumption in shaking flasks on rotary shaking machines: II. Nondimensional description of specific power consumption and flow regimes in unbaffled flasks at elevated liquid viscosity, *Biotechnol Bioeng* **68**(6), 594–601.
- Büchs, J. and Zoels, B.: 2001, Evaluation of maximum to specific power consumption ratio in shaking bioreactors, *J. Chem. Eng. Jpn* **34**(5), 647–653.
- Butler, M.: 2005, Animal cell cultures: recent achievements and perspectives in the production of biopharmaceuticals, *Appl Microbiol Biot* **68**(3), 283–291.
- Chadd, H. E. and Chamow, S. M.: 2001, Therapeutic antibody expression technology, *Curr Opin Biotech* **12**(2), 188–94.
- Chandler, M. and Zydney, A.: 2004, High throughput screening for membrane process development, *J Membr Sci* **237**, 181–188.
- Cherlet, M. and Marc, A.: 1999, Hybridoma cell behaviour in continuous culture under hyperosmotic stress, *Cytotechnology* **29**, 71–84.
- Chisti, Y.: 1993, Animal cell culture in stirred bioreactors: Observations on scale-up, *Bioprocess Biosyst Eng* **9**(5), 191–196.

- Chisti, Y.: 2001, Hydrodynamic damage to animal cells, *Crit Rev Biotechnol* **21**(2), 67–110.
- De Jesus, M. J., Girard, P., Bourgeois, M., Baumgartner, G., Jacko, B., Amstutz, H. and Wurm, F. M.: 2004, Tubespin satellites: a fast track approach for process development with animal cells using shaking technology, *Biochem Eng J* **17**, 217–223.
- Deshpande, R. R. and Heinzle, E.: 2004, On-line oxygen uptake rate and culture viability measurement of animal cell culture using microplates with integrated oxygen sensors, *Biotechnology Letters* **26**(9), 763–767.
- dcZengotita, V. M., Kimura, R. and Miller, W. M.: 1998, Effects of CO₂ and osmolality on hybridoma cells: growth, metabolism and monoclonal antibody production, *Cytotechnology* **28**(1), 213–227.
- Dinnis, D. M. and James, D. C.: 2005, Engineering mammalian cell factories for improved recombinant monoclonal antibody production: lessons from nature?, *Biotechnol Bioeng* **91**(2), 180–189.
- Doig, S. D., Baganz, F. and Lye, G. J.: 2006, High throughput screening and process optimisation, *Basic Biotechnology* **3**.
- Doig, S. D., Pickering, S. C. R. and Lye, G. J.: 2005, Modelling surface aeration rates in shaken microtitre plates using dimensionless groups., *Chem Eng Sci* **60**(10), 2741–2750.
- Doig, S. D., Pickering, S. C. R., Lye, G. J. and Woodley, J. M.: 2002, The use of microscale processing technologies for quantification of biocatalytic Baeyer-Villiger oxidation kinetics, *Biotechnol Bioeng* **80**(1), 42–49.
- Doran, P. M.: 1995, *Bioprocess Engineering Principles*, Academic Press, London.
- Dove, A.: 2002, Uncorking the biomanufacturing bottleneck, *Nat Biotechnol* **20**, 777–779.

- Duetz, W. A., Ruedi, L., Hermann, R., O'Connor, K., Büchs, J. and Witholt, B.: 2000, Methods for intense aeration, growth, storage, and replication of bacterial strains in microtiter plates, *Appl Environ Microb* **66**(6), 2641–2646.
- Duetz, W. A. and Witholt, B.: 2001, Effectiveness of orbital shaking for the aeration of suspended bacterial cultures in square-deepwell microtiter plates, *Biochem Eng J* **7**(2), 113–115.
- Duetz, W. A. and Witholt, B.: 2004, Oxygen transfer by orbital shaking of square vessels and deepwell microtiter plates of various dimensions, *Biochem Eng J* **17**, 181–185.
- Elmahdi, I., Baganz, F., Dixon, K., Harrop, T., Sugden, D. and Lye, G. J.: 2003, pH control in microwell fermentations of *S. erythraea* CA 340: influence on biomass growth kinetics and erythromycin biosynthesis, *Biochem Eng J* **16**(3), 299–310.
- Fenge, C., Klein, C., Heuer, C., Siegel, U. and Fraune, E.: 1993, Agitation, aeration and perfusion modules for cell culture bioreactors, *Cytotechnology* **11**, 233–244.
- Ferreira-Torres, C., Micheletti, M. and Lye, G.: 2005, Microscale process evaluation of recombinant biocatalyst libraries: application to Baeyer–Villiger monooxygenase catalysed lactone synthesis, *Bioprocess Biosys Eng* **28**(2), 83–93.
- Freyer, S. A., König, M. and Kunkel, A.: 2004, Validating shaking flasks as representative screening systems, *Biochem Eng J* **17**, 169–173.
- Ge, X., Hanson, M., Shen, H., Kostov, Y., Brorson, K., Frey, D., Moreira, A. and Rao, G.: 2006, Validation of an optical sensor-based high-throughput bioreactor system for mammalian cell culture, *J Biotechnol* **122**(3), 293–306.
- Gill, N. K., Appleton, M., Baganz, F. and Lye, G. J.: 2007, Design and characterisation of a miniature stirred bioreactor system for parallel microbial fermentations, *Biochem Eng J* p. IN PRESS.
- Girard, P., Jordan, M., Tsao, M. and Wurm, F. M.: 2001, Small-scale bioreactor system for process development and optimization, *Biochem Eng J* **7**(2), 117–119.

- Guarino, R. D., Dike, L. E., Haq, T. A., Rowley, J. A., Pitner, J. B. and Timmins, M. R.: 2004, Method for determining oxygen consumption rates of static cultures from microplate measurements of pericellular dissolved oxygen concentration, *Biotechnol Bioeng* **86**(7), 775–787.
- Gupta, A. and Rao, G.: 2003, A study of oxygen transfer in shake flasks using a non-invasive oxygen sensor, *Biotechnol Bioeng* **84**(3), 351–358.
- Hadjiev, D., Sabiri, N. E. and Zanati, A.: 2006, Mixing time in bioreactors under aerated conditions, *Biochem Eng J* **27**(3), 323–330.
- Harms, P., Kostov, Y. and Rao, G.: 2002, Bioprocess monitoring, *Curr Opin Biotech* **13**(2), 124–127.
- Hataya, T., Inoue, A. K. and Shikata, E.: 1994, A PCR-microplate hybridization method for plant virus detection., *J Virol Methods* **46**(2), 223–36.
- Heath, C. and Kiss, R.: 2007, Cell culture process development: advances in process engineering, *Biotechnol Prog* **23**(1), 46–51.
- Hermann, R., Lehmann, M. and Büchs, J.: 2003, Characterization of gas-liquid mass transfer phenomena in microtiter plates, *Biotechnol Bioeng* **81**(2), 178–186.
- Hertzberg, R. P. and Pope, A. J.: 2000, High-throughput screening: new technology for the 21st century, *Curr Opin Chem Biol* **4**(4), 445–451.
- Jackson, N. B., Liddell, J. M. and Lye, G. J.: 2006, An automated microscale technique for the quantitative and parallel analysis of microfiltration operations, *J Membrane Sci* **276**(1-2), 31–41.
- Jansen, M., Veurink, J. H., Euverink, G. J. and Dijkhuizen, L.: 2003, Growth of the salt-tolerant yeast *Zygosaccharomyces rouxii* in microtiter plates: effects of NaCl, pH and temperature on growth and fusel alcohol production from branched-chain amino acids., *FEMS Yeast Res* **3**(3), 313–8.

- John, G. T., Klimant, I., Wittmann, C. and Heinzle, E.: 2003, Integrated optical sensing of dissolved oxygen in microtiter plates: A novel tool for microbial cultivation, *Biotechnol Bioeng* **81**(7), 829–836.
- Kato, Y., Peter, C. P., Akgün, A. and Büchs, J.: 2004, Power consumption and heat transfer resistance in large rotary shaking vessels, *Biochem Eng J* **21**(1), 83–91.
- Kensy, F., John, G. T., Hofmann, B. and Büchs, J.: 2005, Characterisation of operation conditions and online monitoring of physiological culture parameters in shaken 24-well microtiter plates, *Bioprocess Biosyst Eng* **28**(2), 75–81.
- Kensy, F., Zimmermann, H. F., Knabben, I., Anderlei, T., Trauthwein, H., Dingerdissen, U. and Büchs, J.: 2005, Oxygen transfer phenomena in 48-well microtiter plates: determination by optical monitoring of sulfite oxidation and verification by real-time measurement during microbial growth, *Biotechnol Bioeng* **89**(6), 698–708.
- Kimurat, R. and Miller, W. M.: 1996. Effects of Elevated pCO₂ and/or Osmolality on the Growth and Recombinant tPA Production of CHO Cells, *Biotechnol Bioeng* **52**, 152–160.
- Kumar, S., Wittmann, C. and Heinzle, E.: 2004, Minibioreactors., *Biotechnol Lett* **26**(1), 1–10.
- Kusnadi, A. R., Nikolov, Z. L. and Howard, J. A.: 1997, Transgenic Plants: Practical Considerations, *Biotechnol Bioeng* **56**(5).
- Laken, H. and Leonard, M.: 2001, Understanding and modulating apoptosis in industrial cell culture., *Curr Opin Biotechnol* **12**(2), 175–9.
- Lamping, S. R., Zhang, H., Allen, B. and Ayazi-Shamlou, P.: 2003, Design of a prototype miniature bioreactor for high throughput automated bioprocessing, *Chem Eng Sci* **58**, 747–758.
- Langheinrich, C. and Nienow, A.: 1999, Control of pH in large-scale, free suspension

- animal cell bioreactors: alkali addition and pH excursions, *Biotechnol Bioeng* **66**(3), 171–179.
- Langheinrich, C., Nienow, A. W., Eddleston, T., Stevenson, N. C., Emery, A. N., Clayton, T. M. and Slater, N. K. H.: 1998, Liquid homogenisation studies in animal cell bioreactors of up to 8m³, *Trans IChemE* **76**, 107–116.
- Larrick, J. W. and Thomas, D. W.: 2001, Producing proteins in transgenic plants and animals, *Curr Opin Biotech* **12**(4), 411–418.
- Lee, P. J., Hung, P. J., Rao, V. M. and Lee, L. P.: 2006, Nanoliter scale microbio-reactor array for quantitative cell biology, *Biotechnol Bioeng* **94**(1), 5–14.
- Li, F., Hashimura, Y., Pendleton, R., Harms, J., Collins, E. and Lee, B.: 2006, A systematic approach for scale-down model development and characterization of commercial cell culture processes, *Biotechnol Prog* **22**(3), 696–703.
- Lin, J., Takagi, M., Qu, Y., Gao, P. and Yoshida, T.: 1999, Enhanced monoclonal antibody production by gradual increase of osmotic pressure, *Cytotechnology* **29**(1), 27–33.
- Liu, C. and Hong, L.: 2001, Development of a shaking bioreactor system for animal cell cultures, *Biochem Eng J.* **7**(2), 121–125.
- Lloyd, D. R., Leelavatcharamas, V., Emery, A. N. and Al-Rubeai, M.: 1999, The role of the cell cycle in determining gene expression and productivity in CHO cells, *Cytotechnology* **30**(1), 49–57.
- Lodish, H., Berk, A., Zipursky, S., Matsudaira, P., Baltimore, D. and Darnell, J.: 1999, *Molecular Cell Biology*, 4th edn, W.H. Freeman and Company.
- Lye, G. J., Ayazi-Shamlou, P., Baganz, F., Dalby, P. A. and Woodley, J. M.: 2003, Accelerated design of bioconversion processes using automated microscale processing techniques., *Trends Biotechnol* **21**(1), 29–37.
- Maier, U. and Büchs, J.: 2001, Characterisation of the gas-liquid mass transfer in shaking bioreactors, *Biochem Eng J* **7**(2), 99–106.

- Maier, U., Losen, M. and Büchs, J.: 2004, Advances in understanding and modeling the gas-liquid mass transfer in shake flasks, *Biochem Eng J* **17**(3), 155–167.
- Marks, D. M.: 2003, Equipment design considerations for large scale culture, *Cytotechnology* **42**, 21–33.
- Mazza, C. B., Rege, K., Breneman, C. M., Sukumar, N., Dordick, J. S. and Cramer, S. M.: 2002, High-throughput screening and quantitative structure-efficacy relationship models of potential displacer molecules for ion-exchange systems, *Biotechnol Bioeng* **80**(1), 60–72.
- Meier, S.: 2005, Cell Culture Scale-Up: mixing, mass transfer, and use of appropriate scale-down models, *Biochemical engineering XIV: Frontiers and advances in biotechnology, biological and biomolecular engineering*, Harrison Hot Springs, BC, Canada.
- Merten, O. W.: 2006, Introduction to animal cell culture technology: past, present and future, *Cytotechnology* **50**(1), 1–7.
- Micheletti, M., Barrett, T., Doig, S. D., Baganz, F., Levy, M., Woodley, J. M. and Lye, G. J.: 2006, Fluid mixing in shaken bioreactors: Implications for scale-up predictions from microlitre-scale microbial and mammalian cell cultures, *Chem Eng Sci* **61**, 2939–2949.
- Micheletti, M. and Lye, G. J.: 2006, Microscale bioprocess optimisation, *Curr Opin Biotech* **17**(6), 611–618.
- Miller, W. M., Blanch, H. W. and Wilke, C. R.: 2000, A kinetic analysis of hybridoma growth and metabolism in batch and continuous suspension culture: effect of nutrient concentration, dilution rate, and pH., *Biotechnol Bioeng* **67**(6), 853–871.
- Minas, W., Bailey, J. E. and Duetz, W.: 2000, Streptomycetes in micro-cultures: Growth, production of secondary metabolites, and storage and retrieval in the 96-well format, *Antonie van Leeuwenhoek* **78**(3), 297–305.

- Mollet, M., Ma, N., Zhao, Y., Brodkey, R., Taticek, R. and Chalmers, J. J.: 2004, Bioprocess equipment: characterization of energy dissipation rate and its potential to damage cells, *Biotechnol Prog* **20**(5), 1437–1448.
- Mrotzek, C., Anderlei, T., Henzler, H. J. and Büchs, J.: 2001, Mass transfer resistance of sterile plugs in shaking bioreactors, *Biochem Eng J* **7**(2), 107–112.
- Muething, J., Kemminer, S. E., Conradt, H. S., Šagi, D., Nimtz, M., Kaerst, U. and Peter-Katalinić, J.: 2003, Effects of buffering conditions and culture pH on production rates and glycosylation of clinical phase I anti-melanoma mouse IgG 3 monoclonal antibody R 24, *Biotechnol Bioeng* **83**(3), 321–334.
- Muller, N., Girard, P., Hacker, D. L., Jordan, M. and Wurm, F. M.: 2005, Orbital shaker technology for the cultivation of mammalian cells in suspension, *Biotechnol Bioeng* **89**(4), 400–406.
- Nealon, A. J., Titchener-Hooker, N. J. and Lye, G. J.: 2006, Quantification and prediction of jet macro-mixing times in static microwell plates, *Chem Eng Sci* **61**(15), 4860–4870.
- Nealon, A. J., Willson, K. E., Pickering, S. C. R., Clayton, T. M., O’Kennedy, R. D., Titchener-Hooker, N. J. and Lye, G. J.: 2005, Use of operating windows in the assessment of integrated robotic systems for the measurement of bioprocess kinetics, *Biotechnol Prog* **21**(1), 283–291.
- Nienow, A. W.: 2006, Reactor Engineering in Large Scale Animal Cell Culture, *Cytotechnology* **50**(1), 9–33.
- Nienow, A. W., Langheinrich, C., Stevenson, N. C., Emery, A. N., Clayton, T. M. and Slater, N. K. H.: 1996, Homogenisation and oxygen transfer rates in large agitated and sparged animal cell bioreactors: Some implications for growth and production, *Cytotechnology* **22**, 87–94.
- Oh, S. K. W., Vig, P., Chua, F., Teo, W. K. and Yap, M. G. S.: 1993, Substantial overproduction of antibodies by applying osmotic pressure and sodium butyrate, *Biotechnol Bioeng* **42**(5), 601–610.

- Osman, J. J.: 2001, *Response of GS-NS0 mouse myeloma cells to pH fluctuations relevant to those found in large scale fermentation*, PhD thesis, The University of Reading.
- Osman, J. J., Birch, J. and Varley, J.: 2001, The response of GS-NS 0 myeloma cells to pH shifts and pH perturbations, *Biotechnol Bioeng* **75**(1), 63–73.
- Osman, J. J., Birch, J. and Varley, J.: 2002, The response of GS-NS0 myeloma cells to single and multiple pH perturbations, *Biotechnol Bioeng* **79**(4), 398–407.
- Ozturk, S. S.: 1996, Engineering challenges in high density cell culture systems, *Cytotechnology* **2**, 3–16.
- Ozturk, S. S. and Palsson, B. O.: 1991a, Effect of medium osmolarity on hybridoma growth, metabolism, and antibody production, *Biotechnol Bioeng* **37**, 989–993.
- Ozturk, S. S. and Palsson, B. O.: 1991b, Growth, metabolic, and antibody production kinetics of hybridoma cell culture: 2. Effects of serum concentration, dissolved oxygen concentration, and medium pH in a batch reactor, *Biotechnol Prog* **7**(6), 481–494.
- Peter, C. P., Suzuki, Y. and Büchs, J.: 2006, Hydromechanical stress in shake flasks: correlation for the maximum local energy dissipation rate, *Biotechnol Bioeng* **93**(6), 1164–1176.
- Pfeifer, T. A.: 1998, Expression of heterologous proteins in stable insect cell culture, *Curr Opin Biotech* **9**(5), 518–521.
- Pickering, S. C. R.: 2007, Engineering characterisation of shaken microwell plates for bacterial cultures. PhD thesis for submission to University College London.
- Puskeiler, R., Kaufmann, K. and Weuster-Botz, D.: 2005, Development, parallelization, and automation of a gas-inducing milliliter-scale bioreactor for high-throughput bioprocess design(HTBD), *Biotechnology and Bioengineering* **89**(5), 512–523.

- Raval, K., Kato, Y. and Büchs, J.: 2007, Comparison of torque method and temperature method for determination of power consumption in disposable shaken bioreactors, *Biochem Eng J* **34**(3), 224–227.
- Reddy, S. and Miller, W. M.: 1994, Effects of abrupt and gradual osmotic stress on antibody production and content in hybridoma cells that differ in production kinetics, *Biotechnol Prog* **10**(2), 165–173.
- Rege, K., Ladiwala, A., Tugcu, N., Breneman, C. M. and Cramer, S. M.: 2004, Parallel screening of selective and high-affinity displacers for proteins in ion-exchange systems, *J Chromatogr A* **1033**(1), 19–28.
- Rege, K., Pepsin, M., Falcon, B., Steele, L. and Heng, M.: 2006, High-throughput process development for recombinant protein purification, *Biotechnol Bioeng* **93**(4), 618–630.
- Ruitenbergh, E. J., Brosi, B. J. M. and Steerenberg, P. A.: 1976, Direct measurement of microplates and its application to Enzyme-Linked Immunosorbent Assay, *J Clin Microbiol* **3**(5), 541–542.
- Ryu, J. S. and Lee, G. M.: 1997, Influence of hyperosmolar basal media on hybridoma cell growth and antibody production, *Bioprocess Eng* **16**(6), 305–310.
- Samorski, M., Muller-Newen, G. and Büchs, J.: 2005, Quasi-continuous combined scattered light and fluorescence measurements: A novel measurement technique for shaken microtiter plates, *Biotechnol. Bioeng* **92**, 61–68.
- Sauer, P. W., Burky, J. E., Wesson, M. C., Sternard, H. D. and Qu, L.: 2000, A high-yielding, generic fed-batch cell culture process for production of recombinant antibodies, *Biotechnol Bioeng* **67**(5), 585–597.
- Schmid, G., Blanch, H. W. and Wilke, C. R.: 1990, Hybridoma growth, metabolism, and product formation in HEPES-buffered medium: I. Effect of passage number, *Biotech Lett* **12**(9), 627–632.

- Schulz, C., Scampavia, L. and Ruzicka, J.: 2002, Real-time monitoring of lactate extrusion and glucose consumption of cultured cells using a lab-on-valve system, *Analyst* **127**, 1583–1588.
- Sen, A., Kallos, M. S. and Behie, L. A.: 2001, Effects of hydrodynamics on cultures of mammalian neural stem cell aggregates in suspension bioreactors, *Ind Eng Chem Res* **40**(23), 5350–5357.
- Severns, M. L., Schoeppner, S. L., Cozart, M. J., Friedman, L. I. and Schanfield, M. S.: 1984, Automated determination of ABO/Rh in microplates, *Vox Sang* **47**(4), 293–303.
- Shmanai, V. V., Nikolayeva, T. A., Vinokurova, L. G. and Litoshka, A. A.: 2001, Oriented antibody immobilization to polystyrene macrocarriers for immunoassay modified with hydrazide derivatives of poly(meth)acrylic acid, *BMC Biotechnology* **1**(4).
- Simon, L. and Karim, M.: 2002, Control of starvation-induced apoptosis in Chinese hamster ovary cell cultures, *Biotechnol Bioeng* **78**(6), 645–657.
- Singh, V.: 1999, Disposable bioreactor for cell culture using wave-induced agitation, *Cytotechnology* **30**, 149–158.
- Strobel, R., Bowden, D., Bracey, M., Sullivan, G., Hatfield, C., Jenkins, N. and Vinci, V.: 2001, High throughput cultivation of animal cells using shaken microplate techniques, *Animal Cell Technology: From Target to Market*, Kluwer Academic.
- Sucosky, P., Osorio, D., Brown, J. and Neitzel, G.: 2004, Fluid mechanics of a spinner-flask bioreactor, *Biotechnol Bioeng* **85**(1), 34–46.
- Sullivan, E. J. and Rosenbaum, M. A. X. J.: 1967, Methods for preparing tissue culture in disposable microplates and their use in virology, *Am J Epidemiol* **85**(3), 425.

- Sumino, Y., Akiyama, S. and Fukada, H.: 1972, Performance of the shaking flask.i. power consumption, *J Ferment Technol* **50**, 203208.
- Szita, N., Boccazzi, P., Zhang, Z., Boyle, P., Sinskey, A. and Jensen, K.: 2005, Development of a multiplexed microbioreactor system for high-throughput bio-processing, *Lab Chip* **5**, 819–826.
- Tait, A. S., Brown, C. J., Galbraith, D. J., Hines, M. J., Hoare, M., Birch, J. R. and James, D. C.: 2004, Transient production of recombinant proteins by Chinese hamster ovary cells using polyethyleneimine/DNA complexes in combination with microtubule disrupting anti-mitotic agents, *Biotechnol Bioeng* **88**(6), 707–721.
- Vailejos, J., Kostov, Y., Ram, A., French, J., Marten, M. and Rao, G.: 2006, Optical analysis of liquid mixing in a minibioreactor, *Biotechnol Bioeng* **93**(5), 906–911.
- van Suijdam. J. C. and Metz, B.: 1981, Influence of engineering variables upon the morphology of filamentous molds, *Biotechnol Bioeng* **23**(1), 111–148.
- Varley, J. and Birch, J.: 1999, Reactor design for large scale suspension animal cell culture, *Cytotechnology* **29**, 177–205.
- Verma, R., Boleti, E. and George, A. J.: 1998, Antibody engineering: comparison of bacterial, yeast, insect and mammalian expression systems, *J Immunol Methods* **216**(1-2), 165–181.
- Weiss, S., John, G. T., Klimant, I. and Heinzle, E.: 2002, Modeling of mixing in 96-Well microplates observed with fluorescence indicators, *Biotechnol Prog* **18**(4), 821–830.
- Weuster-Botz, D.: 2005, Parallel reactor systems for bioprocess development, *Adv Biochem Eng Biotechnol* **92**, 125–143.
- Weuster-Botz, D., Altenbach-Rehm, J. and Arnold, M.: 2001, Parallel substrate feeding and pH-control in shaking-flasks, *Biochem Eng J* **7**(2), 163–170.
- Wurm, F. M.: 2004, Production of recombinant protein therapeutics in cultivated mammalian cells, *Nat Biotechnol* **22**(11), 1393–1398.

- Xie, L., Metallo, C., Warren, J., Pilbrough, W., Peltier, J., Zhong, T., Pikus, L., Yancy, A., Leung, J., Aunins, J. G. and Zhou, W.: 2003, Large-scale propagation of a replication-defective adenovirus vector in stirred-tank bioreactor PER.C6 cell culture under sparging conditions, *Biotechnol Bioeng* **83**(1), 45–52.
- Xie, L., Pilbrough, W., Metallo, C., Zhong, T., Pikus, L., Leung, J., Auniņš, J. and Zhou, W.: 2002, Serum-free suspension cultivation of PER. C 6[®] cells and recombinant adenovirus production under different pH conditions, *Biotechnol Bioeng* **80**(5), 569–579.
- Yoon, S., Song, J. and Lee, G.: 2003, Effect of low culture temperature on specific productivity, transcription level, and heterogeneity of erythropoietin in Chinese hamster ovary cells, *Biotechnol Bioeng* **82**(3), 289–298.
- Zanzotto, A., Boccazzi, P., Gorret, N., Van Dyk, T. K., Sinskey, A. J. and Jensen, K. F.: 2006, *In situ* measurement of bioluminescence and fluorescence in an integrated microbioreactor, *Biotechnol Bioeng* **93**(1), 40–47.
- Zhang, H.: 2004, *Application of computational fluid dynamics to micro-titre plates scale bioreactors*, PhD thesis, The University of London.
- Zhang, H., Williams-Dalson, W., Keshavarz-Moore, E. and Shamlou, P.: 2005, Computational-fluid-dynamics (CFD) analysis of mixing and gas-liquid mass transfer in shake flasks., *Biotechnol Appl Biochem* **41**(1), 1–8.
- Zhang, Z., Szita, N., Boccazzi, P., Sinskey, A. and Jensen, K.: 2005, A well-mixed, polymer-based microbioreactor with integrated optical measurements, *Biotechnol Bioeng* **93**(2), 286–296.
- Zimmermann, H. F., John, G. T., Trauthwein, H., Dingerdissen, U. and Huthmacher, K.: 2003, Rapid evaluation of oxygen and water permeation through microplate sealing tapes, *Biotechnol Prog* **19**(3), 1061–1063.



UNIVERSITY OF LONDON

SENATE HOUSE. MALET STREET, LONDON, WC1E 7HU



REPRODUCTION OF THESES

A thesis which is accepted by the University for the award of a Research Degree is placed in the Library of the College and in the University of London Library. The copyright of the thesis is retained by the author.

As you are about to submit a thesis for a Research Degree, you are required to sign the declaration below. This declaration is separate from any which may be made under arrangements with the College at which you have pursued your course (for internal candidates only). The declaration will be destroyed if your thesis is not approved by the examiners, being either rejected or referred for revision.

Academic Registrar

To be completed by the candidate

NAME IN FULL (please type surname in BLOCK CAPITALS)

TIMOTHY ALAN BARRETT

THESIS TITLE

Microwell evaluation of mammalian cell lines for large scale culture

DEGREE FOR WHICH THESIS IS PRESENTED Please select either... PHD

DATE OF AWARD OF DEGREE (To be completed by the University):

DECLARATION

1. I authorise that the thesis presented by me in [2008] for examination for the MPhil/PhD Degree of the University of London shall, if a degree is awarded, be deposited in the library of the appropriate College and in the University of London Library and that, subject to the conditions set out below, my thesis be made available for public reference, inter-library loan and copying.
2. I authorise the College or University authorities as appropriate to supply a copy of the abstract of my thesis for inclusion in any published list of theses offered for higher degrees in British universities or in any supplement thereto, or for consultation in any central file of abstracts of such theses.
3. I authorise the College and the University of London Libraries, or their designated agents, to make a microform or digital copy of my thesis for the purposes of inter-library loan and the supply of copies.
4. I understand that before my thesis is made available for public reference, inter-library loan and copying, the following statement will have been included at the beginning of my thesis: The copyright of this thesis rests with the author and no quotation from it or information derived from it may be published without the prior written consent of the author.
5. I authorise the College and/or the University of London to make a microform or digital copy of my thesis in due course as the archival copy for permanent retention in substitution for the original copy.
6. I warrant that this authorisation does not, to the best of my belief, infringe the rights of any third party.
7. I understand that in the event of my thesis being not approved by the examiners, this declaration would become void.

*Please state year by hand, using a pen.

DATE 20/9/2007 SIGNATURE _____

Note: The University's Ordinances make provision for restriction of access to an MPhil/PhD thesis and/or the abstract but only in certain specified circumstances and for a maximum period of two years. If you wish to apply for such restriction, please enquire at your College about the conditions and procedures. External Students should enquire at the Research Degree Examinations Office, Room 261, Senate House.